Study of drug-excipient interactions regarding solubility enhancement in diluted aqueous media and solid state transformations

Inauguraldissertation

zur
Erlangung der Würde eines Doktors der Philosophie
vorgelegt der
Philosophisch-Naturwissenschaftlichen Fakultät
der Universität Basel

von

Wiebke Svea Saal

aus Leverkusen, Deutschland

Basel, 2018

Originaldokument gespeichert auf dem Dokumentenserver der Universität Basel
edoc.unibas.ch

Genehmigt von der Philosophisch-Naturwissenschaftlichen Fakultät

auf Antrag von

Fakultätsverantwortlicher	Herr Prof. Dr. Georgios Imanidis
Korreferentin	Frau Prof. Dr. Christel Bergström

Basel, den 20.06.2017

Prof. Dr. Martin Spiess

Dekan

The significant problems we have cannot be solved at the same level of thinking with which we created them.

Albert Einstein

Abstract

Nearly all marketed dosage forms comprise pharmaceutical excipients that have multiple functions, for example, improvement of wettability, solubilization, or absorption enhancement, while they can also have further technical functions such as diluent, glidant, disintegrant, or preservative. The selection of appropriate excipients is crucial for a suitable dosage form design and therefore an important step during the drug development process. Excipients have traditionally been considered as pharmacologically inert; however, they can interact with the drugs in the dosage form. Such interactions can be of physicochemical nature or even biological effects may occur that are critical for oral drug absorption. These interactions can be especially of relevance when formulating poorly water-soluble drugs. Different formulations are needed for the various development phases, where eventually different requirements have to be considered. In early phases, time lines and drug amounts are very limited and therefore, formulation development has to be fast and compound saving but long-term stability does not have to be given. Since the choice of excipients is such a crucial step, a better mechanistic understanding is targeted by pharmaceutical scientists to avoid a purely empirical trial-and-error approach. A thorough general mechanistic understanding of drug-excipients interactions is helpful for designing a robust formulation.

In academic and industrial research, there is a huge interest in understanding the different mechanisms of drug-excipient interactions with regards to formulation processes or with respect to dissolution and absorption. The present work centers around the latter aspects and makes use of miniaturized test methods to obtain comparatively large experimental datasets.

The present thesis consists of six studies, which all focus on excipient effects on the solubility and solid state of poorly water-soluble drugs. Excipients effects were studied at low concentrations that are relevant for solution and suspension formulation in early phases but the effects are of equal importance for oral solid dosage forms upon dissolution and dilution in the gastrointestinal (GI) tract. New methods were introduced to study kinetic solubility and possible solid state transformation in a miniaturized scale to save material and to obtain multiple results in a short time frame.

The first study introduces a miniaturized X-ray powder diffraction (XRPD) assay for quantification of polymorphic mixtures. This approach was applied to simultaneously study kinetic solubility and time evolution of optional solid state changes. Additionally, the influence of four excipient vehicles and biorelevant media on the solid state and the solubility were tested. Excipient effects could be differentiated into effects in the solid and liquid phase of the slurries as enabled by the parallel study of kinetic concentrations and XRPD. As a result, effects were rather specific and no general interaction type was found for the two excipient classes tested.

The second study introduced image and fractal analysis into the pharmaceutical field of solvent-mediated phase transformation to gain an improved mechanistic understanding. It was possible to monitor the fractal dimension of crystallized compound in different media and it could be interpreted as an indicator of the cluster growth phase of the hydrate crystals. Additional, parallel tests based on a miniaturized scale, provided similar excipient trends for the solid state transformation. There were no general polymer or surfactant trends, and each excipient appeared to have specific effects on the kinetics.

The third study focusses on surfactant effects at low concentrations by studying solid state and solubility of 13 model compounds in parallel. It was found that solid state transformations played a minor role for the extent of solubility enhancement. However, the surfactants showed individual effects on solid state transformations of some drugs, which needs to be considered for formulation development. The obtained dataset demonstrated high solubilization correlations among pegylated surfactants of

similar type. Such correlations may be used to omit individual surfactants for a resource-saving solubilization testing in preformulation.

In the fourth study, we focused on a methacrylic copolymer (Eudragit EPO) which is already known for interacting with anionic drugs and is applied for stabilizing them in an amorphous state. These ionic interactions led also to a great solubility enhancement in aqueous environment of eight crystalline, anionic model compounds. With ^{1}H nuclear magnetic resonance (NMR) spectroscopy, we could also detect hydrophobic interaction that contributed to the overall interaction additionally to the expected ionic interactions. An additional and important finding was the correlation between diffusion data measured by diffusion ordered spectroscopy (DOSY) and the solubility enhancement.

The understanding of the interaction mechanism, resulted in the fifth study, where we investigated the solubility enhancing effect of the same polymer on six basic compounds. Unexpected high solubility enhancement was obtained considering that polymer and drugs are equally charged in the aqueous environment. DOSY-experiments indicated that the polymer undergoes conformational changes in presence of the drugs which may contribute to the interaction mechanism.

Finally, such *in vitro* obtained results were tested *in vivo* in rats in the sixth study. Two formulations with Eudragit EPO (EPO) were compared to conventional formulation approaches such as a pH-adjusted solution or suspensions. The *in vitro* obtained solubility enhancement did not translate into improved *in vivo* bioavailability in rats; however, the pharmacokinetics were significantly influenced. Delayed and decreased absorption of the drugs was most likely due to hydrophobic drug polymer interactions and co-precipitation of the compound with polymer in the gastrointestinal tract of the rats. Solid state analysis showed an absence of crystalline compound in the co-precipitate. The polymeric co-precipitation *in vivo* can be used for high-dose *in vivo* studies in the early phases of pharmaceutical development like toxicology or pharmacokinetic studies to circumvent high peak to trough plasma ratios.

In summary, this thesis provides new analytical methods and an improved mechanistic understanding of drug-excipient interactions *in vitro* as well as *in vivo*. However, it was seen that excipient effects especially on the solid state are highly

specific between drug and excipient, which makes it hard to formulate general rules or guidelines. Due to choosing the same experimental conditions, excipient effects can be better compared and the concomitant study of solid state and kinetic concentrations is key for a better understanding of molecular drug-excipient interactions in a dispersed system. The obtained findings can be used to guide early formulation development and the mechanistic insights may be help to decrease the number of experiments and needed amounts of compound, which is highly desirable in preformulation or early development.

Contents

Acknowledgements

I would like to express my gratitude to Prof. Georgios Imanidis for giving me the opportunity to carry out my PhD at the University of Basel and at the University of Applied Sciences and Arts Northwestern Switzerland. Thank you for your support, your interest and the scientific discussions.

Many thanks also go to Prof. Martin Kuentz for his supervision, help and support during my study. Thank you for the enthusiasm and many fruitful discussions.

I would like to thank Prof. Christel Bergström of the University of Uppsala for being the co-referee for this thesis.

Many thanks go also to F. Hoffmann- La Roche who kindly funded my doctoral studies. My thanks go to many people in this company, who collaborated with me, helped me in practical concerns and guided me with your expert knowledge. Especially, I would like to thank Dr. Nicole Wyttenbach and Dr. Jochem Alsenz for having great ideas, sharing their experience with me and their valuable input. Thank you for your great support during my PhD-work. Additionally, I would like to thank Rainer Alex for his support, Elisabeth Haenel, Barbara Jost and Pauline du Castel for their help in the laboratory. Also to the other members of the group – thanks for welcoming me and helping whenever needed. I also thank Olaf Grassmann, Alfred Ross and Björn Wagner for their collaboration and sharing their professional expertise.

Many thanks go to my colleagues at the Institute of Pharma Technology. I enjoyed common lunches, evenings at the riverside, Christmas dinners and breakfasts. Thank you for a great time at IPT. A special mention goes to Katka, who did not only shared the lab with me but also supported me generously during a very exciting period of the PhD work.

My thanks go also to the students that carried out their Bachelor-thesis under my supervision: Dominik Buser, Mladen Kovacevic and Patricia Tanner. Thank you for your work in the laboratory.

Ein ganz herzliches Dankeschön gilt meiner Familie, insbesondere meinen Eltern und meiner Schwester, für ihre Unterstützung während des Studiums und der Doktorarbeit.

Zum Schluss möchte ich mich bei dir bedanken, Stefan, für deine Unterstützung und deine Geduld. Du warst und bist eine grosse Stütze, nicht nur während der Doktorarbeit, sondern bei allen Unternehmungen und Projekten, die ich bzw. wir uns vorgenommen haben.

Chapter 1

Introduction

1.1 Background

The increased use of high throughput (HT) combinatorial and parallel chemical synthesis processes has led to an enormous library of compounds that can be used for lead identification in drug development. While such early screening tests target effective receptor binding, other physicochemical drug properties are considered typically at a later stage. Consequently, the compounds are often highly selective and potent, but essentially difficult to formulate. It is often barely possible to administer them in high doses as needed in toxicology studies. Also adequate clinical drug exposure might be difficult to achieve, which can increase further the attrition rate in development.

It is estimated that approximately 40% of all lead compounds have a high molecular weight and are rather lipophilic.[1] Based on their solubility and permeability, drug substances can be classified according to the biopharmaceutical classification system (BCS) (Figure 1.1).[2] BCS class II compounds have a limited oral absorption due to insufficient drug solubility. Bulter and Dressman[3] proposed a further development of the BCS, the so-called developability classification system (DCS), which includes a modified version of the solubility definition. The authors proposed estimation of a solubility limited absorbable dose together with effective permeability. This modification additionally allows a differentiation between dissolution-rate limited or solubility-limited class II compounds. This characteristic is especially important when choosing an appropriate formulation strategy for improving the oral bioavailability of these compounds.[4-6]

In addition to their poor water solubility, BCS class IV drugs exhibit insufficient membrane permeability, which is difficult to improve with formulation strategies. The use of permeability enhancers is limited by safety of the drug product so the best way to improve this property of absorption is to go back to the discovery phase to optimize a substance by modifying the chemical structure.

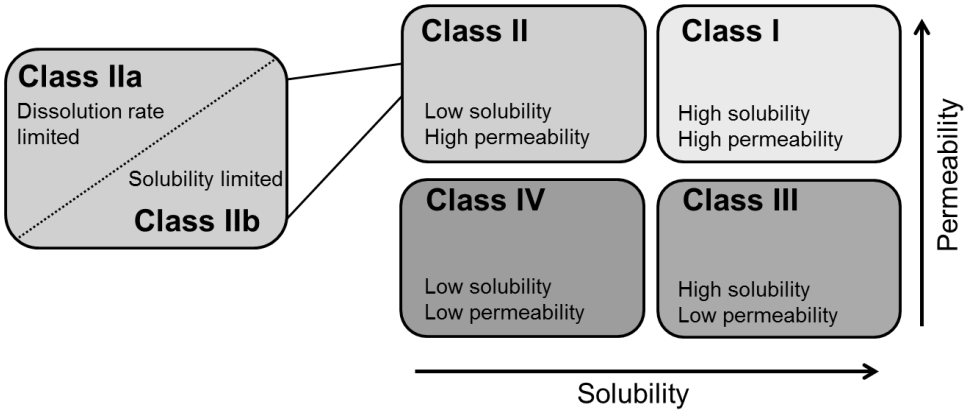

Figure 1.1: Biopharmaceutical classification system (BCS)[2] modified from Fahr and Liu[4] with the inclusion of the developability classification system by Butler and Dressman.[3]

Formulation strategies for oral bioavailability enhancement are either based on an improvement of the dissolution rate or on enhancing the solubilization of the compound. Unfortunately, not all formulation strategies can be applied in early development phases since there is only a limited amount of compounds available. In addition to small drug quantities, the synthesis process is not finalized at this stage and therefore the physical quality might not be ideal for the formulation process. The most common dosage forms in early phases are rather simple systems such as solutions, suspensions, or emulsions.[7, 8] In case of solutions, pH adjustment and the use of cosolvents, cyclodextrins, and surfactants are the most commonly applied strategies to dissolve the drug compounds.[7]

Based on this, pharmaceutical buffers can be used to adjust the pH of weak bases and acids that ionize at physiological pH between 2 and 9. As described in the Henderson-Hasselbalch-equation (Equation 1.1), the total solubility of a compound increases when its ionized fraction increases. The pH that is chosen for the formulation depends

on drug solubility and stability. However, extreme pH values can cause biocompatibility issues such as tissue irritation or potential drug precipitation.

$$pH = pK_a + \log\frac{[A^-]}{[HA]} \qquad \text{Eq. 1.1}$$

Cosolvents are known for their enormous capacity for solubilizing poorly water-soluble compounds especially for neutral compounds that cannot be formulated by pH-adjustment.[9] The most commonly used cosolvents are propylene glycol, polyethylene glycol, and glycerin.[9, 10] However, it is important to note that drug precipitation can occur when cosolvent-solutions are diluted *in vivo* with aqueous media (blood or intestinal fluid). This is not only an issue for intravenously administered formulations but may also lead to lacking tolerability or erratic absorption from oral dosage forms.

Polymers and surfactants are of particular importance as pharmaceutical excipient category. Micellar systems play for example an important role during the drug development process. They enhance drug solubilization, improve particle wettability and dissolution and may also hinder precipitation of drugs. Surfactants are used in many dosage forms, e.g. solutions, emulsions, capsules or tablets.[9, 11] In addition to solutions, suspensions are broadly employed in animal studies. In these dosage forms, a small percentage of hydrophilic polymers and surfactants are often added to aqueous vehicles. Polymers are used for particle suspending and homogeneity, while surfactants are used for particle wetting and dispersing. The major concern of suspensions is the physical stability since particle aggregation, sedimentation or changes in particle morphology are frequent problems.[7, 8]

All of these different formulation approaches include the use of a variety of excipients that are influencing mainly drug solubility. A selection of excipients was established on an empirical knowledge obtained over years in formulation development. More recently, there is particular interest in better understanding the mechanisms of drug-excipient interactions in formulation manufacturing processes [12-16] but also during drug dissolution[17] as well as resulting effects on drug absorption.[6, 18]

Drug-excipient interactions regarding drug solubilization are not only of interest with respect to the liquid phase but by considering the solid phase, as there is a solid-liquid

phase equilibrium (SLE). It is desired that already in the early phases of the drug development process, drug solubilization is combined with an assessment of the residual solid drug form and results obtained are likely to affect the following formulation strategy.

1.2 Objective

The aims of this thesis address the challenges to formulate poorly water-soluble drugs with comparatively simple formulation approaches. Considering the high number of poorly water-soluble compounds emerging from the discovery process, special attention was paid to solubility enhancement. Since solubility strongly depends on the solid state of the drug substance, the solid state was studied in parallel. A special focus in the experimental sections was the performance of experiments in miniaturized and high-though put approaches to conduct solubility and solid state studies already in an early development phases when time-lines are stretched and compounds are limited. The thesis is subdivided into individual chapters addressing different kinds of drug-excipient interactions and it additionally introduces methods for quantitative and qualitative analysis of drug-excipient interactions.

Background information on the formulation aspects of solubility and solid state are presented in the theoretical section (Chapter 2) as well as established miniaturized assays and reported/latest studies on drug-excipient interactions.

Chapter 3 introduces a quantification method on a miniaturized scale for polymorphic mixtures. The aim of this method was to study excipients' influence on solid state transformations of active compounds.

For a more mechanistic understanding, image and fractal analyses were applied to solid state transformations in excipient vehicles in Chapter 4. The focus is on gaining an improved understanding of the excipient effects in aqueous environment on hydrate formation. Additionally, the excipient effects were classified according to their influence in the liquid and the solid phase and these effects were compared regarding their influence on the final drug's solubility.

The primary aim of Chapter 5 is to broadly study drug solubilization by surfactants at a rather low concentration that should mimic dilution of an oral dosage form. Potential solid state changes are again checked by means of XRPD. Based on these results, a second aim is to correlate solubility enhancement factors among different surfactants. Such correlations can be used for decreasing the number of surfactant that need to be tested in preformulation for a more focused early solubility screening.

The Chapters 6 to 8 emphasize the application of a known excipient for enabling formulations, a polyelectrolytic polymer (Eudragit EPO), in a rather simple formulation approach to test specific drug-excipient interactions regarding solubilization and optional solid state changes. Additionally, nuclear magnetic resonance (^{1}H NMR) methods are evaluated to assess the strength of drug-excipient interactions. This polymer was applied to formulate not only acidic drugs but also basic compounds with the same charge as the polymer. It was aimed to show that excipient selection should not only be based on obvious ionic interactions but a more refined view of molecular interactions is required in the selection of solubilizing excipients. The rather counterintuitive interactions of Eudragit EPO with a basic and a neutral drug were also studied in a pharmacokinetic rat study to better assess biopharmaceutical consequences of these molecular interactions.

Chapter 2

Theoretical section

2.1 Solid state properties

The probability that a drug can exist in different polymorphic forms is reported to be between 50 and 80%.[19] The existence of different crystal forms can translate into changes in physicochemical properties such as solubility, melting point, chemical stability, or wettability (Table 2.1).[20-22] These alterations do not only influence the technical processes during formulation development, but they might also result in bioavailability changes. Additionally, the presence of metastable or amorphous forms can lead to recrystallization as a stability issue. The occurrence of polymorphs often follows Ostwald's rule of stages[23], which states that metastable forms appear first and are followed by crystallization of the thermodynamically most stable form. This results in polymorphic mixtures of drugs, during not only the production or storage, but also possibly during dissolution. In order to avoid these undesired polymorphic changes, a proper understanding about polymorphism of a drug substance is very important.

Table 2.1: Physical properties that can differ among polymorphic forms adjusted based on Brittian et al.[24]

Packing properties	Molar volume and density
	Refractive index
	Hygroscopicity
Thermodynamic properties	Melting or sublimation temperature
	Enthalpy
	Heat capacity
	Thermodynamic activity
Kinetic properties	Dissolution rate
	Solubility
	Stability
Surface properties	Surface free energy
	Crystal habit
Mechanical properties	Hardness
	Tensile strength
	Compatibility
	Flowability

The stability of polymorphs depends on their free energies. Under defined experimental conditions, only one polymorphic form has the lowest free energy. This polymorph is the thermodynamically stable form, whereas other polymorphs are thermodynamically unstable and therefore named metastable forms. A metastable polymorph might be desirable for formulation development as it may result in e.g. higher bioavailability. However, polymorphic changes can be induced during manufacturing and processing and are studied more in detail in the next chapter.

In general, the solid state of drugs can be divided into three main categories, namely polymorphs, solvates and amorphous forms (Figure 2.1). According to McCrone's definition, polymorphic forms are only represented by different crystal arrangements of the same chemical composition.[25]

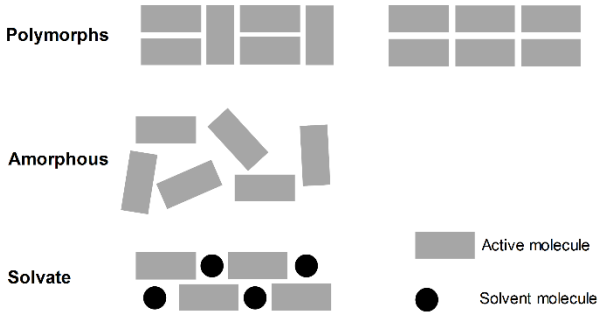

Figure 2.1: Classification of solid state based on Hilfiker.[26]

Solvates are no polymorphic forms according to this strict definition[25] as they do not have the exact same chemical composition as the other polymorphic forms. Instead, solvates differ in their chemical composition through the inclusion of one or more solvent molecules per unit cell.[26] Therefore the term pseudopolymorphism was introduced for solvates. Based on this, hydrates are a special example within the group of solvates, where the solvent associated with the molecule in the crystal is water. Solvates can be classified according to the ratio of drug and solvate molecules: stoichiometric solvates have a definite ratio, whereas for non-stoichiometric solvates the ratio of solvent to drug molecule may vary continuously. Another classification of solvates is based on analytical results and distinguishes between isolated site solvates, channel solvates and ion associated solvates.[27] Approximately one third of all active pharmaceutical ingredients (APIs) have the ability to form hydrates.[24] In many stages of the pharmaceutical development, drugs are exposed to solvents or solvent vapor, where solvate-formation might occur. These include precipitation, crystallization, wet granulation, and spray drying.

The amorphous forms build a special category within polymorphic forms. Amorphous solids are defined as non-crystalline solids, as the consequence of the absence of long-range molecular order. Amorphous materials can be prepared by several techniques including quench cooling, milling, spray drying or freeze-drying.[28, 29] There is a high interest in amorphous pharmaceutical solids because they provide great advantages in terms of solubility and bioavailability due to the high energetic state.[24]

A variety of analytical methods are available to obtain qualitative and quantitative information about the solid state. They have been extensively described in several reviews and textbooks.[24, 26, 30, 31] Table 2.2 summarizes commonly used analytical techniques and the unique information that are obtained by applying these methods.

Appropriate methods have to be chosen according the particular case and the investigated properties. Moreover, the system (pure drug, drug-excipient mixtures, formulations) and the experimental set-up (aqueous environment, scale) has to be considered when choosing the analytical method. Usually, a combination of several techniques is used to achieve a comprehensive understanding of the solid state properties.

Table 2.2: Analytical techniques commonly used for solid state characterization.

Analytical technique	Information	Limitation
X-ray diffraction (XRPD)[32-34]	Crystallographic properties like structural information and degree of crystallinity	Preferred orientation effects No information about the chemical structure
Infrared (IR) spectroscopy[35, 36]	Chemical information like intramolecular vibrations and H-bonding	Sample preparation can induce solid state transformation
Near infrared (NIR) spectroscopy[35, 37]	Chemical information from vibrational overtones and combinations of vibrations	Low sensitivity and selectivity Chemometrics might be needed for analysis
Raman spectroscopy[14, 36]	Chemical information from molecular vibrations and complementary to IR spectroscopy	Local heating of the sample Photodegradation
Solid state nuclear magnetic resonance spectroscopy (ss-NMR)	Chemical information like nuclei and chemical environment within a molecule	Long data acquisition time and expensive method
Differential scanning calorimetry (DSC)[38, 39]	Thermal events e.g. glass transition (T_g), crystallization (T_c) and melting temperature (T_m)	Destructive method Nature of thermal events is not determined Overlapping thermal events at the same temperature cannot be differentiated
Thermogravimetric analysis (TGA)[38]	Transitions related to a gain or loss in mass, decomposition temperature	Destructive method Unsuitable for materials that degrade at low temperatures
Dynamic vapor sorption (DVS)[40]	Hygroscopicity behavior	Interference with water-containing excipients possible
Isothermal microcalorimetry (IMC)	Heat changes in reaction e.g. heat of crystallization	Large amount of sample is required Low specificity

Table 2.2: Continued.

Analytical technique	Information	Limitation
Microscopy, polarized light microscopy (PLM), scanning electron microscopy (SEM)[41-44]	Morphology, color, crystal habit, topographical properties, crystallinity	No quantitative information are available Careful sample preparation is required (SEM)
Hyperspectral imaging (UV, Raman, IR, NIR)[45-49]	Visualization of crystallization, morphology, drug dissolution behavior, distribution of chemical components	Local heating of (dry) samples (Raman) Depending on pixel resolution

2.1.1 Process-induced transformations

Solid state transformations that occur during processing steps of the drug development process are important to monitor and understand, which should ensure an appropriate quality and stability of the final drug product. Process-induced transformations are caused by mechanical or thermal stress or they follow an exposure to solvents. Figure 2.2 represents possible phase transitions during pharmaceutical processing and their resulting effect on the solid state of the drug product.

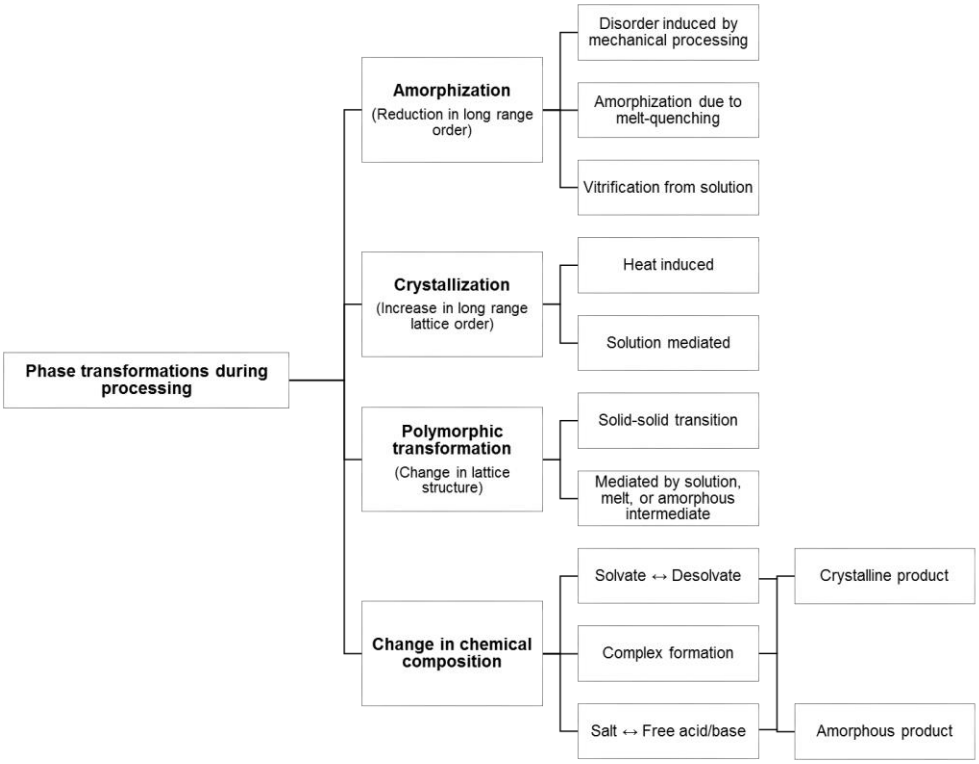

Figure 2.2: Representation of possible process-induced phase transformations.

During pharmaceutical processing, solid state changes cannot only occur in the active ingredients but also the solid state of excipients might be affected. Such changes in excipients can also have an important influence on the product quality and the final performance and therefore need to be considered.

Phase transformations can be classified by their underlying mechanism as proposed by Zhang et al.[50] Some solid state changes occur without passing through an intervening transient, liquid or vapor phase. This mechanism is strongly affected by the environmental factors such as temperature, pressure or relative humidity but also by the presence of crystalline defects, particle size and distribution, and impurities. A phase transition might as well occur when heating a compound above its melting point and subsequently cooling it back to ambient temperatures. The final solid state after melting is depending on the nucleation, crystal growth, and cooling rate. Additionally, impurities or excipients can affect the crystallization. Many processes in pharmaceutical development include the complete or partial dissolution of a compound in a solvent, usually water. Removing the solvent can induce solid state

transformations from a stable to a metastable phase or vice versa. The final solid form may also be a mixture of different solid states depending on the rate of solvent removal, the nucleation and crystal growth rate and the processing conditions. The undissolved drug may serve as seeds for crystallization of the original form but impurities or insoluble excipients provide surfaces for heterogeneous nucleation of different phases. The fourth possible mechanism is solvent-mediated phase transformation. It only allows transition from a metastable phase to the stable phase. Since the focus of this work was on solid state transformations in aqueous environments such as formulation vehicles for suspensions and solutions or during dissolution, solvent-mediated phase transformations will be discussed in more detail in the next chapter.

2.1.2 Solvent-mediated phase transformations

Cardew and Davey described solvent- or solution-mediated phase transformation as a two-step process as shown in Figure 2.3.[51, 52] The metastable form dissolves first, which results in a supersaturated solution with respect to the stable form and this stable form subsequently crystallizes out. The crystallization step is started with a nucleation of the stable form followed by growth of the crystals. The nucleation step may occur in the bulk phase or it is primarily a surface process.

Figure 2.3: Schematic representation of solvent-mediated phase transformation process.

Solvent-mediated phase transformations can be either dissolution- or crystallization-controlled depending on the relative kinetics of the dissolution and crystallization steps. The dissolution process is affected by the thermodynamic solubility of the metastable form, the particle size, and hydrodynamics. More details on dissolution rates of solids will be discussed in Chapter 2.2. Usually, the nucleation or the crystal growth is rate limiting and therefore any factors influencing nucleation or crystal growth will influence the overall transformations. Nucleation occurs when a solution

is supersaturated with respect to the stable phase, which is necessary for the growth of the more stable phase. Primary nucleation can be divided into two types, homogeneous and heterogeneous nucleation. Homogeneous nucleation does not occur very often as it requires significant supersaturation levels. Heterogeneous nucleation occurs when e.g. impurities or grain boundaries act as nucleation seed and lower therefore the free energy barrier. The primary nucleation rate J_1 can be described in these cases by the classical nucleation theory.[53]

$$J_1 = A'Se\frac{B'v_0^2\gamma^3}{(kT)^3 ln^2 S} \qquad \text{Eq. 2.2}$$

Where *A'* is a kinetic factor that is proportional to the number of nucleation-active centers, *B'* is a factor of shape and homogeneity, v_0 is the molecular volume of the crystalline phase and γ is the interfacial energy per unit area of the crystal. Moreover, *k* holds for the Boltzmann constant, *T* is the temperature and *S* the drug supersaturation.

In crystal suspensions it is more likely that the suspension itself serves as crystallization nuclei as a result of secondary nucleation. Secondary nucleation describes any nucleation mechanism that requires the presence of suspended parent solute crystals as it is caused by interaction of existing crystals with the vessel, impeller or by collisions and providing thereby new seed crystals through breakage. The secondary nucleation J_2 rate can be described by an empirical equation, taking the agitation rate (ω), the suspension density (ρ_s) and the supersaturation (σ) into account:[53]

$$J_2 = k_N \omega^l \rho_s^j \sigma^i \qquad \text{Eq. 2.3}$$

The secondary nucleation rate constant is described by k_N and the exponents *i, j, l* are empirically determined.

2.2 Solubility and dissolution

In addition to a detailed solid state characterization of a drug substance, there are other key parameters that need to be determined during the drug discovery process. Physicochemical properties such as the ionization constant (pK_a) or the partitioning

and distribution coefficient (log*P*, log*D*), are calculated or measured along with stability and permeability measurements. Moreover, aqueous solubility is one of the most important drug properties in the discovery and development process. These measured parameters together with initial results of *in vivo* exposure are used to make decisions on the biopharmaceutical developability of new APIs.

In principle, thermodynamic solubility is an easy parameter to measure, since it is defined as the concentration reached at equilibrium between the solid drug substances in a liquid solvent to form a homogenous solution of the solute in the solvent.[54] It is typically determined using the shake-flask technique where the pure crystalline compound is incubated in a saturated suspension containing the medium of interest for several days [55] In this experimental set-up, it can be tested if equilibrium has been reached. In addition, the solid state of the residual solid and the end pH of the medium should be investigated[56] even though this is often neglected. However, depending on the experimental set-up, solubility measurements can define apparent, intrinsic or thermodynamic solubility (see Table 2.3 for definitions).[57]

Table 2.3: Solubility definitions according to Bergström et al.[55]

Thermodynamic solubility (S)	Saturated solution in equilibrium with the thermodynamic stable polymorph
Intrinsic solubility (S_0)	Equilibrium solubility at pH where the API is in its neutral form
Apparent solubility (S_{app})	Solubility measured under given assay conditions

Thermodynamic solubility is often regarded as the "true" solubility of a compound.[57] However, experimental factors such as the polymorphic form at the start and end of the experiment, the pH, the mixing conditions or compound purity can influence the measured values. Therefore, solubility values should be seen rather in context of the experimental conditions and values may slightly differ from one experimental test protocol to another.

For the oral absorption processes not only the thermodynamic solubility, but also the dissolution rate needs to be considered. Noyes and Whitney conducted the first dissolution experiments in 1897.[58] The authors mathematically defined the proportional relation of the rate of dissolution and the difference between

instantaneous concentration *C* at time *t* and the saturation solubility C_s, known as the Noyes-Whitney-law (Equation 2.4), where *k* is a constant.

$$\frac{dC}{dt} = k(C_s - C) \qquad \text{Eq. 2.4}$$

Later on, the Noyes-Whitney equation was modified, considering the exposed surface, stirring rate, temperature, structure of the surface and the type of apparatus.[59] The work of Nernst and Brunner followed, which was based on the diffusion layer concept and Fick's second law known as the Nernst-Brunner equation (Equation 2.5).[58, 60] This equation replaces the constant k_1 ($k = k_1 S$) that was introduced by Bruner and Tolloczko:[59]

$$\frac{dC}{dt} = \frac{DS}{Vh}(C_S - C) \qquad \text{Eq. 2.5}$$

Here, *D* is the diffusion coefficient, *h* the thickness of the diffusion layer and *V* is the volume of the dissolution medium. For an overview of more recent theoretical developments of diffusion-controlled dissolution, Wang et al. have written an excellent review.[61]

Nowadays, dissolution studies are an essential part in drug development and provide useful information especially for administration via the oral route. There are several methods known to measure the dissolution rate of a pure drug, drug-excipient mixtures or even complete formulations. Many of these methods aim to use only small amounts of compounds and were reviewed recently.[62] Additionally, there are several techniques available for a real-time analysis of the dissolution behavior. They are usually based spectroscopic techniques such as UV, Raman or IR, but also potentiometric principles and a method based on the ultrasound resonator technology were applied to dissolution studies.[62]

Although solubility and dissolution rate are in principal easy to determine, there is still the need to define and validate solubility measurement techniques to ensure the comparability of obtained results. Within a European project about oral biopharmaceutical tools (OrBiTo project), an inter-laboratory comparison of small-scale solubility and dissolution measurements were performed.[63] Therefore, solubility and dissolution experiments were performed at 12 different laboratories including

industry and academia. Values from individual protocols were compared with values obtained by an established protocol used by all institutions. Andersson et al. found that establishing of standardized protocols is required for the experimental design but also for the data analysis to decrease the variability of obtained results.[63] Moreover, the authors identified experimental factors contributing to the variability like the quality of the standard curve or the amount of undissolved particles in powder dissolution measurements.

2.3 Miniaturized assays

Although, HT approaches have been intensively used in the discovery phase for synthesis of new compounds and crystallization screening, the following development phases use barely similar HT approaches. This has resulted in some disconnect between the discovery and development stage. In recent years, scaled down methods were developed to determine various compounds' characteristics such as to rapidly identify solubility-enhancing formulations.[11, 55] These approaches allowed the scientists in pharmaceutical profiling to provide feedback to the discovery researchers for improving the "developability" of candidate molecules.

Investigation of the physical form of a drug candidate has two major benefits. On the one side, the performance can be optimized by choosing a polymorphic form that has a high oral bioavailability or the maximum chemical stability.[64, 65] On the other hand, the risk of developing a metastable form is typically avoided because this could lead to a conversion later on that compromises the pharmaceutical performance. Solid state screenings coupled with crystallization optimization are hence powerful methods for exploring and optimizing the polymorphic form of a drug substance and product in the early development process. Critical elements during the screening include the crystallization technique, handling procedure, detection method, data processing, and storage. Solid form screenings are typically used to understand the effects of crystallization variables on the polymorphic outcome. Hilfiker et al.[19] combined high throughput screening and crystallization optimization for the example of carbamazepine. They showed that by designing good crystallization processes,

commercial advantages can be obtained. However, for this process a profound knowledge of the physicochemical characteristics of the drug is required.

Screening of the solid form and determining the aqueous solubility of critical importance in pharmaceutical discovery and development. There are several approaches described that evaluate kinetic solubility.[11, 57] Kinetic solubility measurements are based on a dilution of a drug solution in an organic solvent (often dimethyl sulfoxide) in aqueous media. When the drug reaches its solubility in the aqueous medium, the excess of drug precipitates and is detected by turbidity or UV absorption.[11] These experiments are simple to perform in a HT format since organic stock solution can be provided easily. However, the residual organic solvent additionally to the solid state of the precipitate influences the solubility and might therefore lead to values that are higher compared to the equilibrium solubility. Traditional methods to determine the thermodynamic equilibrium are not practical for testing a large number of samples with low compound availability and stretched time-lines. Therefore, thermodynamic solubility assays were developed on a smaller scale. They can be divided into scaled-down shake-flask and solvent-evaporation methods. Drug concentrations are usually measured with UV spectroscopy or high performance liquid chromatography (HPLC).[56, 66] Some assays also include a final pH measurement and solid state determination.[56] The detection methods applied are the limiting points for the use of these miniaturized assays. HPLC with a UV detector or UV spectroscopy are only possible for compounds which have a suitable chromophore. In case of the solvent-evaporation methods, polymorphic changes are likely to occur during the evaporation step, which can lead to substantial changes in the solubility values.

Also later on in the preformulation phase, only rather limited amounts of the compounds are available. However, during this stage not only physicochemical parameters need to be determined but also suitable formulation vehicles have to be supplied for pharmacokinetic or toxicology studies. Screening experiments using excipients and entire formulation vehicles are more challenging to handle on a miniaturized scale due to different viscosities and even dispending of solid excipients. There are still several miniaturized assays described in the literature for example regarding compound and excipient compatibility or to identify polymers for

stabilizing amorphous compounds.[67-69] Additional approaches are available in a 96-well format to examine the tendency of APIs alone and in presence of excipients to supersaturate[70] in media like buffers as well as simulated fluids.[71, 72]

2.4 Excipient effects on solubility and solid state

Regardless of the dosage form, drug characteristics, or administration route, nearly all drug products contain mainly excipients. The active compound represents typically only a small percentage of the dosage form. There is certainly much literature about the diverse excipient effects on quality attributes and aspects of industrial additive selection can be inferred from a recent article.[73]

Since excipients are used for a wide variety of functions in drug product, also the effect mechanisms are diverse. A focus of this work is the influence of excipients on the solubility and the solid state of drugs in aqueous environment (Figure 2.4). Solubility is one of the most important properties in drug discovery and strongly dependent on the solid state of the active compound. A drug already has several possibilities for interaction with itself as either in the solid form or as self-association in solution.[74, 75] The drug can further interact with an excipient in the liquid bulk or in a solid phase (Figure 2.4).

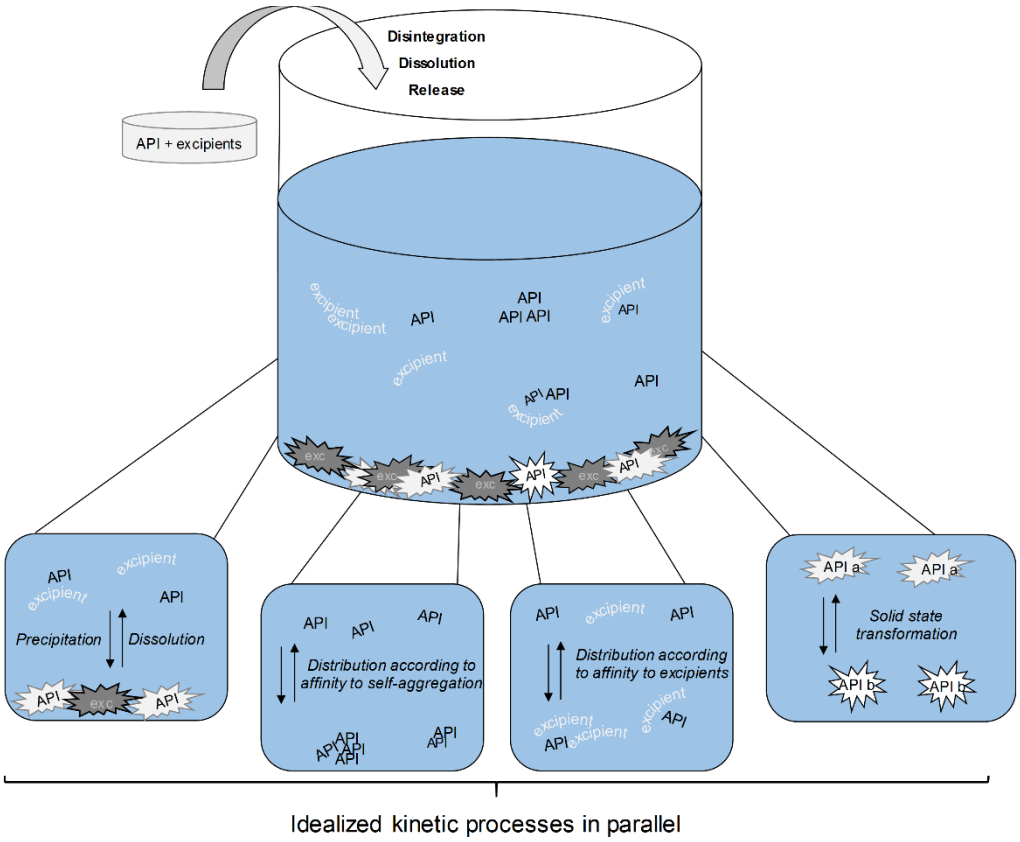

Figure 2.4: Schematic overview over different states, in which the active pharmaceutical ingredient (API) may occur upon aqueous dispersion with possible drug-excipient interactions.

These different drugs states with and without excipient already provide some complexity. Such complexity may be further increased by different interaction motifs of a given drug and excipient.[76] The idealized states depicted in Figure 2.4 come with kinetic processes that are expected to occur at least partially in parallel

The kinetic aspect is especially of interest when performing *in vitro* tests. Upon aqueous dispersion in the GI tract, the release rate of both, excipients and drug is key for molecular interactions. Different kinetic scenarios can be imagined. For example, if the excipient dissolves very fast, whereas the API is dissolution limited, it might happen that the undissolved API remains in e.g. the stomach but the excipient is already transported to the small intestine. This would result in minor drug-excipient interactions during the absorption process since excipients and drug exhibit differences in spatial and temporal distribution thereby preventing molecular interactions that may increase drug solubilization. When administering already

dissolved API and excipient, as e.g. in a solution formulation, the chances are higher, that both excipient and API will be transported together through the GI tract. However, APIs and excipients might be pH-dependent soluble and therefore precipitate in a certain section of the GI tract. For example, dissolved acidic APIs are very likely to precipitate in the stomach depending on their pK_a. However, such precipitation can be influenced by excipients regarding the precipitation rate or the solid state of the precipitate.

More recently, modern methods such as real-time spectroscopy revived the interest in better characterization and understanding of drug-excipient interactions by considering the solid state.[13, 20, 77] This interest can be motivated with respect to manufacturing processes or it may rather stem from a biopharmaceutical perspective.

In many pharmaceutical processes the active compound is exposed to water or water vapor which increases the likelihood of hydrate appearance. Especially during wet milling, wet granulation or dissolution, solvent-mediated phase transformations might occur and may lead to substantial changes in drug substance or drug product characteristics. Gift et al. studied transformation kinetics in presence of different polymeric excipients in high-shear wet granulation[12] and aqueous slurries.[16] They showed that the addition of certain polymeric excipients can inhibit hydrate formation of few model compounds. Very little amounts of polymers can lead via two mechanisms to a decrease in hydrate formation. On the one hand, polymers adsorb granulation liquid and thereby reduce the amount of available water. On the other hand, polymers interact with the surfaces' of particles, which leads to a smoothed surface and therefore also to reduced crystal growth. Wikstroem et al.[78] came to similar conclusions when studying the hydrate formation of theophylline during high-shear wet granulation. They also studied kinetics of anhydrate-to-hydrate formation of several model compounds and saw that not only solubility and dissolution play a role in solvent-mediated phase transformations but also surface properties and external factors such as shear force or the presence of seeds play an important role.[15] However, they also showed a noticeable retardation of hydrate formation by addition of polymeric excipients.[78] The mechanisms, they identified were similar to those from Gift et al. since they were arguing with a smoothing of the particles' surface by adsorption of the polymer and therefore decreasing of possible nucleation points.

Christensen et al.[79] studied not only the influence of polymeric excipients but also added cosolvents like ethanol. They identified high water-absorbing polymers and cosolvents with water-activity reducing characteristics as suitable for delaying the hydrate formation of their model compound, piroxicam. Ilevbare et al. published several results on the influence of polymers on the crystallization rate from supersaturated compounds.[43, 80, 81] They identified physicochemical characteristics of the polymers like hydrophobicity or functional groups to influence specific drug-excipient interactions and therefore also be responsible for the effectiveness of the crystallization inhibition. These structural relationships may also help to develop new excipients with excellent crystallization inhibition characteristics.

Polymeric excipients are not only useful for stabilization of a metastable solid state but they were also studied regarding their influence in liquid-liquid phase separation. Jackson et al.[82] studied the influence of three different polymers on the liquid-liquid phase separation and additional crystallization of danazol from supersaturated solutions. Liquid-liquid phase separation is observed for highly lipophilic compounds that are known to form aggregates in solutions. Although self-aggregation has been widely observed for chemically diverse compounds, the mechanism is not well understood yet. Liquid-liquid phase separation results in a two phase system, consisting of a solute-riche and a solvent-riche phase. This phenomenon is well known for protein solutions and organic crystallization. However, liquid-liquid phase separation in aqueous solutions of lipophilic drugs has only recently been studied more thoroughly. Ilevbare et al.[83] tested the influence of several experimental conditions like temperature and ionic buffer strength on the aggregation behavior of ritonavir and applied well-known thermodynamic principles to predict concentrations at which phase separation can occur.

There were also attempts to use miniaturized experimental set-ups to study a larger number of compounds in combination with various excipients. Avdeef et al.[84] studied the influence of frequently used liquid excipient vehicles on the solubility enhancement of eight model compounds to mimic conditions that can be expected after dissolution and dilution of dosage forms in the gastrointestinal tract. They also took into account in their study that several APIs are known to aggregate with themselves when they are dissolved in aqueous media. For the authors, it was possible

to classify excipients' effects and identify trends; however there are still mechanistic questions unanswered and an additional examination of solid state properties was not reported. However, Wyttenbach et al.[56] studied the solubility and the solid state of three compounds in parallel in aqueous and non-aqueous vehicles. Although, the study was intended to introduce a miniaturized approach for testing these two key parameters in parallel, the obtained data can be used when choosing model compounds or excipient vehicles for further studies since the research is providing solubility and solid state data in common formulation vehicles as well as in biorelevant media.

Not only polymeric excipients can influence solvent-mediated phase transformations but also surfactants can have an influence on transformation kinetics. Rodriguez-Hornedo and Murphy studied the influence of two anionic surfactants on the hydrate formation of carbamazepine.[85] Since carbamazepine anhydrate is transforming to its hydrate via a solvent-mediated process, the transformation kinetics is very sensitive to solution conditions such as pH, temperature or additives. When adding two anionic surfactants, an increase in the transformation rate was reported.[85] However, this influence of the surfactants was highly specific and depended on the molecular structure, concentration, and supramolecular association. The influence of surfactants plays also during the dissolution in the human body a major role. During the digestion process, drug formulations are exposed to gastric and intestinal media, which contain biorelevant surfactants. Lehto et al.[17] studied therefore the influence of simulated intestinal fluid on the solvent-mediated phase transformation of carbamazepine. Also with biorelevant media, specific drug-excipient interactions were found to occur via hydrogen bonding that were inhibiting crystal growth on the surface and therefore also inhibited the hydrate formation.[17] To obtain relevant results for the *in vivo* performance of drug product, it is very important to choose biologically representative dissolution media that mimic the situation *in vivo*.

Although there was important research done on excipients' effects on solubility and solid state, these studies often lack a large number of model compounds and experimental conditions like excipient concentrations and pH values differ from one study to another. Pronounced difference in these conditions are especially given when studies are compared that were about aqueous manufacturing processes as opposed to

in vitro experiments that were intended to reflect biopharmaceutical performance. Therefore, it is hard to compare the mechanisms and specific excipients effects within these studies and only trends can be noticed. For an improved understanding of drug-excipient interaction, a focus must be defined for example to mimic oral formulation performance. Same conditions in terms of excipient concentrations and pH should be maintained and it is important to study both, solubility and solid state in parallel to distinguish between effects in the solid phase and in the liquid phase.

Chapter 3

Miniaturized X-ray powder diffraction assay (MixRay) for quantitative kinetic analysis of solvent-mediated phase transformations in pharmaceutics

Summary

Many pharmaceutical compounds exhibit polymorphism, which may result in solvent-mediated phase transformations. Since the polymorphic form has an essential influence on physicochemical characteristics such as solubility or dissolution rate, it is crucial to know the exact polymorphic composition of a drug throughout pharmaceutical development. This study addressed the need to perform quantitative X-ray analysis of polymorphic mixtures on a 96-well scale (MixRay). A calibration of polymorphic mixtures (anhydrate and hydrate) was performed with three model drugs, caffeine, piroxicam, and testosterone, and linear correlations were obtained for all compounds. The MixRay approach for piroxicam was applied to a solubility and residual solid screening assay (SORESOS) to quantify the amount of hydrate and anhydrate corresponding to kinetic bulk concentrations. Changes in these drug concentrations correlated well with the kinetic changes in the residual solid. The influence of excipients on the solid state and kinetic concentrations of piroxicam was also studied. Excipients strongly affected polymorphic transformation kinetics of piroxicam and concentrations after 24 h depended on the excipient used. The new

Kirchmeyer et al. Miniaturized X-ray powder diffraction assay (MixRay) for quantitative kinetic analysis of solvent-mediated phase transformations in pharmaceutics. *Journal of Pharmaceutical and Biomedical Analysis*, **2016**, 131, 195-201.

calibration X-ray method combined with bulk concentration analysis provides a valuable tool for both pharmaceutical profiling and early formulation development.

3.1 Introduction

The majority of pharmaceutical compounds exhibit polymorphism. Since different polymorphic forms of a drug can have different bioavailability and behavior during processing,[86, 87] it is important to properly characterize the solid form of the drug already early on. Sensitive analytical methods are required especially in case of polymorphic mixtures. A thorough understanding of potential solvent-mediated phase changes is needed for clinical candidates' selection and for in-process controls to avoid quality issues of the final drug product.

An early solid state screening is nowadays typically conducted as part of the pharmaceutical profiling work aiming at the selection of the most suitable polymorph of a compound for development.[19, 31] Here, not only qualitative information is needed but also a quantification of polymorphic mixtures would be desirable.

At an early stage of development, high-throughput (HT) methods for compound characterization (solubility, stability) or testing drug-excipient compatibility are convenient because only a small amount of compound is available. HT-experiments provide the opportunity to test a number of different drugs and excipients, for e.g. solubility determination, in parallel at a miniaturized scale. Parallel testing has also already been reported in the field of drug discovery for the screening of polymorphic forms and for crystallization optimization.[31, 64] In the field of API-excipient interactions and solubility measurements, some HT-approaches have previously been reported.[56, 57, 88] In some of these assays, solid state analysis on a miniaturized scale has already been introduced but only on a qualitative level.[56] Thus there is clearly a need to also quantitatively determine drug solid state changes in a HT-format throughout kinetic processes for example during solubility and dissolution studies.

Today, solid state characterization of pharmaceuticals is typically performed for bulk powders on a much larger scale than HT-experiments. The different bulk

characterization methods include X-ray powder diffraction (XRPD),[33, 89] optical and electron microscopy,[90] spectroscopic methods like Raman spectroscopy,[13] near infrared (NIR) spectroscopy,[13, 91] and thermal methods such as differential scanning calorimetry (DSC).[92] Among these different methods, XRPD has been used for quantitative solid phase analysis for almost a century.[93] It is based on direct proportionality of X-ray reflection intensity and the weight fraction of the phase for which the scattering is characteristic. The technique was also successfully utilized for quantification of solid state changes of diverse active pharmaceutical compounds,[33, 89] the drug amounts required in these studies are usually in the 100 mg range. Single peaks or entire diffraction patterns of XRPD spectra can be used to establish correlations between phase composition and quantification. In general, quantification methods based on single peak measurements do require limited knowledge about the phases to be quantified, whereas whole pattern methods, such as the Rietveld method, are based on refinement of crystal structure parameters. Single peak methods are often more sensitive but also suffer from higher variability due to the influence of diverse experimental factors such as preferred orientation.[32] Among the whole pattern methods there are examples that do not require prior knowledge of the crystal structure like the factor-based Partial Least Square (PLS) analysis[94] and the whole pattern method described by Smith et al.[95] These methods require no knowledge of crystal structure date since they are based on empirically-derived correlation of intensities from one or more diffraction regions as a function of the analyte concentration.

XRPD quantitative analysis using Bragg-Brentano parafocusing configuration is currently most widely used.[96] In this reflection geometry, the specimen thickness exceeds the penetration depth of the X-ray beam into the powder bed and the powder volume contributing to scattering is consistent throughout a series of samples with comparable density. However, reflection mode XRPD requires sample amounts in the 100 mg range and the method is prone to effects of preferred orientation and specimen height. Thus, careful sample preparation, usually incl. powder milling, is a prerequisite for reflection mode XRPD quantification. In contrast, the orientation and specimen height effects are less relevant for transmission mode XRPD, and usually less sample is required. However, in transmission geometry the sample volume that

contributes to XRPD scattering usually varies considerably from one sample preparation to another. The addition of an internal standard to the measured sample can be used to normalize diffraction intensities in support of quantification a polymorphic mixture. However, the internal standard method is not applicable for polymorph screening applications. Therefore, a novel miniaturized X-ray powder diffraction quantification method (MixRay) is applied in the present study. Accordingly, the contribution of air/background scattering is quantified for each sample using an appropriate air/background reference pattern. Then, a least squares fit is performed that uses the references of the crystalline polymorphic forms and the air/background reference pattern to quantify the fractions in the polymorphic mixture. As the air/background pattern is not a "true" component of the polymorphic mixture the quantities of the crystalline constituents are normalized to 100%.

In the present study, the MixRay is applied to monitor solvent-mediated phase changes in a 96-well based HT test. First, three known hydrate-forming drugs were selected, caffeine,[97] piroxicam,[98, 99] and testosterone.[100] Anhydrates and hydrates of these drugs were used to perform HT-XRPD-calibrations on a miniaturized scale. Moreover, solid state transformation of the model compound piroxicam was studied in vehicles with different excipient and compared with drug solubility at different time points. The novel HT-test provides kinetic data of the changes in both the solid and liquid phase. The MixRay will help to better understand solvent-mediated phase changes in the presence of various excipients to support formulation development.

3.2 Materials and Methods

3.2.1 Materials

Anhydrous piroxicam (PRXAH), caffeine (CAFAH), and testosterone (TESAH) were purchased from TCI Europe N.V. (Zwijndrecht, Belgium), Sigma-Aldrich Chemie GmbH (Buchs, Switzerland), and TCI Europe N.V., respectively. Piroxicam monohydrate (PRXMH) was prepared by stirring PRXAH in 10 ml of deionized water

for 72 h, followed by filtration, and drying at 25 °C /45 % relative humidity as described in the literature.[98] Caffeine hydrate (CAFH) was purchased from MP Biomedicals LLC (Santa Ana, California, USA). Testosterone hydrate (TESMH) was prepared by suspending TESAH in water for 72 h, filtering, and drying for 24 h at room temperature. Complete transformation of piroxicam and testosterone to the hydrate form was confirmed by thermogravimetric analysis (TGA) and XRPD analysis.

Hydroxypropylmethylcellulose (HPMC) was obtained from Harke Group (Mülheim a.d. Ruhr, Germany), carboxymethylcellulose sodium salt (NaCMC) from Sigma-Aldrich Chemie GmbH, polysorbate 80 from Croda Europe Ltd. (Cowick Hall, UK) and sodium dodecyl sulfate (SDS) from Stepan Company (Northfield, Illinois, USA). Sodium chloride and sodium phosphate monobasic anhydrous were from Sigma-Aldrich Chemie GmbH and sodium chloride from Sigma Aldrich Co. (St. Louis, Missouri, USA). N-methyl-2-pyrrolidone, trimethylamine and methansulfonic acid were obtained from Sigma-Aldrich Chemie GmbH. Hydrochloric acid (0.1 M), sodium hydroxide (0.1 M) and ethanol were purchased from Merck KGaA (Darmstadt, Germany). Heptane and acetonitrile was from Biosolve BV (Valkenswaard, Netherland) and SIF® powder from Biorelevant (Croydon, UK).

3.2.2 Thermal gravimetric analysis (TGA)

Thermogravimetric analyses were performed with a TGA/DSC 1 STARe system from Mettler-Toledo AG (Greifensee, Switzerland). Samples (2–3 mg) were heated at 10 °C/min in 40 µl aluminum pans with pierced aluminum lids (Mettler-Toledo AG) to a maximum temperature of 300°C. Nitrogen was used as a protective gas at a flow rate of 100 ml/min. TGA was used to confirm the pseudopolymorphic transformation of the active pharmaceutical ingredients (APIs).

3.2.3 X-ray powder diffractometry (XRPD)

The polymorphic form of all materials (hydrates/anhydrates) was verified experimentally with XRPD using a STOE Stadi P Combi diffractometer equipped with primary Ge-monochromator (CuKα radiation), imagine plate position sensitive detector (IP-PSD), and 96-well plate sample stage. The IP-PSD allowed simultaneous recording of diffraction patterns on both sides of the primary beam. The software STOE WinXPOW was used for improving XRPD data quality by merging both 2-theta ranges and for calculating the composition of the mixtures. Effects related to poor crystal orientation statistics were reduced by summing up diffracted beam intensities on both sides of the primary beam. Each well of the imaging plate was exposed to X-ray radiation for 5 min. Samples were analyzed directly in the 96-well filter (polycarbonate membrane) plate (in triplicate) without prior preparation or additional processing.

3.2.4 Microscopy

Microscopic images were obtained by using a Zeiss Axiolab (Carl Zeiss AG, Jena, Germany) polarizing optical microscope. Powder samples of the different polymorphic forms were placed onto a glass slide, dispersed in silicone oil, and roofed with a cover slip. Photomicrographs were taken using an AxioCam MRc 5 and AxioVision software (version 4.6).

3.2.5 Preparation of polymorphic mixtures

Binary mixtures of hydrate and anhydrate were prepared by mixing proportions of components from 0% to 100% in steps of 10%. The total amount of drug per well in a 96-well filter plate (MultiScreen®HTS, Merck Millipore Ltd., Carrigtwohill, Ireland) was 10 mg. The powder was subsequently suspended in n-Heptane (100 µl) and stirred for 30 min to evaporate the heptane to achieve homogenous mixing of the 2 polymorphic forms. Subsequently, the 96-well plate was left for 12 h at RT to

evaporate heptane. Residual heptane in the dried powders of random samples was finally determined by using TGA as described in section 3.2.1.1.

3.2.6 XRPD data analysis

Win XPow Kombi/Quant was used for quantitative analysis of X-ray diffractograms. This program analyzes any powder diffraction pattern as a mixture of its possible standard components. It is assumed that at any 2theta the intensity $I(2\Theta)$ of the mixture can be expressed as

$$I(2\theta) = \sum_i x_i S_i(2\theta) \qquad \text{Eq. 3.1}$$

where the x_i is the mass fraction of the standard i present in the mixture and $S_i(2\Theta)$ holds for the observed intensities of the same amount of the pure phase at this 2theta angle. The x_i values are determined by a linear least squares procedure and then rescaled to give a total of 100%.

To account for different scattering volumes, the analyzed samples were normalized with the air/background scattering. Therefore, an air/background reference pattern recorded under identical conditions was used to account for air/background scattering contribution of the samples and quantified as a "component" of the mixture. Subsequently, the ratio of the crystalline polymorph phase was normalized by the "content" of the air/background "component".

3.2.7 Kinetics of drug concentrations and polymorphic transformation

3.2.7.1 Preparation of solutions

The effect of formulations vehicles with polymers and surfactants on the solid state transformation kinetics were compared with biorelevant media. To keep the systems as simple as possible only excipient solutions with one excipient were used instead of excipient mixtures. Thus, pure water and biorelevant phosphate buffer (pH 6.5) were

selected as reference media. All solutions were adjusted to a pH of 6.5 before incubation to minimize the differences between the media. For each group of excipients, two examples were selected, one charged (NaCMC, SDS) and one neutral additive (HPMC, polysorbate 80).

Phosphate buffer, pH 6.5 (hereafter named blank-buffer) was prepared by dissolving sodium hydroxide (0.42 g/l), sodium phosphate monobasic anhydrous (3.44 g/l), and sodium chloride (6.19 g/l) in deionized water followed by adjusting the pH to 6.5 (25°C). A standard medium composition was used to mimic intestinal fluid:[101] Fasted state simulated intestinal fluid (FaSSIF) was prepared using SIF® instant powder according to the manufacturer's preparation protocol[102] for FaSSIF solution.

Excipient solutions were prepared by dissolving HPMC, NaCMC, SDS or polysorbate 80 at 0.5 % (w/w) in deionized water and adjusting the pH to 6.5 with hydrochloric acid or sodium hydroxide at 25°C.

3.2.7.2 Kinetic concentration and residual solid analysis

Kinetic concentrations of piroxicam were determined in different excipient solutions by using a slightly modified SORESOS (SOlubility and REsidual SOlid Screening) assay.[56] PRXAH (ca. 7 mg), TESAH (ca. 6 mg) and CAFAH (ca. 15 mg) was dispensed in a 96-well flat bottom plate (Corning Inc., Durham, New York, USA) using the so-called powder-picking-method.[103] After adding stir bars and 150 µl excipient vehicle, the plate was sealed with pre-slit silicon caps. The mixtures were agitated by head-over-head rotation for 10, 20, 30, 45, 60, 90, 120, 180, 240, 300, 360 and 1440 min at room temperature. The suspensions were transferred into 96-well filter plates (MultiScreen®HTS) and liquid was separated from residual solid by centrifugation. Filtrates of piroxicam and testosterone were diluted with N-methyl-2-pyrrolidone and filtrates of caffeine with ethanol. Drug concentrations were determined using a Waters Acquity Ultra Performance Liquid Chromatographic (UPLC) system equipped with a 2996 Photodiode Array Detector and an Acquity UPLC BEH C18 column (2.1x50 mm, 1.7 µm particle size) from Waters (Milford, Massachusetts, USA). An isocratic flow was applied for 0.3 min at a flow rate of 0.75

ml/min. Subsequently, the concentration of solvent B was linearly increased to 100% within 0.5 min. Table 3.1 lists the composition of the mobile phase during isocratic flow and the wavelength of detection. Solid state analysis of residual solid was performed by XRPD.

Table 3.1: Experimental conditions used for UPLC analysis.

	Gradient (A:B)[a] [%]	Detection wavelength [nm]
Caffeine	95:05	273
Piroxicam	65:35	342
Testosterone	60:40	244

[a]Mobile phase A: deionized water with 0.1% (v/v) triethylamine adjusted to pH 2.2 with methanesulfonic acid Mobile phase B: acetonitrile.

3.3 Results and Discussion

3.3.1 Characterization of raw materials

The X-ray diffractograms of anhydrous polymorphs and hydrates of caffeine and piroxicam are shown in Figure 3.1. The diffractograms agreed well with published data.[97-99] For TESMH, there was no reference pattern available in the literature. Therefore a reference powder pattern was calculated by the program mercury[104] based on a single crystal cif-file from the Cambridge Structural Database (CSD). The obtained diffraction pattern was compared with experimental data and good agreement with the calculated reference was evidenced. Figure 3.1 shows diffractograms of the model compounds and indicates that the hydrates can be well differentiated by both unique peaks and intensities.

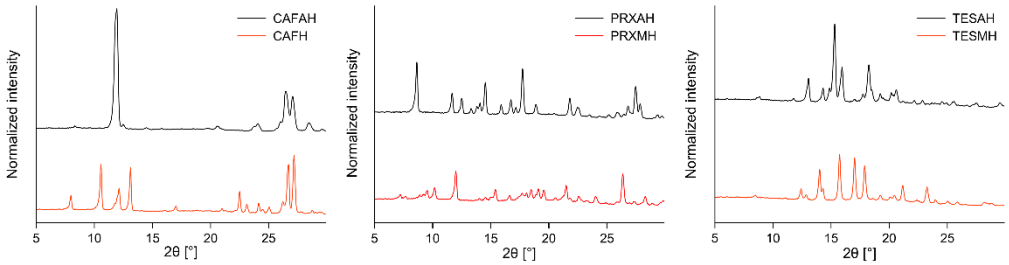

Figure 3.1: X-ray diffractograms of anhydrous polymorphs and hydrates of caffeine (CAFAH/CAFH), piroxicam (PRXAH/PRXMH), and testosterone (TESAH/TESMH).

Results of TGA measurements of anhydrous and hydrated raw materials are listed in Table 3.2. The stoichiometry that was inferred from thermal analysis agreed well with those reported in the literature.[98, 100, 105] Thus, piroxicam and testosterone were shown to form the expected 1:1 molecular monohydrates, whereas caffeine hydrate was different due to the specific channel structure and has therefore been previously described as a 4/5 hydrate.[105]

Table 3.2: Thermoanalytical results.

	$\frac{n_{heptane}}{n_{drug}}$ [a]	$\frac{n_{water}}{n_{drug}}$ [b]
Caffeine anhydrous	0.00	
Caffeine hydrate		0.80
Piroxicam anhydrous	0.00	
Piroxicam hydrate		0.98
Testosterone anhydrous	0.07	
Testosterone hydrate		0.95

[a] $n_{heptane}/n_{drug}$ is the molar ratio of heptane and drug after supending in heptane and drying of the samples, [b] n_{water}/n_{drug} is the molar ratio of water and drug in hydrate forms

According to the thermal analysis, there was no residual heptane in caffeine and piroxicam (Table 3.2). Only in TESAH a small amount of residual heptane (heptane: drug molar ratio 0.07) could be detected; however, this does not seem to affect XRPD

analysis since no difference was detected between the diffractograms of TESAH and TESAH suspended in heptane (data not shown).

3.3.2 XRPD calibration

XRPD patterns from binary mixtures were analyzed with Win XPow Kombi/Quant by considering the pure anhydrous, pure hydrated drug, and additionally the background as standard components. Validation of mixtures was carried out in the 5-35° 2Θ range. Calculated compositions of the different binary mixtures were plotted against weight fractions (not shown). For all compounds this resulted in linear correlation; however the respective correlation coefficients differed (R^2 (CAF) = 0.9375, R^2 (PRX) = 0.9734, R^2 (TES) = 0.9284).

Likely sources of variation are differences in scattering intensities or particle sizes and shapes; the latter is known to cause errors in quantitative analysis using XRPD.[33] Thus, the lower correlation coefficient for caffeine mixtures might be caused by the caffeine hydrate that has long, needle-like crystals[13] as shown in Figure 3.2b.

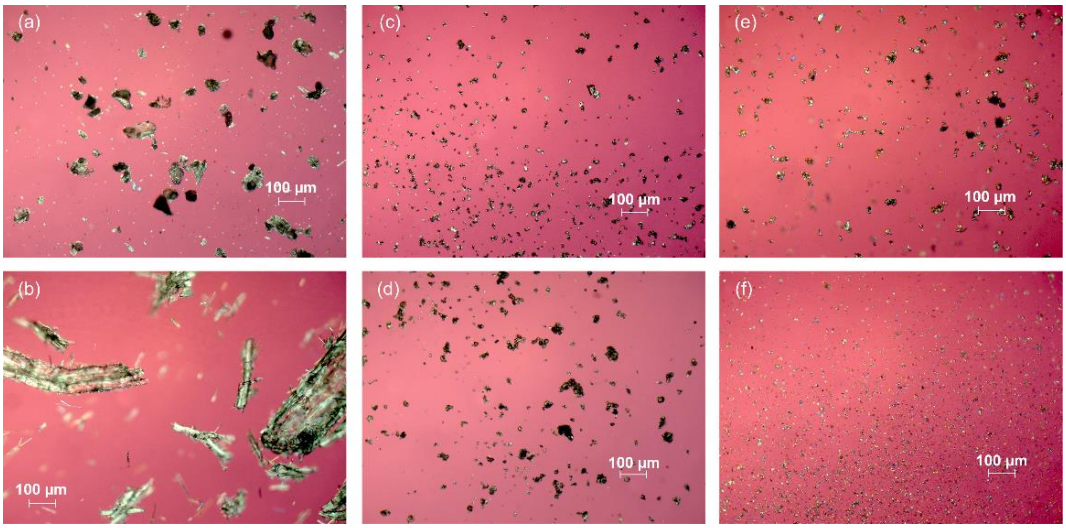

Figure 3.2: Microscopic images of crystals of CAFAH (a), CAFH (b), PRXAH (c), PRXMH (d), TESAH (e), and TESMH (f).

Given the miniaturized nature of the MixRay, the obtained regression models were considered in all cases as sufficiently good. It was beyond the scope of this study to further optimize the HT-method and to determine parameters such as the limit of quantification or detection; further method optimization and validation would then be part of later stage development. The intended use of the miniaturized calibration is the early screening phase in combination with other assays such as SORESOS [56]. Here many different compounds are tested with various excipients and it is primarily important to gather much information on a short time scale. For a faster and less work-intensive preparation process compared to the method described in section 3.2.5, the polymorphic mixtures were prepared by mixing different volumes of suspensions of pure PRXAH and PRXMH in heptane (100 mg/ml), followed by heptane evaporation. Calibration measurements resulted here also in a linear regression (data not shown).

3.3.3 Piroxicam in excipient-solutions and biorelevant medium

3.3.3.1 Kinetic concentrations and qualitative analysis of residual solids - Screening test

The kinetic SORESOS assay[56] was used to determine kinetic concentrations of PRXAH in four different excipient-vehicles, FaSSIF, blank-buffer pH 6.5, and pure water as a reference. In parallel, solid state properties of the residual solid was qualitatively analyzed with XRPD. The time-dependent concentration curves of PRXAH and the corresponding composition of solids are shown in Figure 3.3.

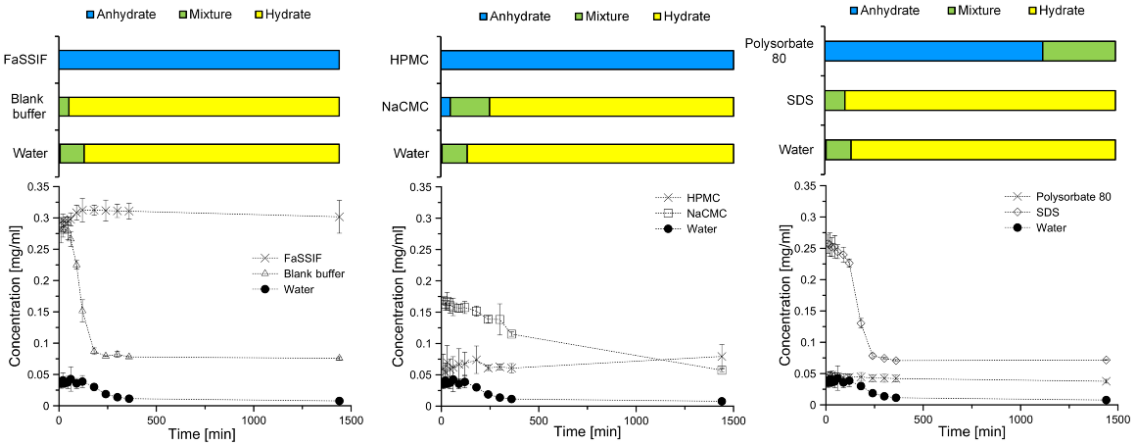

Figure 3.3: Solid state (bars at the upper section) and concentrations (curves in the lower section) of piroxicam in excipients-vehicles (0.5%, pH 6.5) and water. Time points of solid state and concentrations are the same in the upper and lower part of the figure.

To use the assay as a "quick test", i.e., for qualitative determination of occurrence and classification of the kinetics of drug phase transformations (fast vs slow), we only distinguished between the different polymorphic forms or mixtures thereof. As expected, the initial drug concentration decreased in the media where PRXMH was formed because the PRXMH solubility is lower compared to PRXAH.[56, 90] The appearance/disappearance of hydrate/anhydrate (Figure 3.3) can here only be roughly related to the measured kinetic drug concentrations in the bulk phase of the different excipient media. However, these "screening test" results can be analyzed further to gain more in depth kinetic knowledge as described in section 3.3.3.2.

3.3.3.2 Kinetic concentrations and quantitative analysis of residual solids - MixRay assay

For a more detailed analysis of polymorphic transformations, the established MixRay calibration curve for piroxicam was used to quantitate anhydrate to hydrate conversion in the residual solids. In a previous paper, similar excipient effects were observed,[90] but solid state was determined only after 24 h at the end of the solubility experiments, which makes a profound difference to the present work. It is from a

biopharmaceutical perspective relevant to learn about more detailed kinetic changes as they are likely to impact *in vivo* drug absorption.

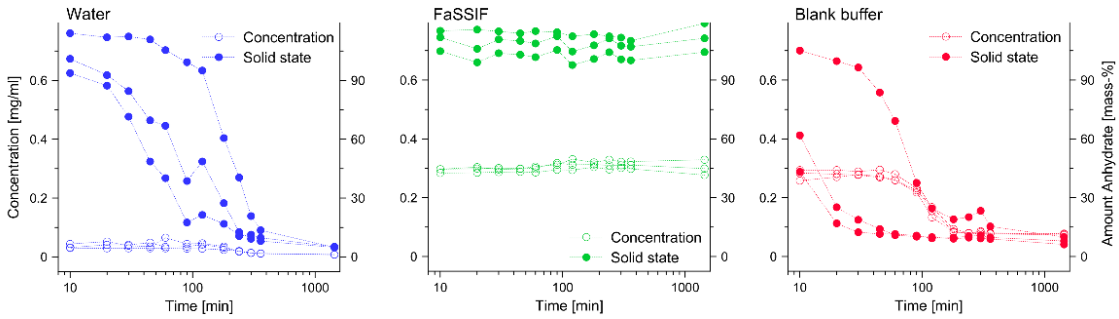

Figure 3.4: Concentrations (empty circles) and solid state (filled circles) of piroxicam in (a) water, (b) FaSSIF, and (c) blank-buffer.

In water, solid state transformation to PRXMH started instantaneously once PRXAH was added PRXAH could be detected up 200 min and conversion to PRXMH was completed after 6 h. Among the vehicles tested, PRX-solubility was lowest in water after 24 h (Figure 3.4).

In the biorelevant FaSSIF medium, PRXMH formation was completely inhibited (Figure 3.4). In contrast, PRXMH transformation in blank-buffer (FaSSIF without phospholipids and bile salts) was fast and after 10 min already 30% hydrate was formed. Transformation was more rapid than in pure water and completed after only 2 h at RT. The faster transformation of PRXMH in blank-buffer compared to water may be attributed to the ion composition and/or pH of the blank-buffer medium. Bulk drug concentrations correlated well with the solid state analysis. Kinetic drug concentrations in FaSSIF remained high at 0.3 mg/ml over 24 h, whereas the high initial concentration in blank-buffer decreased rapidly when PRXAH was completely transformed into PRXMH. Similar results have been reported for carbamazepine where sodium taurocholate and lecithin were also shown to inhibit hydrate formation;[17] in the latter study the observed increased piroxicam concentration in FaSSIF compared to blank-buffer in the bulk was attributed to drug solubilization in micelles.

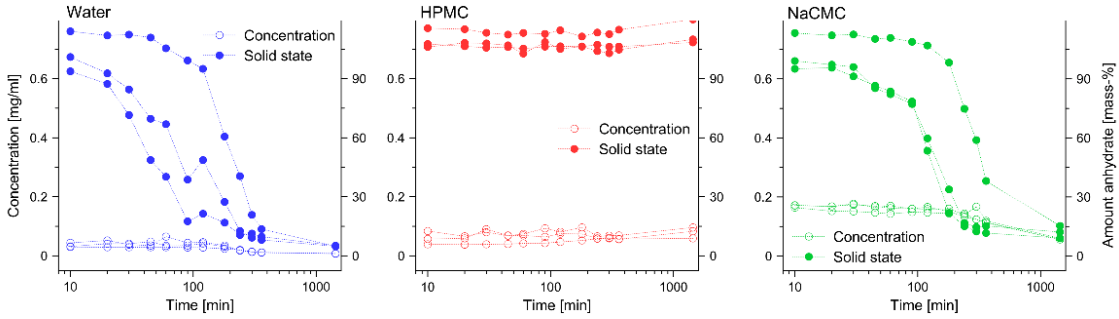

Figure 3.5: Concentrations (empty circles) and solid state (filled circles) of piroxicam in (a) water, (b) HPMC (0.5%), and (c) NaCMC (0.5%).

Polymer-solutions had different effects on piroxicam pseudopolymorphic transformation. HPMC completely inhibited PRXMH formation. In contrast, NaCMC only delayed PRXMH formation compared to water alone (Figure 3.5c). Solid state transformation kinetics in NaCMC can be divided into two phases, an initial slow one where only 10% of the PRXAH was transformed to PRXMH within 1.5 h followed by a fast conversion of remaining PRXAH to PRXMH within the next 3 h. Compared to water, piroxicam kinetic concentrations were slightly increased in HPMC solutions and remained almost constant for 24 h. In contrast, drug concentration rapidly decreased in NaCMC-solution when hydrate was formed and even after 24 h, equilibrium solubility was presumably not yet reached.

The difference between the two tested polymers may be related to different charges. Polymers typically inhibit polymorphic transformations by adsorption onto particles' surfaces.[70] At the test pH of 6.5, HPMC is neutral and NaCMC and piroxicam are negatively charged. Thus, in case of NaCMC, repulsion between piroxicam and NaCMC molecules may have reduced polymer adsorption to the surface of piroxicam particles and hence PRXAH to PRXMH conversion may be more pronounced than with HPMC. Kinetic concentrations of piroxicam in HPMC and NaCMC after 24 h were both higher than in water. This may result from an incomplete transformation to PRXMH or an increase in drug solubility by the polymers.

The two surfactants used, SDS and polysorbate 80, also affected piroxicam hydrate formation differently (Figures 6b and c). SDS slightly accelerated PRXMH formation compared to water (30 min), whereas polysorbate 80 delayed PRXMH formation for up to 20 h. An influence on the kinetic concentrations was not noticed although about 10% hydrate was detected after 24 h. Probably the better soluble species (PRXAH) was dominating bulk concentrations, which might be a more general case as long as a sufficient amount of the more soluble form is present. Moreover, pseudopolymorphic transformation kinetics are strongly influenced by a variety of factors, such as pH differences, contaminations or ionic strength of the media, and it is therefore quite common that repeated results may vary from well to well.[56] These variations between the polymorphic compositions in the single wells seem to not influence the solubility significantly, since in Figures 6a and c, the curves of the solid state transformation vary whereas the solubility curves are almost identical.

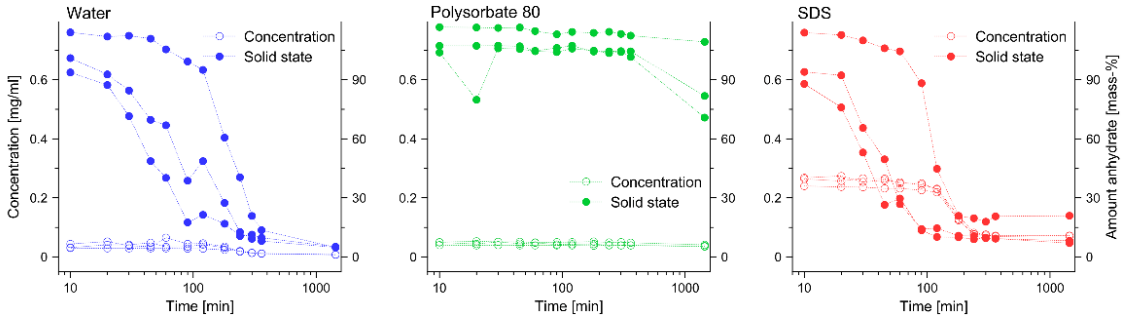

Figure 3.6: Concentrations (empty circles) and solid state (filled circles) of piroxicam in (a) water, (b) polysorbate 80 (0.5%), and (c) SDS (0.5%).

Transformation of piroxicam in polysorbate 80-solution was not completed after 24 h and drug concentration remained almost constant over 24 h (Figure 3.6b). In contrast, piroxicam concentrations in SDS-solution decreased from 0.27 mg/ml to 0.075 mg/ml after hydrate transformation was completed.

Noteworthy is that for all excipient solutions, the pH was rather stable (± 0.5) around the initial value.[90] The only exception was polysorbate 80, where the pH dropped from 6.5 to 4.27 (±0.39).

For those systems where hydrate formation was completely inhibited (like FaSSIF and HPMC-solution) no additional information was obtained from the more detailed quantitative results (MixRay) of solid state transformation. Here the "screening test" without calibration would obviously provide sufficient information on the given pseudopolymorphic transformation.

3.4 Conclusions

This study presents a miniaturized, high throughput X-ray method (MixRay) that was developed for quantification of different polymorphic forms in mixtures. The introduction of the correction of X-ray pattern with measured background pattern allowed the detection of much smaller quantities of polymorphic forms in binary mixtures than in previous studies. [33, 89] The method allows the determination of both solid state transformations and kinetic concentrations in parallel in a single assay. A simplified version of the assay may analyze a phase transformation also without polymorphic quantification, which provides as a kind of “screening test”. Both, the MixRay and the simpler kinetic assay can support pharmaceutical profiling of a clinical candidate and solvent-mediated phase transformations can be studied to screen excipients as part of formulation development. The new promising assay may in the future also be used to study kinetic changes of amorphous compounds or of metastable polymorphs.

Chapter 4

Influence of excipients on solvent-mediated hydrate formation of piroxicam studied by dynamic imaging and fractal analysis

Summary

Hydrate formation of pharmaceutical compounds can affect critical drug properties such as solubility and dissolution. There is early on in development a need for a deeper understanding of how excipients influence mechanistically hydrate formation. The influence of excipients and of biorelevant medium on the kinetics of hydrate formation of piroxicam was studied with the aim to describe the kinetic changes of both the bulk suspension and the drug compact surface. Kinetic experiments were based on a miniaturized method using x-ray diffraction for solid state analysis and ultra-high pressure liquid chromatography for drug concentration determination in bulk solution. Surface changes on drug compacts were monitored by dynamic image analysis of microscopic pictures and subsequent determination of a fractal dimension using box counting. Surface analysis correlated well with bulk monitoring of the piroxicam hydrate formation. Individual excipients exhibited highly specific effects on the kinetics of hydrate formation but at equilibrium, the finally obtained fractal dimensions reached the same value of 1.85. The cluster structure of hydrate particles and therefore the recrystallization process were hardly affected by excipients; in contrast excipients strongly affected the kinetics of hydrate formation which is of pharmaceutical relevance.

Kirchmeyer et al. Influence of excipients on solvent-mediated hydrate formation of piroxicam studied by dynamic imaging and fractal analysis. *Crystal Growth & Design*, **2015**, 15, 5002-5010.

4.1 Introduction

More than a third of pharmaceutical compounds are known to form hydrates.[86] Different types of hydrates exist, ranging from crystal structures with isolated hydrate sites (lattice hydrates) to channel-type structures (channel hydrates) and finally to hydrate forms, where the water is primarily associated with ions (ion associated hydrates).[27] Since the crystal structure of a hydrate can be quite different from its anhydrous form, several important solid state properties of drugs can be affected by hydrate formation such as for example solubility and dissolution rate.[106] Hydrates often have lower solubility than their corresponding anhydrous form. Uncontrolled hydrate formation may result in impaired or erratic oral absorption, which can result in reduced drug absorption.[107] This is a prime concern during pharmaceutical development of novel drug candidates and it is important to identify hydrate formation or any other crystal structure changes (salt formation, polymorphic changes) early on as part of a pharmaceutical solid state screening.

For polymorphic or pseudopolymorphic changes it is important to evaluate the rate of conversion under defined conditions. Comparatively rapid conversion kinetics can lead to solvent-mediated solid phase transformations already during pharmaceutical processing. An example was recently reported by Wikstroem et al. who studied various factors influencing the anhydrate-to-hydrate transformations in aqueous medium[15] with emphasis on the process of high-shear wet granulation.[78] The authors found that external parameters like seeding and agitation conditions influence the hydrate formation. Excipients also had strong effects on hydrate formation and could even prevent their formation during high-shear wet granulation.

Hydrate formation may even be fast enough to occur in the gastrointestinal tract after oral drug administration. For example, Letho et al.[17] studied carbamazepine anhydrate to hydrate conversion in simulated intestinal fluids with Raman spectroscopy in a channel flow cell. They observed that transition kinetics was greatly influenced by medium composition; for example hydrogen bonding between carbamazepine and the bile salt sodium taurocholate inhibited hydrate formation. Other studies focussed on aqueous slurries to identify excipient effects on the kinetics of hydrate formation.[16, 22,

[107, 108] In these studies, no general effect of excipients was found but drug-excipient interactions were rather specific. Excipients may interfere via several mechanisms with hydrate formation. The classical Cardew and Davey model[109] described solvent-mediated phase transformations as a multi-step process and additives may affect the kinetics of anhydrate dissolution and/or subsequent nucleation and growth steps of a hydrate. Due to this complexity, additional data are needed to gain more insight into excipient effects on anhydrate-to-hydrate conversions. This could then be the basis for a more rational excipient selection for the formulation development of hydrate forming drugs.

This work focuses on piroxicam (PRX). PRX has two pK_a values (2.3 (acid), 5.3 (base)) and its different solid state forms have been studied previously.[98, 99, 110] Piroxicam anhydrate (PRXAH) has a substantially different crystal lattice compared to the hydrate. The crystal structure of the anhydrate of PRX is based on the neutral molecule, whereas the piroxicam monohydrate (PRXMH) contains the zwitterionic molecule (Figure 4.1).[111] Interestingly, the anhydrous form is colorless, whereas PRXMH has a bright yellow appearance.[98, 112]

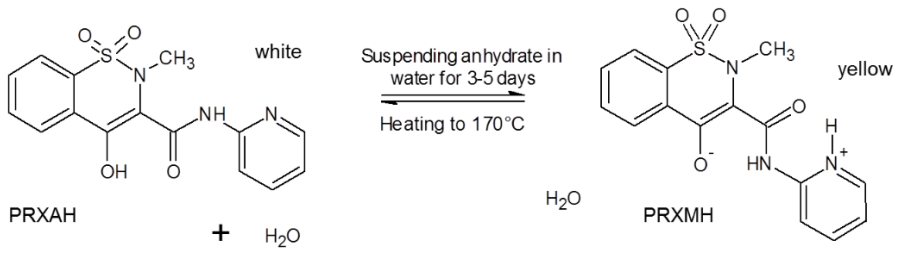

Figure 4.1: Anhydrate-to-hydrate transformation of piroxicam. Adapted from Sheth et al.[98]

A recent paper emphasized particularly the effect of sodium dodecyl sulfate on solvent-mediated phase changes of piroxicam.[22] In this study, 1% SDS (w/w) in a slurry inhibited conversion of PRXAH to PRXMH. However, more data of such excipient effects are needed for practical formulation development and to ultimately gain better mechanistic understanding.

The current work addresses the need for more data by analysing effects of additional excipients and simulated intestinal medium on the kinetics of hydrate formation. Image analysis was used in line with recent advancements in characterizing poorly water-soluble drugs.[49] A particular new idea was to apply fractal analysis to dynamic surface imaging. Concepts of fractal geometry describe the heterogeneous nature of a structure or process. This is different from other models that describe homogenous structures and systems. Such models based on homogeneity assumption have been proposed to describe solvent-mediated phase transformations.[109, 113, 114] It is likely that a consideration of structural heterogeneity and fractal geometry could lead to further insights into the pseudopolymorphic changes. Since the pioneer article by Kopelman in "Science",[115] other applications of fractal geometry have been reported in chemical and pharmaceutical sciences,[116, 117] e.g. a recent study demonstrated fractal-like drug dissolution kinetics in biorelevant media.[118] The present study introduces a fractal analysis of the solid surface to the field of solvent-mediated phase transformations. Fractal dimensions are determined during the PRXAH to PRXMH transition in presence of different additives to better understand the underlying physicochemical process.

4.2 Materials and Methods

4.2.1 Materials

Piroxicam was from Sigma Aldrich (Buchs, Switzerland). Sodium chloride, sodium hydroxide pellets and sodium phosphate monobasic anhydrous were from Fluka Analytical Ltd. (Buchs, Switzerland). SIF® powder was obtained from Biorelevant (Croydon, UK). Hydrochloric acid (1 M) and sodium hydroxide solution (1 M) were from Scharlau (Barcelona, Spain) and paraffin was purchased from Hänseler AG (Herisau, Switzerland).

Hydroxypropylmethylcellulose (HPMC) was obtained from Harke Group (Mülheim a.d. Ruhr, Germany), carboxymethylcellulose sodium salt (NaCMC) from Sigma-

Aldrich (Buchs, Switzerland), Polysorbate 80 (P80) from Croda Europe Ltd. (Cowick Hall, UK), and sodium dodecyl sulfate (SDS) from Stepan Company (Northfield, USA).

4.2.2 Preparation of solutions

Phosphate buffer, pH 6.5 (hereafter named blank-buffer) was prepared by dissolving sodium hydroxide (0.42 g/l), sodium phosphate monobasic anhydrous (3.44 g/l), and sodium chloride (6.19 g/l) in deionized water and adjusting the pH to 6.5 (25°C). A standard medium composition was used to mimic intestinal fluid[101]: Fasted state simulated intestinal fluid (FaSSIF) was prepared using SIF® instant powder according to the manufacturer's preparation protocol[102] FaSSIF solution.

Excipient solutions were prepared by dissolving HPMC, NaCMC, SDS or P80 (0.5 % (w/w)) in deionized water, adjusted to a pH 6.5 by hydrochloric acid or sodium hydroxide, and the final pH was verified again at 25°C.

4.2.3 Preparation of piroxicam monohydrate

For preparation of piroxicam monohydrate (PRXMH), 1 g piroxicam anhydrate was added to 10 ml deionized water and stirred for 72 h at room temperature. After filtration and drying at 25°C, 45% relative humidity, the PRXMH was obtained as previously described in the literature.[98]

4.2.4 Differential scanning calorimetry (DSC)

A differential scanning calorimeter DSC 8500 from Perkin Elmer Ltd. (Schwerzenbach, Switzerland) was used to characterize the thermal properties of the drug and its corresponding hydrate. Samples of PRXAH and PRXMH (average weight: 2 mg) were placed in hermetically sealed aluminum pans (50 µl) and heated at 5°C min^{-1} from 20°C to 220°C under a nitrogen purge (20 ml/min). Melting

temperature and heat of fusion of piroxicam samples were determined from the peak onset and the area under the peak using the Pyris Analysis software (V. 11.0.0.0449) from Perkin Elmer (Schwerzenbach, Switzerland). All measurements were conducted in triplicates.

4.2.5 X-ray powder diffraction (XRPD)

Crystal structures of all materials (hydrate/anhydrous forms) were verified by XRPD using a STOE Stadi P Combi diffractometer with primary Ge-monochromator (CuKα radiation), imagine plate position sensitive detector (IP-PSD), and 96-well plate sample stage. The IP-PSD allowed simultaneous recording of diffraction pattern both sides of the primary beam. The software STOE WinXPOW was used for improving XRPD data quality by merging both 2-theta ranges. Effects related to poor crystal orientation statistics were reduced by summing up diffracted beam intensities both side of primary beam. The imaging plate was exposed for 10 min to X-ray radiation for each well. Samples were analyzed directly in a 96-well filter plate without prior preparation and additional processing and the measurements were conducted in triplicate.

4.2.6 Raman spectroscopy

Raman spectra were recorded with a 785-nm excitation laser in the backscattering mode using a Raman RXN1 analyzer (Kaiser Optical systems Inc., Ann Arbor, USA). The system was equipped with a charge-coupled device (CCD) camera. A laser power of 400 mW was given and background Rayleigh scattering was removed by a holographic filter during acquisition of the spectra. Raman spectra were recorded with a single fiber probe (spot size 0.007 mm^2) of powder samples obtained from slurries as well as powdered raw materials. A single spectrum of the powder was acquired in the backscattering mode using a 30 sec acquisition time. Finally, three scans were averaged to generate a single spectrum. The baseline was corrected and intensities were normalized by setting the maximum peak to unity. Data acquisition, spectral pre-

processing, and the subsequent analysis were based on the iC Raman (V. 3.0) software from Mettler-Toledo AutoChem Inc. (Columbia, USA).

4.2.7 Solubility and residual solid analysis

Kinetic solubility of piroxicam in different excipient solutions was determined by using a slightly modified 96-well solubility assay (SORESOS).[56] PRXAH (ca. 7 mg) was dispensed using the powder-picking-method[103] in a 96-well flat bottom plate (Corning Inc., Durham, USA). After adding stirring bars and excipient vehicles (150 µl) the plate was sealed with pre-slit silicon caps. Filling steps were performed at different time points over a period of 24 h so that the incubation times were variable (10 min, 30 min, 60 min, 120 min, 240 min, 360 min and 1440 min) and a time depending kinetic was obtained. The mixtures were agitated by head-over-head rotation at room temperature. After mixing, the suspension was transferred into 96-well filter plates and liquid was separated from residual solid by centrifugation. Filtrates were collected, diluted with N-methyl-2-pyrrolidone and drug content in filtrates was determined using a Waters Acquity Ultra Performance Liquid Chromatographic (UPLC) system equipped with a 2996 Photodiode Array Detector and an Acquity UPLC BEH C18 column (2.1x50 mm, 1.7 µm particle size) from Waters (Milford, USA). Mobile phase A and B consisted of 0.1% (v/v) triethylamine in deionized water adjusted to pH 2.2 with methanesulfonic acid and acetonitrile. An isocratic flow of 65:35% (v/v) (A:B) was applied for 0.3 min at a flow rate of 0.75 ml/min. Subsequently, the concentration of solvent B was linearly increased from 35% to 100% B within 0.5 min. The wavelength of detection was at 342 nm. Solid state analysis of residual solid was performed by XRPD with an exposure time of 5 min per well. Moreover, the pH of the samples was measured in a slightly larger scale (500 µl) after 24 h using the experimental setup of the other kinetic measurements.

4.2.8 Microscopy

For microscopy studies, samples were prepared with a diameter of 7 mm by compacting 110 mg of PRXAH using a Korsch XP0 tablet press (Korsch AG, Berlin,

Germany). Compact strength was measured and a comparable value targeted to achieve a standardized degree of particle consolidation (data not shown). To assure that no hydrate seeds were present on the compact surface, the samples were dried for 24 h at 100 °C at a reduced pressure (75 mbar) as previously described.[119] The compacts were embedded in paraffin leaving one of the surfaces uncovered.

Compacts were placed in a crystallization dish under the Olympus microscope SZX10 (Olympus Corporation, Tokyo, Japan) and were covered with the medium (30 ml). Images were recorded every 0.5 hour over a period of 24 hours at room temperature. The microscope was equipped with a CCD chip camera UC30 from Olympus (Olympus Corporation, Tokyo, Japan) and a VisiLED ringlight (Lightning and Imaging SCHOTT North America Inc., Southbridge, USA). Picture acquisition was conducted with the Olympus Stream (V. 1.8.5) from Olympus Corporation (Tokyo, Japan).

4.2.9 Data analysis

4.2.9.1 Image and fractal analysis

The acquired images were converted to black-and-white (binary) pictures by using the image processing software GIMP (V. 2.8.10).[120] For each image the contrast was increased and a conversion to grey-scale was performed. For creation of the final binary images a threshold value from 180 was used (where 0 and 255 resulted in an entirely white and black image). The final pictures had a size of 2080 x 1544 pixels.

A standard box-counting method was used for fractal analysis. The pre-processed binary images were used with white pixels as background. All image calculations were based on the integrated fractal analyzing module Fraclac[121] of ImageJ[122], which employed a maximum box size of 45% relative to the whole image size.

For box counting, an image is covered by a series of grids with decreasing caliber. The number (N) of these calibers (boxes) containing any part of the structure is counted for each box size (ε). The principle of box counting is depicted in Figure 4.2.

The obtained counts are related to the caliber with the negative fractal dimension (*D*) as exponent, Equation 4.1.

$$N(\varepsilon) \propto \varepsilon^{-D} \qquad \text{Eq. 4.1}$$

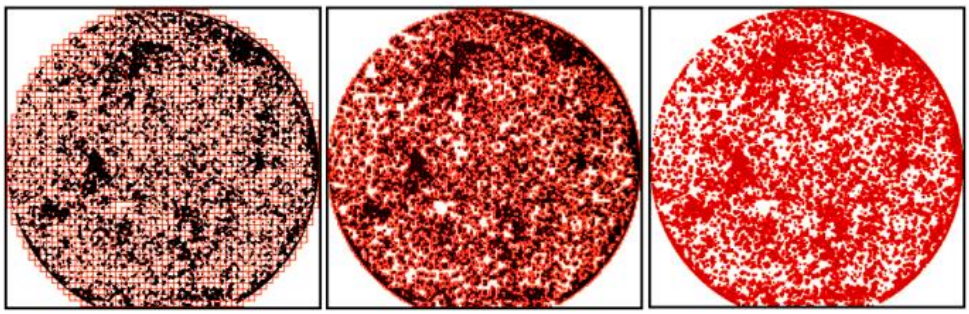

Figure 4.2: Principle of box-counting method: The object is covered by a series of grids with decreasing caliber. For each box size the amount of boxes that cover any part of the structure is counted.

For fractal objects a double-logarithmic plot yields a straight line, and *D* can be determined as the absolute value of the slope:

$$\ln N(\varepsilon) = -D \ln \varepsilon + c \qquad \text{Eq. 4.2}$$

The constant *c* describes the ordinate intercept[123] and a typical plot of double-logarithmic plot of box counting is shown in Figure 4.3. The bias caused by the circular surface of the tablet was taken into account for the fractal analyses.

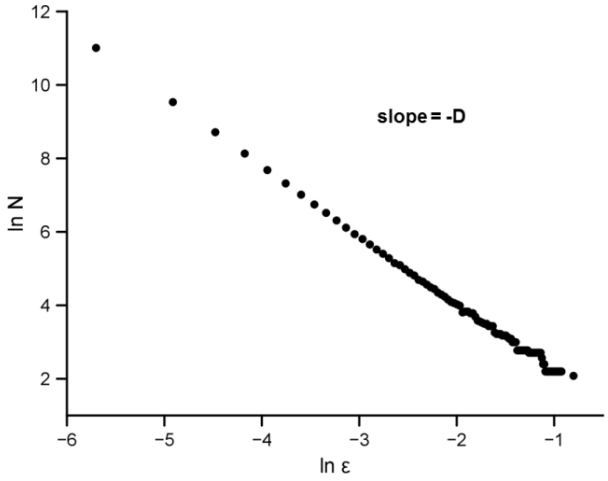

Figure 4.3: Example of a double logarithmic plot of number of boxes (*N*) against box size (ε) for calculating the fractal dimension, *D*.

4.2.9.2 Statistical analysis

The STATGRAPHICS Centurion XVI ed. Professional (V. 16.2.04) software from Statpoint Technologies Inc. (Warrenton, USA) was used for statistical processing. Analysis of variance (ANOVA) was used to estimate the repeatability and reproducibility of the measurement system in terms of the fractal dimension in the plateau. Mean values of fractal dimension (*D*) in the plateau were compared for three different excipients. Included in the ANOVA a F-test was performed to identify any significant differences among the means.

4.3 Results

4.3.1 Initial characterization of piroxicam

According to the thermal analysis, Raman spectroscopy and XRPD results, the purchased PRX was the form I described by Vrečer et al.[99] and by Sheth et al.[110] The same methods were used for characterization of prepared hydrate samples and results agreed well with published data.[22, 77, 98, 119]

4.3.2 Solubility and residual solid analysis of piroxicam in excipient-solutions

The solubility of PRX was determined in four different excipient-vehicles, FaSSIF and blank-buffer pH 6.5 (Table 4.1). As a reference, the solubility of PRX was analyzed in pure water (Milli-Q-water). In addition to the kinetic solubility, residual solid drug was analyzed by XRPD. The diffractograms indicated that after 24 h (at room temperature) PRXAH was not converted in all media to PRXMH. The monohydrate was clearly detected in water, blank-buffer, NaCMC-, and SDS-solutions but not in HPMC-, P80-solutions, and FaSSIF.

Table 4.1: Kinetic solubility of piroxicam (PRX) in different vehicles and identified crystal forms of the residual solids after an incubation time of 24 h as determined by XRPD.

	Solubility [µg/ml][a]	**Residual solids**	**pH after 24 h[a]**
Water (initial measurement as reference)	37.0 (0.0)[b]	PRXAH[c]	5.29 (0.25)[c]
Water	9.3 (1.5)	PRXMH	5.93 (0.73)
Blank-buffer pH 6.5	75.7 (2.5)	PRXMH	6.50 (0.01)
FaSSIF	307.3 (18.3)	PRXAH	6.39 (0.02)
0.5 % NaCMC in water (w/w)	37.3 (2.5)	PRXMH	6.19 (0.05)
0.5 % HPMC in water (w/w)	73.7 (2.1)	PRXAH	5.72 (0.06)
0.5 % SDS in water (w/w)	70.3 (3.2)	PRXMH	5.92 (0.18)
0.5 % P80 in water (w/w)	66.7 (1.2)	PRXAH	4.27 (0.39)

[a] All measurements were performed at 25±3°C (24 h except for the reference in water), expressed as mean (standard deviation), n=3.
[b] Kinetic (non-equilibrium) solubility after 30 min.
[c] Incubation time was 30 min instead of 24 h and the solid state of PRX was verfied with XRPD.

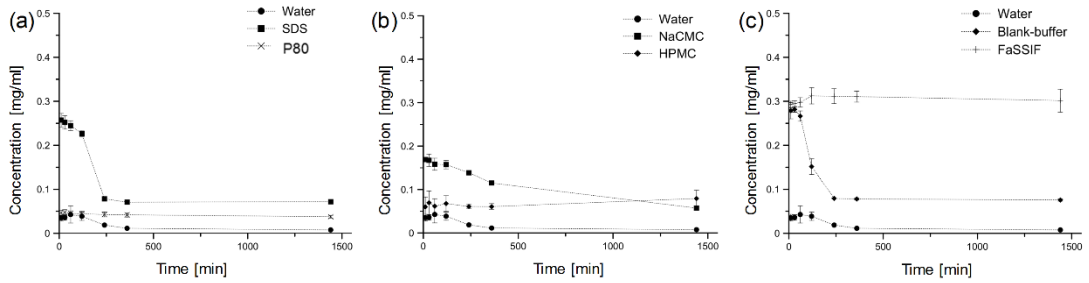

Figure 4.4: Kinetic solubility of PRX in (a) water, 0.5% SDS- and P80-solution, (b) water, 0.5% NaCMC- and HPMC-solution, (c) water, blank-buffer and FaSSIF over 24 h.

The kinetic solubility results of piroxicam are shown in Figure 4.4. During the first hour almost no difference in solubility was observed between water and P80 (Figure 4.4a). Afterwards, concentration decreased in water but not in P80. SDS substantially increased the initial drug concentration; however concentration dropped after 4 h. The final concentration in SDS-solution was still markedly higher than in P80-solution or water.

In NaCMC-solutions, PRX concentrations decreased continuously over 24 h. In the presence of HPMC, drug concentrations remained nearly constant over 24 h, being higher than in water. High drug concentrations were initially observed in both FaSSIF and its blank-buffer. However, in blank-buffer concentration dropped rapidly within the first 3 h, while it remained high in FaSSIF over 24 h. In all media, where PRXMH was formed, initial concentrations decayed. This decrease in solubility is caused by a lower solubility of PRXMH compared to the anhydrous form.

Kinetic solubility results were further evaluated in terms of a supersaturation ratio (Table 4.2). This data presentation better marks the time course of PRXAH to PRXMH conversion than only showing kinetic concentrations (Figure 4.4). The supersaturation ratio was calculated as apparent value by dividing any drug concentration at a given time by its solubility after 24 h. This period was not for all systems long enough to reach equilibrium (=complete formation of PRXMH). Therefore, the solubility in these systems was determined after 72 h and the last two consecutive time points were checked for absence of relevant differences to verify that equilibrium has been reached.

Table 4.2: Apparent supersaturation ratios of piroxicam (PRX) in different vehicles at various time points.

	Supersaturation[a]					
	10 min	**30 min**	**60 min**	**120 min**	**240 min**	**360 min**
Water	4.61 (1.33)	4.70 (1.17)	5.57 (2.96)	5.04 (1.61)	2.43 (0.33)	1.48 (0.19)
Blank-buffer	3.68 (0.37)	3.72 (0.21)	3.52 (0.27)	2.00 (0.30)	1.05 (0.04)	1.03 (0.13)
FaSSIF [b]	3.80 (0.17)	3.83 (0.16)	3.87 (0.21)	4.06 (0.31)	4.05 (0.29)	4.03 (0.24)
0.5 % NaCMC in water (w/w)[b]	4.25 (0.16)	4.21 (0.52)	3.98 (0.50)	3.96 (0.35)	3.49 (0.20)	2.89 (0.13)
0.5 % HPMC in water (w/w) [b]	1.33 (0.67)	1.55 (0.79)	1.37 (0.55)	1.50 (0.59)	1.36 (0.26)	1.35 (0.32)
0.5 % SDS in water (w/w)	3.60 (0.24)	3.52 (0.24)	3.41 (0.18)	3.16 (0.12)	1.09 (0.05)	0.99 (0.03)
0.5 % P80 in water (w/w) [b]	3.56 (0.97)	3.64 (1.05)	3.49 (0.96)	3.38 (0.95)	3.28 (0.93)	3.23 (0.90)

[a]Ratios calculated from the concentration divided by the corresponding 24 h solubility with standard deviations according error propagation (Gauss).

[b]Supersaturation values were calculated by using the solubility of PRXMH in the vehicles after 72 h instead of the solubility after 24 h.

Conversion to the monohydrate within 360 min occurred in water, blank-buffer, and in the excipient solutions of NaCMC and SDS. In all systems, the observed supersaturation values were always below 6. Maximum supersaturation was reached in water after one hour. In blank-buffer and SDS the maximum was achieved earlier, after 30 min and 10 min, respectively. In both systems supersaturation was negligible after 4 h (value close to unity). In NaCMC-solution, drug supersaturation reached its maximum of 4.25 already after 10 min and decreased only gradually to about 3 after 6 h.

4.3.3 Dynamic microscopic imaging and fractal dimensions

Changes of the bulk were measured in suspensions using the described XRPD analysis of the slurries (see Chapter 4.2.5). All experiments in the different media were also investigated in the microscopic studies as a function of time. The experimental details can be inferred from the method description. The yellow colored crystals indicated hydrate formation which is well described in the literature.[8, 12, 13] Moreover, we conducted experiments (DSC, Raman spectroscopy and XRPD) to prove that the appearance of yellow crystals means indeed crystallization of the hydrate. The images of the compacts' surfaces were converted into binary images and the pixels were counted to determine clusters and their extents on the compact surface. In our study yellow color was converted into black, so black pixels were counted for quantification of hydrate formation.

In unbuffered water, PRXAH converted to PRXMH on the surface of the compact (Figure 4.5). Most pronounced changes were detected between 3 h and 17 h, variability between measured samples was high.

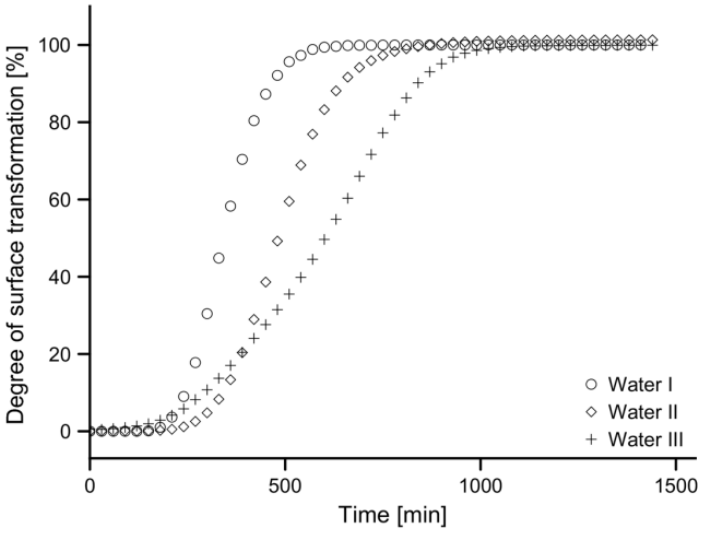

Figure 4.5: Solid state transformation of piroxicam in water monitored by microscopic imaging.

In the presence of the excipients P80 and HPMC complete inhibition of the conversion was observed (Figures 4.6b and 4.6d).This is in line with the XRPD results obtained in bulk suspension experiments (Figure 4.4). NaCMC almost completely inhibited PRXAH transformation to PRXMH and only a small amount of hydrate (1% of the surface) could be detected in the microscopic study (Figure 4.6c). In the presence of the surfactant SDS (0.5% (w/w)), the surface of the samples was almost completely covered with hydrate after 17 h (Figure 4.6a). The kinetics of the conversion to the monohydrate was similar to water but seemed to be delayed and less variable by the additive.

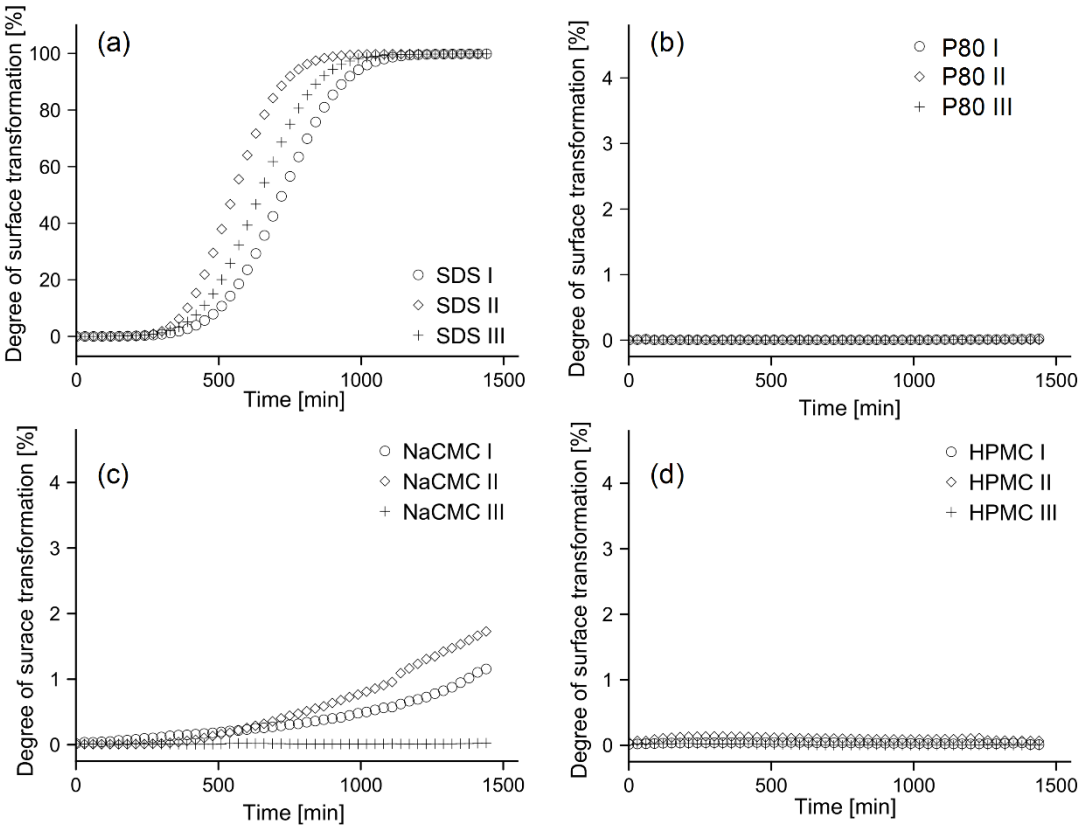

Figure 4.6: Solid state transformation (by microscopic imaging) of piroxicam in (a) SDS-solution 0.5%, (b) P80-solution 0.5%, (c) NaCMC-solution 0.5%, and (d) HPMC-solution 0.5%. All solutions were adjusted to pH 6.5.

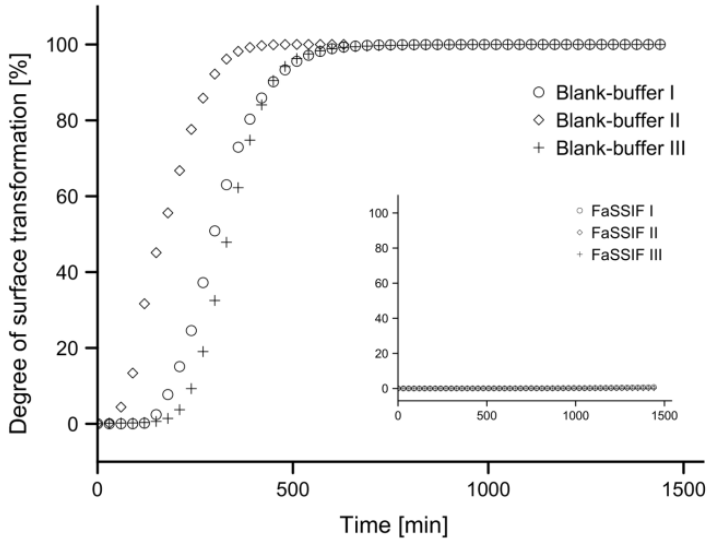

Figure 4.7: Solid state transformation of piroxicam in blank-buffer pH 6.5 and FaSSIF, pH 6.5 (microscopic image analysis).

In blank-buffer pH 6.5, transformation of PRXAH to PRXMH was accelerated compared to water (Figure 4.7). In contrast, FaSSIF did not reveal any transformation to the monohydrate. This result might be attributed to the presence of bile salt and phospholipid in FaSSIF, which is the only difference to blank-buffer. The observed spots of PRXMH on the surface of samples covered with blank-buffer and with water differed (Figure 4.8). In blank-buffer initially only a few spots of PRXMH formed close to the compact's periphery which then grew to cover a wider surface area (Figure 4.8b). In contrast, PRXMH in water initially displayed a higher number of PRXMH nucleation surface spots distributed over the whole surface followed by a growth phase of these dispersed clusters (Figure 4.8a).

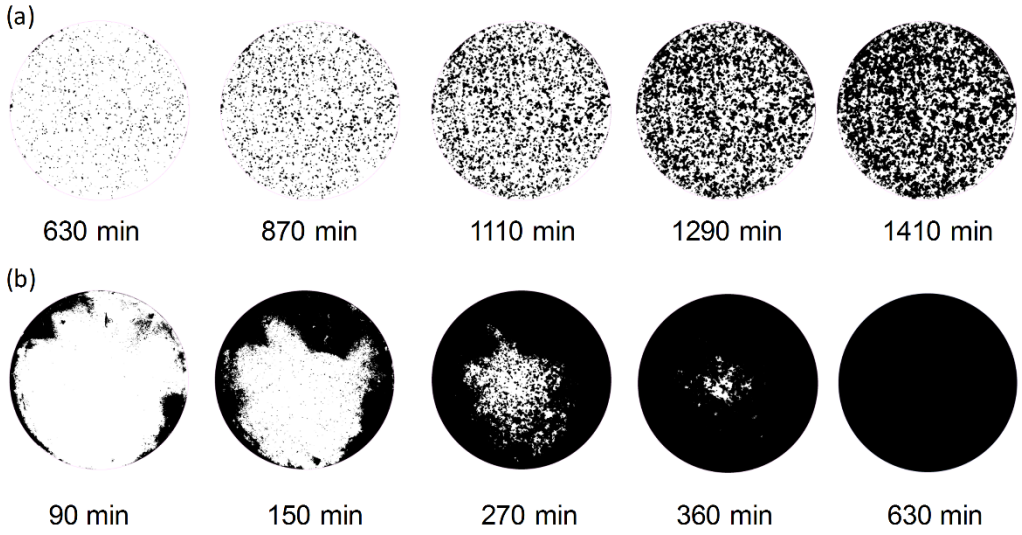

Figure 4.8: Tablet surface in (a) water and (b) blank-buffer at different time points (black: hydrate, white anhydrate).

The analysis from the box-counting method in media in which an almost complete conversion to PRXMH has been reached is shown in Figure 4.9. This data evaluation confirmed the aforementioned kinetic trends. Thus, SDS appeared to delay hydrate formation compared to water, whereas blank-buffer clearly accelerated the process. In water and blank-buffer a considerable variability in conversion was observed at the beginning but results were very reproducible when most of the surface was covered with hydrate. A fractal dimension of less than unity was expected for nucleation and initial formation of clusters. Interestingly, maximal surface coverage in all samples resulted in the same fractal dimension of 1.85.

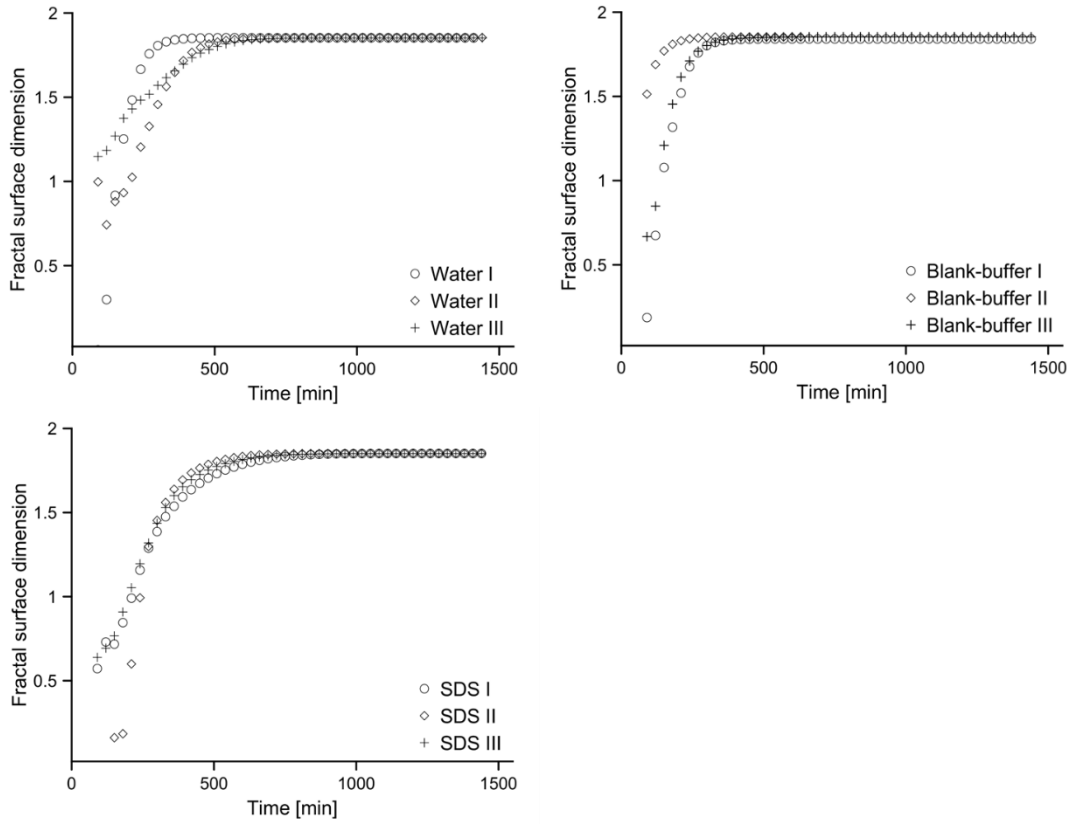

Figure 4.9: Fractal surface dimension of PRXMH obtained by microscopy (box counting method) in water, blank-buffer pH 6.5 and 0.5 % (w/w) SDS-solution.

This fractal dimension was essentially lower than the Euclidean dimension of two because the surface coverage of PRXMH was not complete. Remarkable was that the value appeared to be the same for all samples studied.

Table 4.3: Fractal surface dimension of piroxicam (PRX) in different vehicles after plateau was reached.

Media	**Fractal dimension (*D*) in plateau**
Milli-Q-Water	1.853
	1.854
	1.852
Blank-buffer pH 6.5	1.841
	1.853
	1.854
0.5 % SDS in water (w/w)	1.852
	1.852
	1.851

The ANOVA-analysis confirmed that there was no significant difference between the mean fractal dimensions of media at the 95 % confidence interval.

4.4 Discussion

The effect of excipients on the kinetics of hydrate formation of PRX was studied. A 96-well assay was used to determine both solubility by UPLC and residual solid state changes in suspension by XRPD (SORESOS).[56] Obtained results were compared to surface imaging analysis of API compacts using fractal geometry. These two approaches differ in their experimental set-up for the study of conversion kinetics: in SORESOS, the conversion kinetics of bulk phases is analyzed whereas in dynamic imaging experiments the focus is on the surface analysis of the compacts. The two approaches further differ in stirring conditions and hence in hydrodynamics. Together, both approaches were expected to gain complementary information and to give more insight into anhydrate-to-hydrate transformation of PRX.

Solvent-mediated polymorphic and pseudopolymorphic transformation can be divided in several steps. The classical Cardew and Davey model assumes that an initial dissolution step of the anhydrate is typically followed by heterogeneous nucleation on for example grain boundaries or impurities followed by a growth phase of the nuclei.[109] The authors pointed out that Poisson statistics may be applied for the probability of *r* nuclei per crystal in a monodisperse powder. Based on a random nucleation process and introduction of a growth step, the overall conversion kinetics was mathematically modeled.[109]

For heterogenous nucleation, the classical nucleation theory[53] can be considered in case of anhydrate-to-hydrate transformation:[78]

$$J_1 = A'S\, e^{-\frac{B'v_0^2\gamma^3}{(kT)^3 ln^2 S}} \qquad \text{Eq 4.3}$$

Where J_1 holds for a primary nucleation rate, *A'* is a kinetic factor that is proportional to the number of nucleation-active centers and takes much lower values for heterogeneous compared to homogenous nucleation.[124] *B'* is a factor of shape and

homogeneity, v_0 is the molecular volume of the crystalline phase, and γ is the interfacial energy per unit area of the crystal. Moreover, k holds for the Boltzmann constant, T is the temperature, and S is the drug supersaturation. There are different ways to formulate this classical nucleation rate equation and regarding heterogeneous nucleation, the contact angle of the crystallizing phase on the solid may be considered as part of B'. Heterogeneous nucleation occurs in general on so-called foreign particles like impurities but for anhydrate-to-hydrate transformations, it is primarily the surfaces of the anhydrate that exist in abundance.

For hydrate formation in suspensions, it is possible that depending on the hydrodynamics, a secondary nucleation rate J_2 becomes important.[78] This rate is in theory depending on the density of the crystal suspension and on the agitation rate.[78] It is therefore theoretically expected that different kinetics can occur with the same excipient vehicle when different experimental setups are compared. Considering our experiments, stirred suspensions were studied as well the corresponding monolithic solid samples in liquid. Moreover, the solid concentration and hence the density of the crystal suspensions, differ between the experiments. The bulk analysis employed a solid concentration of about 5% (w/w), whereas for surface analysis the solid concentration was 0.4% (w/w). While the suspension was stirred, the surface analysis was carried out without a stirring device. These different hydrodynamic effects may explain for example the different transformation kinetics of the NaCMC system in both experimental setups (Figures 4.4b and 4.6c).

To go beyond the level of general data interpretations with classical nucleation theory is often difficult because parameters like the kinetic prefactor in Equation 4.3 or interfacial energy of the nuclei are not well experimentally accessible. Moreover, there are various simplifications in the classical nucleation theory. These simplifications have been discussed in several textbook and reviews and the present work focuses on the neglected aspect of fractal geometry. Fini et al. were pioneers to use fractal geometry for studying hydrates of diclofenac sodium.[125, 126] The current study followed a novel approach in the anhydrate-to-hydrate transition by monitoring the changes in fractal dimension of PRXMH clusters. The initial values were below unity indicating that nucleation started from preferred surface points. Such sites could

have been grain boundaries or edges to the sample holder as it was for example observed with the blank-buffer medium (Figure 4.8b). Regardless of this initial nucleation, the fractal dimension reached a final value of 1.85. This fractal dimension was hence lower than the Euclidean embedding two dimensional space. Macroscopically, the surface of the samples appeared to be covered with PRXMH after conversion, however there were still some pixels in the binary images that did not hold for the hydrate. This may either arise from a highly rugged surface due to deposition of PRXMH crystals, while leaving some pixels blank in the projection area. Alternatively, some crystal surface sites may indeed not have been converted to hydrates. It was remarkable that all samples finally reached a value of 1.85 (Table 4.3). This dimension described a resulting PRXMH cluster structure which was likely dominated by the growth process. It is known from phenomena of diffusion-limited aggregation and growth that a fractal dimension of about 1.7 can result in two-dimensional systems or around 1.7-1.8 in three dimensions.[127] For a reaction-limited process in two dimensions, a much lower value of 1.53 was reported.[127] The observed fractal dimension in the current study indicates that drug diffusion to the growing nuclei may have been the limiting step during the growth phase of the PRXMH clusters. It would be interesting to see whether other excipients/drugs also show in solvent-mediated phase transformations a fractal dimension close to the value reported for the reaction-limited process. The nature of the fractal dimension was hence of interest to better understand the mechanisms of hydrate crystallization.

A central emphasis of this work was to study the influence of excipients on conversion kinetics to PRXMH. The excipients' concentration of 0.5% (w/w) was arbitrarily selected and holds for a comparatively high additive concentration regarding the dispersion of typical oral dosage forms in gastrointestinal fluids. Without excipients, unbuffered water displayed rather variable transformation rates, which can be due to differences in pH, impurities, or ionic strength. The presence of excipients generally reduced variability and greatly influenced the conversion kinetics. In HPMC- and P80-solutions, the formation of PRXMH was completely inhibited (Figures 4.4a and 4.6b/d). Antinucleant influences of HPMC on aqueous formulation of piroxicam as well as an inhibition of the pseudopolymorphic transformation were also shown by Pellett et al.[128] in a former study. HPMC was also

found in another study to hinder the nucleation and the growth of carbamazepine hydrate.[16] This is probably caused by HPMC adsorption onto the surface of particles. These findings are in good agreement with our results where HPMC inhibited the solid state transformation in both assays. Chen et al.[129] found that P80 exhibited opposing effects depending on the concentration used. Below the CMC (<0.5 mg/ml), P80 reduced the surface tension, increased nucleation, and caused the transformation to a less soluble polymorphic form. Above the CMC the authors reported that P80 hindered the polymorphic transformation and suggested increased viscosity and adsorption onto the surface of the particles as possible mechanisms. In the present study, P80 concentration was also above the CMC and the inhibitory effect on PRXMH formation observed in our experiments are in line with their results.

In our studies, solid state transformation of PRXAH to PRXMH differed only slightly between SDS and water. In water, on average, the nucleation started 2 h earlier than in presence of SDS. Paaver et al.[22] monitored the solid state transformation of PRX in aqueous slurries using Raman spectrosopy in combination with a partial least square (PLS) regression model. They also found that SDS delayed the onset of the solid state transformation of PRX and claimed that this is caused by an inhibition of nucleation.[22] In contrast, another study reported that SDS promoted the crystallization of carbamazepine dihydrate during dissolution due to a facilitation of surface-mediated nucleation.[85]

The polymer NaCMC inhibited solid state transformation of PRX less than HPMC. A potential reason could be that NaCMC hinders nucleation less than HPMC. Polymers have a general tendency to adsorb onto particle surfaces.[70] They can thus mask preferred sites on the solid surface for nucleation such as grain boundaries of PRXAH. Moreover, adsorbed polymer layer would change the interfacial boundary layer between the crystal and the solution. This can generally hinder diffusion processes that were previously discussed to be rate limiting for the solvent-mediated phase transformation.[70, 112] In contrast to HPMC, NaCMC is negatively charged at pH 6.5 and also over 98% of the PRX molecules are expected to be negatively charged at this pH.[130] This may result in a repulsion between the two molecules, less polymer onto the solid surface, and hence less kinetic inhibition compared to HPMC.

In blank-buffer the solid state transformation was faster than in water and after 10 h compact surface was completely covered with hydrate crystals. Differences in ion composition and/or the pH of the medium could be potential reasons. Interestingly, FaSSIF medium that contained additionally sodium taurocholate and lecithin, showed a complete inhibition of the monohydrate transformation over 24 h. The biorelevant surface active components were evidently dominating the kinetics. Lehto et al.[17] also found for the solvent-mediated conversation of carbamazepine anhydrate to dihydrate an inhibitory effect of FaSSIF on the amount of dihydrate formed. They tested FaSSIF in comparison to a simple buffer solution and found that hydrate formation of carbamazepine was slowed down caused by interaction between carbamazepine and sodium taurocholate. The authors explained their findings by a crystal growth inhibition of carbamazepine dihydrate. In addition, Lehto et al.[17] also emphasized that high carbamazepine solubilization in the micelles of the medium may have contributed to the reduced conversion. Solubilization of PRX in micelles alone may not explain the observed inhibition of PRXMH conversion in our study. The solubility not only in FaSSIF, blank-buffer, and SDS was initially about ten times higher than in in water, however hydrate formation and concomitant decrease in solubility was only observed in blank-buffer and SDS but not in FaSSIF.

The influence of excipients on the solid state transformation generally showed similar trends in both microscopic studies and the 96-well assay. This was remarkable considering the huge differences in hydrodynamics (unstirred vs. stirred) and the differences in the presentation of samples (compact vs. slurry). These differences affected the magnitude of individual excipient effects but general trends for an excipient ranking were similarly reflected by both experimental set-ups. The parallel assay had certainly has the advantage of a higher experimental throughput and drug solubility can be determined in the different media. Such solubility data enable calculation of apparent drug supersaturation as a function of time and thus allow direct monitoring of the driving forces of hydrate crystallization.

4.5 Conclusions

In this study two different approaches were used to determine the solid state transformation of piroxicam. In the miniaturized assay, bulk suspensions were studied and in dynamic imaging the surface of compacts was analyzed. The latter combined with fractal analysis was of high interest from a mechanistic viewpoint. It was possible to monitor the fractal dimension of crystallized PRXMH in different media. A final value of 1.85 was found in all samples and was interpreted as an indicator of the cluster growth phase. Accordingly, drug diffusion to the clusters of PRXMH on the surface and cluster-cluster growth were assumed to dominate the kinetics of the solvent-mediated phase transformation. The fractal dimension appeared to be unaffected by the presence of excipients and it could be universal, which needs to be confirmed with other drugs. The parallel tests based on SORESOS provided similar excipient trends for the anhydrate-to-hydrate conversion of PRX. There were no general polymer or surfactant trends and each excipient appeared to have specific effects on the kinetics of PRXMH formation. All excipients increased the different aqueous concentrations of PRX compared to pure water but in case of SDS, NaCMC, and blank-buffer bulk concentrations then decreased due to the formation of PRXMH.

Knowledge of excipient effects on solvent-mediated phase transformations are of critical importance in pharmaceutical development. It can be applied to liquid dosage forms such as for example suspensions that are often used in preclinical formulations for animal studies. Other applications are development processes that use aqueous solvents for manufacturing of solid dosage forms such as for example wet granulation. Finally, this knowledge can be of considerable relevance for formulated anhydrous drug if they rapidly convert to hydrates in the gastro-intestinal tract after oral administration and hence may have lower or more variable oral bioavailability.

Chapter 5

The quest for exceptional drug solubilization in diluted surfactant solutions and consideration of residual solid state

Summary

Solubility screening in different surfactant solutions is an important part of pharmaceutical profiling. A particular interest is in low surfactant concentrations that mimic the dilution of an oral dosage form. Despite of intensive previous research on solubilization in micelles, there is only limited data available at low surfactant concentrations and generally missing is a physical state analysis of the residual solid. The present work therefore studied 13 model drugs in six different oral surfactant solutions (0.5%, w/w) by concomitant x-ray diffraction (XRPD) analysis to consider effects on solvent-mediated phase transformations. A particular aspect was potential occurrence of exceptionally high drug solubilization. As a result, general solubilization correlations were observed especially between surfactants that share chemical similarity. Exceptional solubility enhancement of several hundred-fold was evidenced in case of sodium dodecyl sulfate solutions with dipyridamole and progesterone. Furthermore, carbamazepine and testosterone showed surfactant-type dependent hydrate formation. The present results are of practical relevance for an optimization of surfactant screenings in preformulation and early development and provide a basis for mechanistic modeling of surfactant effects on solubilization and solid state modifications.

Saal et al. The quest for exceptional drug solubilization in diluted surfactant solutions and consideration of residual solid state. Submitted to *European Journal of Pharmaceutical Sciences*.

5.1 Introduction

A central task of pharmaceutical profiling is to screen solubility of drug candidates in various solvents and excipient solutions that should include different surfactants. These surfactant solutions are typically used for preclinical formulations or they may serve as intermediate bulk solutions for preparation of a final dosage form that should enable oral delivery of poorly soluble compound.[6, 131] While most of these colloidal test solutions contain several percent of surfactant, it is further of interest to extend the solubility screening to diluted surfactant solutions. Such rather low surfactant concentrations of about one percent and less are for example relevant with respect to concentrations in the gastro-intestinal (GI) tract. A recent review article discussed the various effects of surfactants in oral formulations from a biopharmaceutical perspective.[132] Key is here to which extent surfactants can solubilize drugs at rather low surfactant concentration. Although the science of drug solubilization in micelles has a long tradition,[133, 134] it is currently not possible to reliably predict solubilization of new compounds. There are trends known for given surfactant types, for example that an increase of polysorbate alkyl chain from C12 to C18 provided increasing solubilization capacity for barbiturates.[135] Similar effects of varying hydrophobic chain length were also observed with another surfactant series of polyoxyethylene stearates.[136] As for the solubilized compound, there were further trends observed for example that the partition coefficient of steroid hormones into polyoxyethylene lauryl ether micelles was correlated with the partition coefficient between an aqueous solution and octanol (log*P*).[137] There are certainly more studies in the literature that report solubilization trends of a specific drugs with a specific classes of surfactants, which leaves the practical question unanswered if such findings can be generalized.

It has also been tried to quantitatively predict surfactant solubilization based on measured predictors such as the surface pressure at the critical micelle concentration (CMC) and a reference value of surface tension reduction.[138] However, this interesting approach is still limited by a focus on aromatic hydrocarbons and there are experimental input data required. More recently there have been thermodynamic modeling approaches reported in the literature, which appears to be very

promising,[139, 140] but there is still a long way to go before such *in silico* methods are implemented in the practice of drug profiling.

A first step towards any future theoretical approach is to have sufficient experimental data for model validation. However, reliable and comparable solubilization data of drugs are hard to obtain at low surfactant concentrations. It is further desirable to check the residual solid in solubility experiments [56] to account for potential solid phase changes. In general, data of solid state analysis are not available in solubilization studies of surfactants systems. However, this can be a relevant experimental point since a recent study demonstrated that kinetics of a pseudopolymorphic transition (i.e. hydrate formation of piroxicam) was influenced by the presence of 0.5% (w/w) sodium dodecyl sulfate (SDS) or polysorbate 80 (P80), respectively.[141]

The outlined need for solubilization data of diluted surfactant solutions in conjunction with characterization of the residual solid state provided the aim of the current research. A particular objective was to find correlations between different surfactants used and to look for outliers with exceptional drug solubilization. Finally, some guidance for pharmaceutical profiling should be given based on the obtained findings.

5.2 Materials and Methods

5.2.1 Materials

In total, 13 compounds were chosen as model compounds for studying the solubility and solid state changes in surfactant solutions at low concentrations. Acetylsalicylic acid (ASP), carbamazepine (CBZ), diflunisal (DFL), dipyridamole (DPL), estradiol (ESL), flurbiprofen (FLU), haloperidol (HPL), naproxen (NPX), pindolol (PDL), progesterone (PGN), dioctyl sulfosuccinate (DOSS) and cremophor EL (CEL, synonymous name is Kolliphor EL) were obtained from Sigma Aldrich (St. Louis, USA). Furosemide (FRS) was purchased from Molekula GmbH (München, Germany), while ibuprofen (IBU) was from Satwik Drugs Ltd. (Bidar, India).

Testosterone (TES) was from TCI Europe N.V. (Zwijndrecht, Belgium), hydrochloric acid (0.1 M), and sodium hydroxide solution (0.1 M) were supplied by Merck KGaA (Darmstadt, Germany). Polysorbate 80 (P80) was from Croda Europe Ltd. (Cowick, United Kingdom), while sodium dodecyl sulfate (SDS) was from Stepan Company (Northfield, USA), solutol (SOLU, synonymous name is Kolliphor HS 15) was from BASF SE (Ludwigshafen, Germany) and sucrose monolaurate (SUCM) was obtained from Selectchemie AG (Zürich, Switzerland).

5.2.2 Sample preparation

Surfactant solutions were prepared by dissolving P80, solutol, cremophor EL, sucrose monolaurate, SDS, and DOSS (0.5% (w/w)) in deionized water and adjusting the pH of the solutions to pH 6.0 with hydrochloric acid or sodium hydroxide solution at 25°C. All solutions were visually inspected for absence of residual particles.

5.2.3 Solubility and residual solid analysis

Solubility of compounds in surfactant solutions was determined using a slightly modified 96-well SORESOS assay, which measures both equilibrium solubility and solid form of the residual solid.[56] In brief, APIs were dispensed using the powder-picking-method by Alsenz [103] in 96-well flat bottom plates (Corning Inc., Durham, USA), stirring bars and excipient vehicles (150 µL) were added. The plate was sealed with pre-slit silicon caps and the mixtures were agitated by head-over-head rotation for 24 h at room temperature. After equilibration, the suspensions were carefully transferred into 96-well filter plates and liquid was separated from residual solid by centrifugation. Collected filtrates were diluted with N-methyl-2-pyrrolidone and drug content was determined using a Waters Acquity Ultra Performance Liquid Chromatographic (UPLC) system equipped with a 2996 Photodiode Array Detector and an Acquity UPLC BEH C18 column (2.1x50 mm, 1.7 µm particle size) from Waters (Milford, USA). Table 5.1 summarizes the experimental conditions (solvents, composition of mobile phase, detection wave length) used for the drugs. An isocratic

flow of a mixture of solvent A and solvent B was applied for 0.3 min at a flow rate of 0.75 ml/min. Subsequently, the concentration of solvent B was linearly increased to 100% within 0.5 min. Solid state analysis of residual solid was performed by X-ray powder diffraction (XRPD) as described before.[56, 90] Samples were analyzed directly in the 96-well filter plate with an exposure time of 5 min per well.

Table 5.1: Experimental conditions used for UPLC analysis.

Compound	Composition (A:B)[a] [%]	Detection wavelength [nm]
Acetylsalicylic acid (ASP)	80:20	276
Carbamazepine (CBZ)	70:30	285
Diflunisal (DFL)	50:50	314
Dipyridamole (DPL)	81:20	284
Estradiol (ESL)	60:40	280
Flurbiprofen (FLU)	50:50	255
Furosemide (FRS)	75:25	274
Haloperidol (HPL)	70:30	244
Ibuprofen (IBU)	50:50	232
Naproxen (NPX)	55:45	272
Pindolol (PDL)	90:10	264
Progesterone (PGN)	40:60	243
Testosterone (TES)	60:40	244

[a]Mobile phase A: deionized water with 0.1% (v/v) triethylamine adjusted to pH 2.2 with methanesulfonic acid, mobile phase B: acetonitrile.

5.2.4 Correlation and regression analysis

The program STATGRAPHICS Centurion XVI ed. Professional (V. 16.1.15) from Statpoint Technologies Inc. (Warrenton, USA) was used for statistical correlation as well as regression analysis.

5.3 Results and discussion

5.3.1 Drug solubilization screening at low surfactant concentration and analysis of residual solid

In preformulation, solubility screening in surfactant solutions typically includes several percent of surfactant in order to use it directly as a potential vehicle in preclinical formulation or as an intermediate drug product solution. In this work, a concentration of 0.5% (w/w) surfactant at pH 6.0 was used which may represent the surfactant concentration of a dissolved orally administered dosage form in the GI tract. A constant mass concentration was selected as it represents a diluted formulation. However, this practical approach comes with slightly varying molar concentrations. The chosen mass concentration was generally higher than the critical micelle concentrations (CMC) of the different surfactants that were reported in the literature.[142-147] The extent of drug solubilization will certainly depend on their physicochemical properties (Table 5.2) as well as on physicochemical properties of the surfactants (Table 5.3). The 13 compounds comprised acids, bases as well as neutral compounds at the given reference pH.

Table 5.2: Molecular weight (Mw), ionization constant (pK_a) and distribution coefficient (log$D$) at pH 6.0 for the different model compounds.

Compound	Mw [g/mol]	pK_a[a]	Log$D$[b] (pH 6.0)
ASP	180.2	3.7 (a)*	-1.3
CBZ	236.3	-	2.8
DFL	250.2	2.7 (a)*	0.8
DPL	504.6	6.2 (b)	1.8
ESL	272.4	-	3.7
FLU	244.3	4.2 (a)*	2.4
FRS	330.7	3.5 (a)	0.0
HPL	375.9	8.4 (b)*	1.6
IBU	206.3	4.4 (a)*	2.7
NPX	230.3	4.4 (a)*	1.2
PDL	248.3	9.2 (b)*	-1.4
PGN	314.5	-	4.1
TES	288.4	-	3.4

[a]Measured pK_a-values via photometric titration.
[b]Values calculated by the Marvin program suite (V. 16.5.30) (ChemAxon Ltd., Cambridge, USA).
*Calculates pK_a-values by the MoKa-software (V. 2.6.6) (Molecular Discovery, Hertfortshire, UK).

Table 5.3: Molecular weight (Mw), hydrophilic-lipophilic balance (HLB), and critical micelle concentration (CMC) of surfactants.

Compound	Mw* [g/mol]	HLB	CMC [mM]
Polysorbate 80[145, 148]	1310	15	0.01
Solutol[142]	345	14-16	0.37
Cremophor EL[143]	2500*	12-14	0.20
Sucrose monolaurate[144]	525	13[+]	0.34
SDS[146, 149]	288	40	7.80
DOSS[147, 150]	445	11	2.92

*mean molecular weight of pegylated surfactants based on description of excipients' composition.
[+]Calculated with Molecular Modeling Pro, V.6.2.6 (Norgwyn Montgomery Software Inc., North Wales, USA).

The lipophilicity as expressed by the calculated distribution coefficient (log*D* at pH 6.0) exhibited a broad range of values from -1.4 (PDL) to 4.1 (PGN). More lipophilic compounds are more likely to partition into micellar cores, whereas hydrophilic compounds are either predominantly in the bulk phase or interact with the hydrophilic head groups (Figure 5.1). It was shown in a study of electron resonance spectroscopy that not only lipophilicity was decisive for drug location in micelles but also acid/base properties play a role.[151] The study concluded that the tested positively charged β-blockers were primarily located on the surface of SDS and bile salt micelles whereas neutral lipophilic benzodiazepines were in the deeper interior of the micelles. Such a location in the core of micelles can be further differentiated from drugs that are rather accommodated in the palisade region of micelles (Figure 5.1). Amphiphilic compounds appear to prefer this location and a recent study with amlodipine hydrochloride and a nonionic surfactant evidenced formation of mixed micelles.[152]

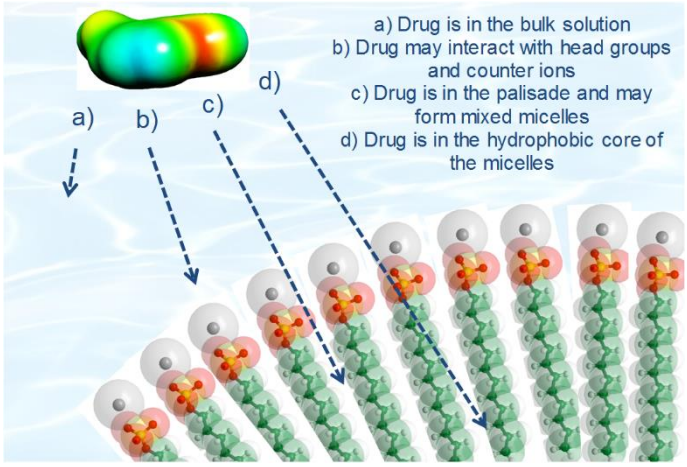

Figure 5.1: Different possible locations and mechanisms of drug solubilization in presence of surfactant micelles (example of sodium dodecyl sulfate). One or several mechanisms are likely to dominate depending on the physical compound properties.

Table 5.4 lists the solubility data for the various compounds and surfactants whereas the solubility enhancement factors are shown in Table 5.5. The comparatively hydrophilic compounds ASP and PDL did not show a pronounced solubilization in the micellar systems, except for a slight enhancement with the charged surfactants

SDS and DOSS. As expected, the more lipophilic steroid drugs showed a clear solubilization in ionic surfactants compared to pure water. SDS increased the solubility of PGN and of DPL almost 200- and 400-times, respectively, compared to water. These results are exceptionally high compared to the other solubilization results. These highest values have in common with other rather high SE results that aqueous drug solubility was in these cases comparatively low. The magnitude of achieved solubilization in such individual cases suggests that it is worthwhile in preformulation to screen for the best drug solubilizer by comparing various surfactant types.

Table 5.4: Solubility (mg/ml) of compounds in 0.5% (w/w) surfactant solutions at room temperature after 24 h. Average values are reported (n=3) with standard deviations.

	Solubility enhancement factor					
Compound	Polysorbate 80	Solutol	Cremophor EL	Sucrose monolaurate	SDS	DOSS
ASP	1.01	0.98	1.01	0.99	1.22	1.10
CBZ	1.7	1.4	1.5	2.3	9.2	2.6
DFL	9.5	8.6	9.0	5.2	6.4	3.8
DPL	21.4	16.3	16.2	23.3	404.0	1.33
ESL	19.9	22.3	20.9	17.0	58.0	5.6
FLU	23.6	19.8	20.5	9.8	20.1	5.9
FRS	161.7	105.7	113.9	112.0	121.3	94.2
HPL	1.5	1.5	1.8	3.4	13.8	0.8
IBU	3.7	3.1	3.5	2.2	4.8	1.7
NPX	6.4	4.8	5.4	3.7	9.6	2.5
PDL	1.8	1.6	1.5	2.5	6.1	3.1
PGN	9.7	10.3	11.5	27.7	189.1	12.6
TES	2.8	2.8	2.6	6.6	36.4	4.8

Table 5.5: Solubility enhancement factors of compounds in 0.5% (w/w) surfactant solutions at room temperature after 24 h.

	Solubility [mg/ml]						
Compound	Polysorbate 80	Solutol	Cremophor EL	Sucrose monolaurate	SDS	DOSS	Water
ASP	4.298 (0.011)	4.174 (0.039)	4.279 (0.036)	4.229 (0.042)	5.175 (0.035)	4.675 (0.052)	4.254 (0.035)
CBZ	0.200 (0.004)	0.168 (0.004)	0.176 (0.002)	0.269 (0.006)	1.082 (0.034)	0.304 (0.009)	0.118 (0.002)
DFL	0.411 (0.011)	0.371 (0.004)	0.391 (0.008)	0.224 (0.008)	0.278 (0.007)	0.162 (0.011)	0.043 (0.024)
DPL	0.064 (0.012)	0.049 (0.009)	0.049 (0.010)	0.070 (0.012)	1.212 (0.087)	0.176 (0.030)	0.003 (0.001)
ESL	0.040 (0.001)	0.045 (0.002)	0.042 (0.001)	0.034 (0.003)	0.116 (0.002)	0.011 (0.002)	0.002*
FLU	0.554 (0.029)	0.466 (0.020)	0.482 (0.026)	0.231 (0.058)	0.473(0.021)	0.139 (0.020)	0.024 (0.002)
FRS	0.270 (0.031)	0.177 (0.021)	0.190 (0.030)	0.187 (0.024)	0.203 (0.054)	0.157 (0.052)	0.024 (0.007)
HPL	0.051 (0.040)	0.051 (0.003)	0.063 (0.005)	0.118 (0.034)	0.472 (0.058)	0.029 (0.001)	0.034 (0.015)
IBU	0.874 (0.007)	0.743 (0.078)	0.824 (0.007)	0.515 (0.033)	1.143 (0.076)	0.414 (0.006)	0.238 (0.045)
NPX	0.308 (0.010)	0.231 (0.003)	0.262 (0.006)	0.179 (0.003)	0.467 (0.054)	0.122 (0.012)	0.049 (0.004)
PDL	0.202 (0.004)	0.185 (0.011)	0.172 (0.003)	0.280 (0.005)	0.694 (0.014)	0.347 (0.007)	0.114 (0.002)
PGN	0.068 (0.005)	0.072 (0.001)	0.080 (0.002)	0.194 (0.003)	1.324 (0.007)	0.088 (0.002)	0.007 (0.000)
TES	0.098 (0.001)	0.095 (0.003)	0.089 (0.001)	0.228 (0.010)	1.260 (0.003)	0.167 (0.003)	0.035 (0.000)

* aqueous solubility literature value [153] because solubility below the limit of quantification.

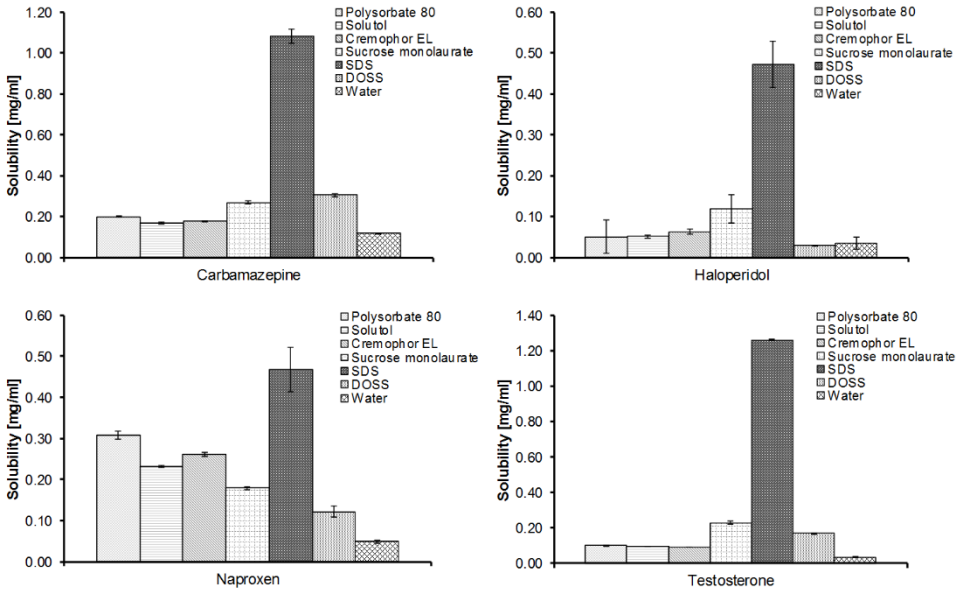

Figure 5.2: Solubility of carbamazepine, haloperidol, naproxen, and testosterone in 0.5% (w/w) surfactant solutions at room temperature after 24 h incubation time.

Figure 5.2 depicts a typical comparison of the different surfactants for selected drugs. The solubilization by SDS was here very pronounced compared to DOSS or the other non-ionic surfactants. Similar solubilization pattern was found for the majority of tested compounds despite of their log*D* values and charges. However, care is needed with any generalization for non-ionic surfactant because even though NPX showed also best solubilization in SDS as well, a previous work showed also excellent solubilization in non-ionic surfactants of the type Brij.[154] The comparative solubilization pattern among surfactants was also found to vary, as in the case of DFL and FLU. Even though these acidic drugs differ in their log*D* values, a similar pattern of preferred solubilization in pegylated non-ionic surfactants was evidenced for these fluorinated aryl acetic acid derivatives (Figure 5.3).

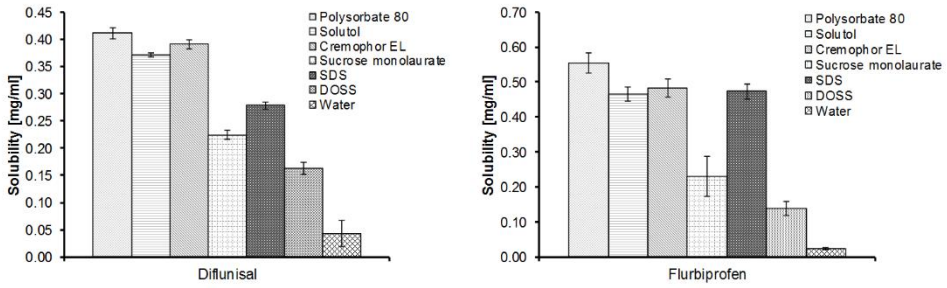

Figure 5.3: Solubility of diflunisal and flurbiprofen in 0.5% (w/w) surfactant solutions at room temperature after 24 h incubation time.

In contrast to most other studies, micellar solubilization at low surfactant concentration was conducted in parallel to the characterization of the residual solid state. Solvent-mediated phase changes were only observed for CBZ and TES (Table 5.6), although also for FLU and DFL hydrate formation is reported in the literature.[155, 156] Only sucrose monolaurate promoted hydrate formation of CBZ, in all other surfactants and in pure water, the anhydrate remained unchanged. In case of TES, hydrates were formed in water, ionic surfactants and non-pegylated non-ionic surfactants.

Table 5.6: Solid state change of CBZ and TES in residual solids after incubation for 24 h in 0.5% (w/w) surfactant solutions at room temperature.

	Solid state characterized by XRPD analysis						
Compound	Polysorbate 80	Solutol	Cremophor EL	Sucrose monolaurate	SDS	DOSS	Water
CBZ	AH	AH	AH	H	AH	AH	AH
TES	AH	AH	AH	H	H	H	H
Other compounds*	AH	AH	AH	AH	AH	AH	AH

*for an overview of the other tested compounds, see Table 5.1; AH: anhydrous form of compound, H: hydrated form of compound

Adsorption of a specific surfactant onto particle surfaces plays an important role in a potential stabilization of anhydrates. Such surfactant effects have recently been studied with piroxicam[90] where imaging showed that the kinetic hydrate transformation was suppressed by 0.5% (w/w) of polysorbate 80. This is in line with the present findings of pegylated surfactants. It can be argued that solubility values with anhydrate as residual solid are not representing true thermodynamic solubility but rather a metastable equilibrium for those compounds where hydrate formation is known. However, from a practical perspective, a pseudo-equilibrium for a certain time might be of interest since formulations are often prepared immediately before administration and not stored for a longer time. For the calculation of SE factors (Table 5.5), solubility values after 24 h incubation time were used without adjusting solubility values from pseudo-equilibria. Although, this calculation is for hydrate-forming compounds not in line with the thermodynamic understanding of SE, it is a practically oriented approach, which is biopharmaceutically meaningful and can be applied for solubility screening. However, present findings underline that proper solid state characterization is an absolute requirement at the end of solubility experiments.

5.3.2 Correlation and regression analysis of solubility enhancement

Similar patterns of drug solubilization among surfactants can be further studied by a correlation analysis. We used for this purpose the logarithmic SE, i.e. the surfactant-mediated solubilization divided by the solubility in pure water (Table 5.5). This normalization is helpful for a comparison among compounds with greatly varying aqueous solubilities. Figure 5.4 shows the results of a Pearson product moment correlation, which is a measure of the linear correlation between the log(SE) values in two surfactants. The correlation coefficients as well as *p*-values are listed in Table 5.7. All correlations between surfactants reached the level of statistical significance but the quality of the correlation differed considerably. Some values were deviating from linearity as the overview of Figure 5.4 displays.

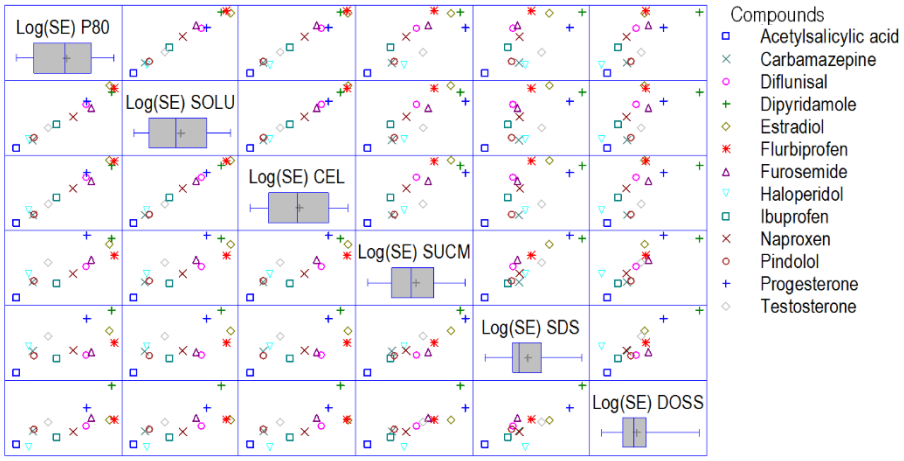

Figure 5.4: Box-and scatter plots of the different solubility enhancements (SE) in 0.5% (w/w) surfactant solutions over water. Surfactants are polysorbate 80 (P80), solutol HS (SOL), cremophor EL (CEL), sucrose monolaurate (SUCM), sodium dodecyl sulfate (SDS), and dioctyl sulfosuccinate (DOSS). Box plots from the lower to upper quartiles are shown for log(SE) of each surfactant with the median lines (and cross for the means). Correlation between any log(SE) values for a pair of surfactants is displayed by individual scatter plots.

Exceptional solubility enhancement was shown for the different steroid compounds as well as for FLU and DPL (Table 5.5). Such high values were expected for the compounds with rather high log*D* value and in case of DPL is notable, that its pK_a value is close to the pH 6.0 of the solutions. It can be expected that slight perturbations would affect partitioning into the micelles. A quantitative measure for such partitioning can be inferred from log(SE) values as it has been reported previously in the literature.[157] It was hence of interest to compare log(SE) with the distribution coefficient log*D*. As a result, these correlations were limited for the different surfactants and notable was mainly SDS that reached r of 0.638 (p=0.014). It was expected that a single molecular property would not provide high correlation due to the complex physicochemistry of partitioning.[158] We therefore focussed primarily on correlations between different surfactants rather than attampting further predicitons based on molecular drug properties.

Table 5.7: Correlation coefficients for the different 0.5% (w/w) surfactant solutions.

	Log(SE) P80	Log(SE) SOLU	Log(SE) CEL	Log(SE) SUCM	Log(SE) SDS	Log(SE) DOSS
Log(SE) P80		0.9912	0.9903	0.8414	0.6341	0.7525
		(*p*= 0.0000)	(*p*= 0.0000)	(*p*= 0.0002)	(*p*= 0.0149)	(*p*= 0.0019)
Log(SE) SOLU			0.9972	0.8682	0.6646	0.7368
			(*p*= 0.0000)	(*p*= 0.0001)	(*p*= 0.0095)	(*p*= 0.0026)
Log(SE) CEL				0.8660	0.6599	0.7174
				(p= 0.0001)	(*p*= 0.0102)	(*p*= 0.0039)
Log(SE) SUCM					0.9108	0.8422
					(*p*= 0.0000)	(*p*= 0.0002)
Log(SE) SDS						0.8373
						(*p*=0.0002)
Log(SE) DOSS						

Correlations were very high among pegylated surfactants, which form a good basis for regression. The surfactant solutol and cremophor EL are very similar since ricinoleic acid and hydroxystearic acid provide similar lipophilic surfactant tails. Figure 5.5a shows the regression line with R^2 of 0.994.

$$\text{Log(SE) CEL} = 0.0251297 + 0.989297 * \text{Log(SE) SOLU} \quad \text{Eq. 5.1}$$

Equation 5.1 describes a relationship that is close to the identity line. Fairly good model can also be formulated for the other relationships among pegylated surfactants as suggested by the *r*-values.

An example is shown by Figure 5.5b where solubility enhancement in cremophor EL correlates well with the values obtained in polysorbate 80 solutions (R^2 = 0.981):

$$\text{Log(SE) CEL} = -0.0117639 + 0.966479 * \text{Log(SE) P80} \quad \text{Eq. 5.2}$$

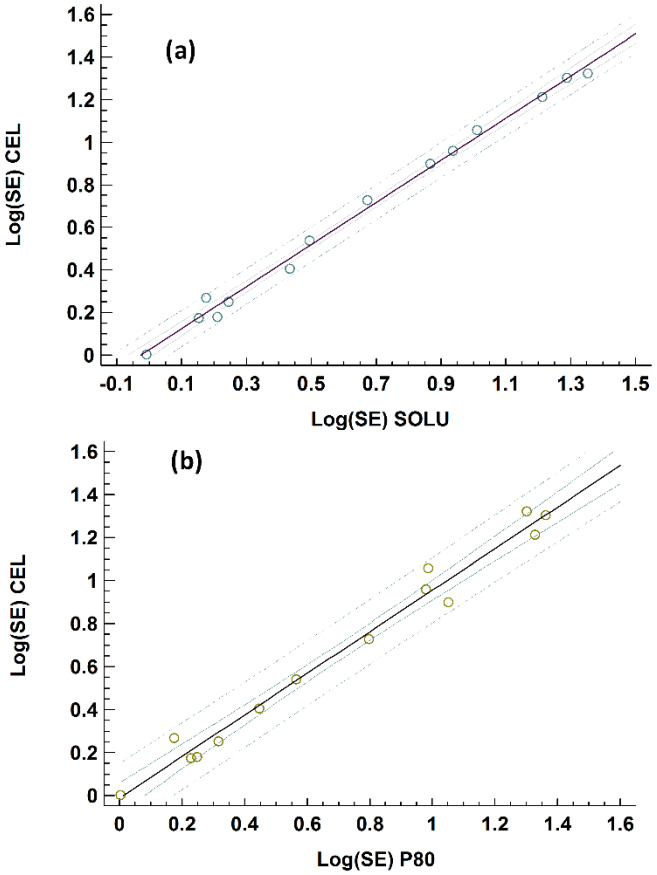

Figure 5.5: Regression analysis of solubility enhancement (SE) in 0.5% surfactant solutions over water in case of (a) cremophor EL versus log(SE) of solutol and (b) cremophor EL versus log(SE) of polysorbate 80.

The high correlations and adequate regression models allow predicting drug solubilization in one pegylated surfactant solution from another based on the results of our study. Thus, it seems to be justified to experimentally determine only one or two pegylated surfactant(s) to save resources in preformulation screening. Later in pharmaceutical development, the initially predicted values can be experimentally grounded when there is a special interest is for a given surfactant. Such an interest may, for example, origin from preformulation of lipid-based formulation if a particular surfactant is attractive because of its phase behavior.[159] Moreover, solubilization may *in vivo* differ due to the presence of bile salts and phospholipids as well as by potential enzymatic hydrolysis of a given surfactant.[160] There are also additional technical aspects that may lead to final excipient selection so that SE values provide only one aspect albeit their biopharmaceutical importance for poorly soluble compounds.[73]

The correlation analysis (Figure 5.4 and Table 5.7) indicates poorer correlations between sucrose monolaurate and anionic surfactants. A potential reason could be the comparatively short tail and sucrose head group which make sucrose monolaurate rather unique in the present study of surfactants. Interestingly, although SDS and DOSS share the negatively charged head group, their correlation is rather limited regarding log(SE) values. A potential reason could be the branched hydrophobic tail group of DOSS which may in many cases be less effective in drug solubilization compared to SDS. Therefore, a predictive regression model for DOSS and SDS was not possible. The current lack of a predictive model for the log(SE) may suggest that both anionic surfactants should be part of an early screening of surfactant solubilization. This inclusion of DOSS is also meaningful because apart from solubilization there is further surfactant performance in drug wettability and dispersion stabilization.

The current dataset shows that remarkable solubility enhancement can be achieved even at rather low surfactant concentrations, which may mimic a realistic range upon dilution of an oral dosage form.

5.4 Conclusions

A surfactant screening has to consider different excipient properties like, for example, tolerability, pharmaceutical quality, and especially its technical and biopharmaceutical performance. For the latter excipient performance, drug solubilization is of crucial importance. We therefore studied drug solubility enhancement at low surfactant concentrations that provide a model for diluted oral dosage forms. A broad screening of drug solubilization was conducted by consideration of optional solvent-mediated phase transformations. Findings suggest that especially charged surfactants like SDS may bear promise to achieve a solubility increase of several hundred-fold compared to water. High solubilization correlations were identified among pegylated surfactants of similar type. These correlations may be used to omit individual surfactants for a resource-saving solubilization testing in preformulation. Our results further stress the

importance of solid state characterization of residual drug since surfactants may affect solvent-mediated phase transformations. Current findings may serve as basis to guide a surfactant screening in preformulation and data may in the future become part of a bigger database. Solubility values are also needed to estimate drug supersaturation upon aqueous formulation dispersion. The values will find additional use for *in silico* models of drug solubilization as well as more complex physiologically-based pharmacokinetic modeling.

Chapter 6

A systematic study of molecular interactions of anionic drugs with a dimethylaminoethyl methacrylate copolymer regarding solubility enhancement

Summary

The methacrylate-copolymer Eudragit EPO (EPO) has raised interest in solubility enhancement of anionic drugs. Effects on aqueous drug solubility at rather low polymer concentrations are barely known despite of their importance upon dissolution and dilution of oral dosage forms. We provide evidence for substantial enhancement (factor 4-230) of aqueous solubility of poorly water-soluble anionic drugs induced by low (0.1-5% (w/w)) concentration of EPO for a panel of seven acidic crystalline drugs. Diffusion data (determined by ^{1}H nuclear magnetic resonance spectroscopy) indicate that the solubility increasing effect monitored by quantitative ultra-pressure liquid chromatography was caused primarily by molecular API polymer interactions in the bulk liquid phase. Residual solid API remained unaltered as tested by X-ray powder diffraction. The solubility enhancement (SE) revealed a significant rank correlation ($r_{Spearman}$= -0.83) with $rDiff_{API}$, where SE and $rDiff_{API}$ are defined ratios of solubility and diffusion coefficient in the presence and absence of EPO. SE decreased in the order of indomethacin, mefenamic acid, warfarin, piroxicam, furosemide, bezafibrate, and tolbutamide. The solubilizing effect was attributed to both ionic and hydrophobic interactions between drugs and EPO. The excellent solubilizing

Saal et al. A systematic study of molecular interactions of anionic drugs with a dimethylaminoethyl methacrylate copolymer regarding solubility enhancement. *Molecular Pharmaceutics*. **2017**, 14(4), 1234-1250.

properties of EPO are highly promising for pharmaceutical development and the dataset provides first steps towards an understanding of drug-excipient interaction mechanisms.

6.1 Introduction

An increasing number of new active pharmaceutical compounds (APIs) exhibit low water solubility which may lead to poor oral bioavailability.[1] Various approaches have been reported to increase drug solubility for these candidates. Formulations were designed to promote intestinal solubility like micro- and nanosuspensions,[161] cyclodextrin complexes,[162-164] and lipid-based formulations.[165, 166] Formulations can also target primarily a transient increase of bulk concentrations by drug supersaturation, which thereby enhances absorptive flux. Supersaturated states can be obtained *in vivo* by pH change when the dissolved compound is transported from the acid stomach into the small intestine or by a loss of solubilization capacity of a formulation as upon dilution, dispersion or digestion in the gastrointestinal tract.[167] Supersaturation is only beneficial if drug crystallization is slower than drug absorption.[70] The most common supersaturating formulations are amorphous solid dispersions that are used to enhance the bioavailability of compounds belonging to biopharmaceutical classification system (BCS) class II or IV.[167, 168]

This work focusses on the copolymer EPO that belongs to the family of methacrylic acid copolymers. EPO is composed of dimethylaminoethyl methacrylate, butyl methacrylate, and methyl methacrylate at molar ratios of 2:1:1 and is positively charged at pH< 8 in aqueous media. Figure 6.1 displays the molecular structure of this copolymer. EPO has been widely used as pharmaceutical excipient for taste masking, moisture protection, enteric film-coating, and sustained release drug delivery.[169]

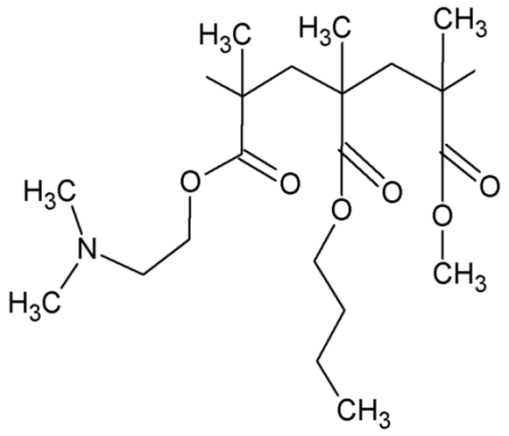

Figure 6.1: Simplified monomer structure of EPO (details are given in the text).

EPO was more recently used to prepare solid dispersions, especially with anionic drugs[170-172], and outstanding results were obtained in terms of solubility and bioavailability enhancement.[170] Priemel et al. also reported *in situ* amorphization with EPO and indomethacin[173] and recently *in situ* amorphization with naproxen and ibuprofen was evidenced.[174]

Different studies attempted to gain insights into the molecular interactions of the copolymer EPO with anionic drugs. Kojima et al. and Higashi et al. used for example nuclear magnetic resonance (NMR) spectroscopy to better understand the molecular basis of solubility enhancement (SE) of solid dispersions and of supersaturated solutions using EPO and mefenamic acid.[170, 171] These important pioneer studies showed that EPO acts not only as a carrier in solid dispersions but also affects drug solubilization and supersaturation of acidic drugs. Formulations with EPO therefore seem to become a research field in its own right. However so far, only few compounds, exclusively in amorphous state, were studied. Moreover, data for rather low polymer concentrations are rare, for example concentrations that would result from dilution of oral dosage forms in the gastrointestinal tract. Another aspect is that combinations of EPO and acidic drugs were primarily studied in the context of solid dispersions.[170] The molecular interactions of the polymer and acidic drugs seem to be also promising for other formulation types but such data are currently lacking.

We therefore studied the influence of EPO in solution on the solubility and solid state of seven poorly water-soluble, acidic, chemically diverse drugs. Our final aim was to better mechanistically understand how the molecular interactions of acidic drugs and EPO would result in specific SE.

6.2 Materials and Methods

6.2.1 Materials

Indomethacin (IMC), mefenamic acid (MFA), tolbutamide (TLB) and warfarin (WFN) were obtained from Sigma Aldrich (St. Louis, USA), while bezafibrate (BZF) and piroxicam (PRX) were from TCI Europe N.V. (Zwijndrecht, Belgium). Furosemide (FRS) was purchased from Molekula GmbH (München, Germany) and amino alkyl metacrylate copolymer E, Eudragit EPO, (EPO) was obtained from Evonik (Darmstadt, Germany). Chemical structures of all model compounds are shown in Figure 6.2. Hydrochloric acid (0.1 M) and sodium hydroxide solution (0.1 M) were supplied by Merck KGaA (Darmstadt, Germany).

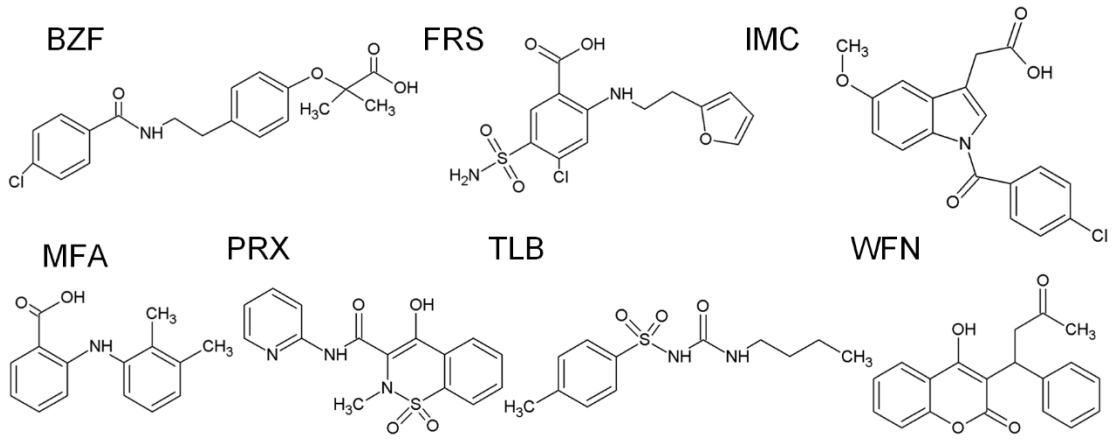

Figure 6.2: Chemical structure of model drugs.

Table 6.1: List of model drugs and selected physicochemical properties.

Compound	Mw [g/mol]	pK_a[a]	Log$D$[b] (pH 6.0)
Bezafibrate (BZF)	361.8	3.2	1.8
Furosemide (FRS)	330.7	3.5	0.0
Indomethacin (IMC)	357.8	4.5	1.4
Mefenamic acid (MFA)	241.3	4.2	3.3
Piroxicam (PRX)	331.4	2.3	-0.4
Tolbutamide (TLB)	270.4	5.1	1.4
Warfarin (WFN)	308.3	5.0	2.2

[a]Measured pK_a-values via photometric titration.
[b]Values calculated by the Marvin program suite (V. 16.5.30) (ChemAxon Ltd., USA).

6.2.2 Sample preparation

Polymer solutions were prepared by dissolving EPO (0.1%, 0.5%, 1%, 2%, 3%, 4%, 5% (w/w)) in deionized water and adjusting the pH of the solutions to pH 6.0 with hydrochloric acid or sodium hydroxide at 25°C. All solutions were visually inspected for absence of residual particles.

6.2.3 Viscosity measurements

Apparent viscosity was measured with a cone-plate-rheometer (Physica MCR 301, Anton Paar GmbH, Graz, Austria) by applying a shear rate of 1000 min^{-1} for 2 min.

6.2.4 Solubility and residual solid analysis

Solubility of compounds in EPO-solutions was determined using a slightly modified 96-well SORESOS[56] assay, which measures both equilibrium solubility and solid form of the residual solid. In brief, APIs were dispensed using the powder-picking-method[103] in 96-well flat bottom plates (Corning Inc., Durham, USA) and stirring bars and excipient vehicles (150 µL) were added. The plate was then sealed with pre-slit silicon caps and the mixtures were agitated by head-over-head rotation for 24 h, 48 h and one week at room temperature. After equilibration, the suspensions were carefully

transferred into 96-well filter plates and liquid was separated from residual solid by centrifugation. Collected filtrates were diluted with N-methyl-2-pyrrolidone and drug content was determined using a Waters Acquity Ultra Performance Liquid Chromatographic (UPLC) system equipped with a 2996 Photodiode Array Detector and an Acquity UPLC BEH C18 column (2.1x50 mm, 1.7 µm particle size) from Waters (Milford, USA). Table 6.2 summarizes the experimental conditions (solvents, composition of mobile phase, detection wave length) used for the drugs. An isocratic flow of a mixture of solvent A and solvent B was applied for 0.3 min at a flow rate of 0.75 ml/min. Subsequently, the concentration of solvent B was linearly increased to 100% within 0.5 min. Solid state analysis of residual solid was performed by X-ray powder diffraction (XRPD) using a STOE Stadi P Combi diffractometer with a primary Ge-monochromator (Cu Kα radiation), imaging plate position sensitive detector (IP-PSD), and a 96-well sample stage. The IP-PSD allowed simultaneous recording of the diffraction pattern on both sides of the primary beam which were summed up by the software STOE WinXPOW to reduce effects related to poor crystal orientation statistics. Samples were analyzed directly in the 96-well filter plate with an exposure time of 5 min per well.

Table 6.2: Experimental conditions used for UPLC analysis.

Compound	Composition (A:B)[a] [%]	Detection wavelength [nm]
BZF	50:50	254
FRS	75:25	274
IMC	50:50	318
MFA	40:60	352
PRX	65:35	342
TLB	60:40	265
WFN	50:50	283

[a]Mobile phase A: deionized water with 0.1% (v/v) triethylamine adjusted to pH 2.2 with methanesulfonic acid, mobile phase B: acetonitrile.

6.2.5 ^{1}H NMR spectroscopy

Solutions for NMR analyses were prepared by incubating APIs for 24 h in a 0.5% (w/w) EPO-solution in deuterium oxide (D_2O) at pH 6.0. Samples were then centrifuged and supernatants (550 µl) were transferred to short disposable 5 mm NMR tubes.

All NMR measurements were performed with a Bruker 600 MHz Avance II spectrometer equipped with a cryogenic QCI probe head at a temperature of 300 K. Spectrometer operation and data processing was done by Topsin 2.1 software (Bruker, Fällanden, Switzerland). For all samples matching/tuning of the probe head and the 90° pulse were determined fully automated. Pseudo 2D ^{1}H diffusion ordered spectroscopy with bipolar gradient pulse pairs and 2 spoil gradients[175] was measured for all samples with presaturation of residual water. Data points (32k) were acquired over 18 ppm sweep-width. The interscan delay was set to 1.5 s and the SMSQ10.100 shaped bipolar gradient was ramped from 2.65 to 50.35 gauss/cm in 16 equidistant steps. A diffusion time of 300 ms was used. Spectra were processed with a lb = 1 exponential filtering.

Diffusion coefficient *D* was fitted by use of the T_1/T_2 relaxation module implemented within the Topsin 2.1 (Bruker, Switzerland). For most molecules at least one API and excipient related NMR signal was identified by visual inspection.

6.2.6 Statistical analysis and molecular modeling

The program STATGRAPHICS Centurion XVI ed. Professional (V. 16.1.15) from Statpoint Technologies Inc. (Warrenton, USA) was used for statistical rank correlation (Spearman) testing.

For graphical representation of the mefenamic acid interaction with EPO, both ionized molecules were assigned to an AMBER force field using the software Chemsite (V. 10.4., Norgwyn Montgomery Software Inc., Northwales, USA). The starting configuration was based on docking the anionic model drug to positively charged nitrogen of the polymer that was modeled as residue of 10 monomers. Following

energy minimization, the molecular dynamics simulation was running for 10 ns while using an implicit Born solvation model (with a relative permittivity of 78.4) at a temperature of 300 K.

6.3 Results

6.3.1 Viscosity

The apparent viscosity was measured under shear (Table 6.3) for all solutions of EPO. A slight increase in viscosity with polymer concentration was observed, however all solutions had a rather low viscosity. These EPO-solutions were used to determine drug solubility after 24 h and 48 h. Most drugs reached equilibrium solubility within 24 h, some compounds (MFA, FRS, TLB) showed differences between the selected time points especially at higher polymer concentration. For those compounds solubility was additionally determined after one week to prove that equilibrium was reached. Finally, 48 h was selected as incubation time for all solubility experiments (shown in Table 6.4 and Figures 6.3 and 6.4) because all systems have reached equilibrium after this time.

Table 6.3: Apparent viscosity of EPO-solutions (25°C, 1000s^{-1}).

Concentration of EPO [%, (w/w)]	**Viscosity [mPas] (standard deviation, n=3)**
0.1	1.1 (0.01)
0.5	1.1 (0.01)
1.0	1.2 (0.01)
2.0	1.5 (0.02)
3.0	1.9 (0.05)
4.0	2.1 (0.01)
5.0	2.3 (0.00)

6.3.2 Solubility and residual solid analysis

All test solutions were adjusted to pH 6.0 and following equilibration, the residual solid was analyzed by means of XRPD. Compared to water, all model compounds displayed an enormous SE in the different EPO-solutions (Figures 6.3-6.4 and Table 6.4) with SE factors of approximately 4-230 fold.

Table 6.4: Drug solubility and pH in water after incubation for 48 h.

Compound	**Solubility in water (standard deviation, n=3) [mg/ml]**	**pH in water (standard deviation, n=3)**
BZF	0.016 (0.003)	4.6 (0.1)
FRS	0.024 (0.007)	4.4 (0.0)
IMC	0.007 (0.003)	5.0 (0.2)
MFA*	< 0.001	6.1 (0.1)
PRX	0.008 (0.001)	5.4 (0.1)
TLB	0.083 (0.007)	5.0 (0.1)
WFN	0.005 (0.001)	5.4 (0.2)

*Aqueous solubility was below the limit of detection.

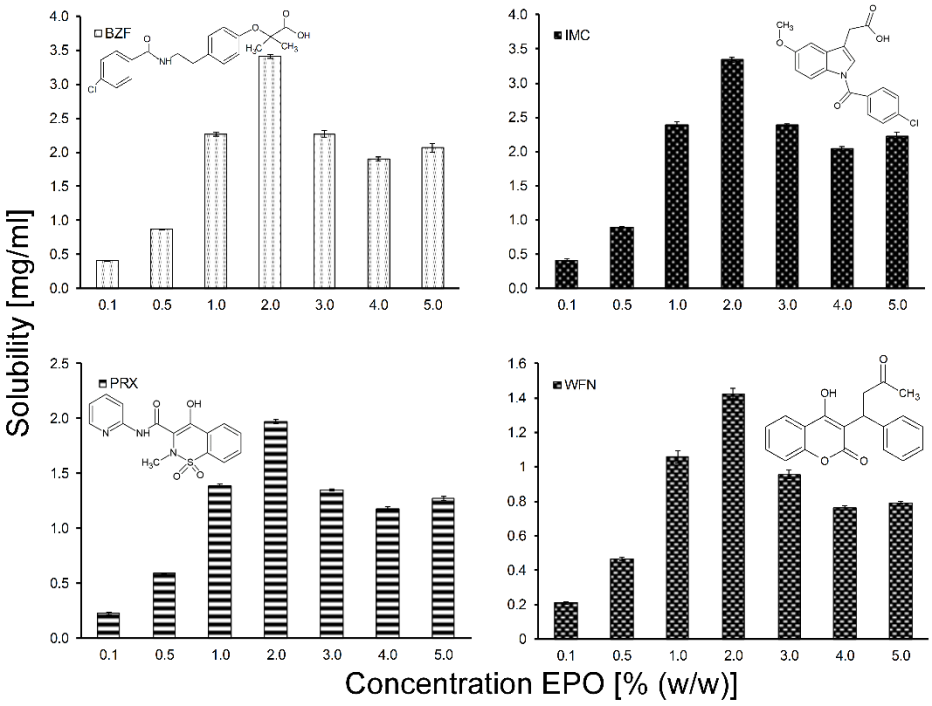

Figure 6.3: Solubility of BZF, IMC, PRX, and WFN in EPO-solutions after 48 h equilibration at room temperature.

BZF, IMC, PRX and WFN (Figure 6.3) reached maximum solubility at 2% EPO (w/w) and their solubility increased with the polymer concentration. Above 2% EPO, solubility decreased again and finally reached a kind of plateau. In contrast, FRS and MFA (Figure 6.4) showed a constant increase of solubility with polymer concentration up to 5% EPO. TLB (Figure 6.4) was the only tested compound that reached a kind of plateau at 2% EPO where the solubility did not decrease at higher EPO concentrations.

The residual solid analysis confirmed that none of the tested compounds changed its polymorphic form. Therefore, it is likely that the SE resulted from drug-EPO interactions in the bulk phase and not from stabilization of a metastable polymorphic form.

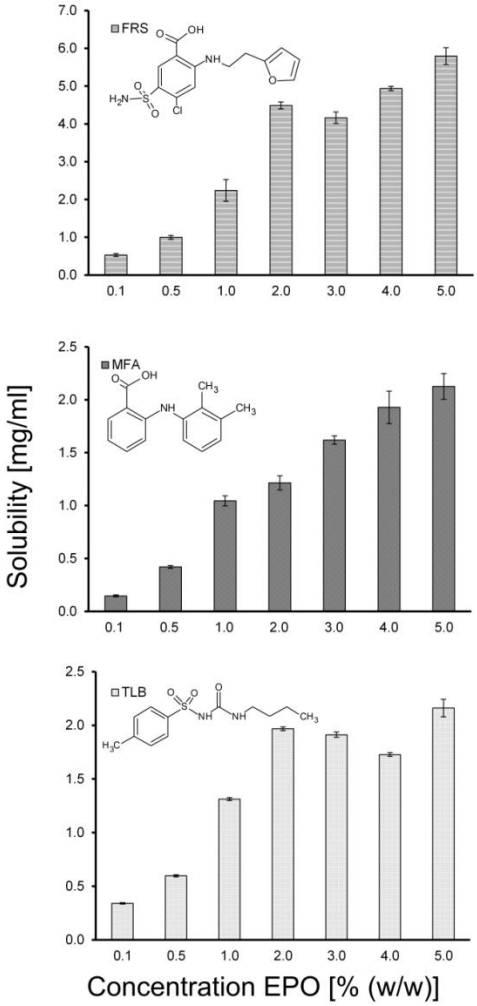

Figure 6.4: Solubility of FRS, MFA, and TLB in EPO-solutions after 48 h equilibration at room temperature.

To address potential pH effects on drug solubility, the pH was measured after 48 h for all substances in EPO (0.5%, 2%, and 5%) (Table 6.5). For most compounds the pH dropped about 0.5 units. Maximum changes were observed in FRS suspensions where the pH dropped to pH 3.6 in 2% EPO and to pH 4.1 in 0.5% and 5% EPO.

Table 6.5: pH of drug suspensions in EPO after 48 h at room temperature.

Compound	pH in EPO 0.5% after 48 h (standard deviation, n=3)	pH in EPO 2% after 48 h (standard deviation, n=3)	pH in EPO 5% after 48 h (standard deviation, n=3)
BZF	4.5 (0.0)	4.6 (0.3)	4.7 (0.0)
FRS	4.1 (0.0)	3.6 (0.0)	4.1 (0.1)
IMC	4.8 (0.0)	4.4 (0.1)	4.9 (0.1)
MFA	5.6 (0.1)	5.2 (0.0)	5.4 (0.0)
PRX	5.4 (0.0)	5.5 (0.1)	5.6 (0.1)
TLB	5.2 (0.1)	5.4 (0.1)	5.6 (0.0)
WFN	5.4 (0.1)	5.4 (0.1)	5.7 (0.1)

As a trend, the pH was slightly higher in 5% EPO compared to the pH in 0.5% and 2% EPO. The dimethylaminoethyl groups in EPO have a rather high pK_a value (8.4)[176] and thus concentration-dependent interactions with the dissolving acidic drugs are likely to affect equilibrium pH.

6.3.3 ^{1}H NMR spectroscopy

^{1}H NMR measurements were performed to evaluate the interactions between EPO and the compounds in solution. Peaks originating from protons of aromatic ring systems (present in all API molecules investigated) were observed between 7.00 and 8.25 ppm in D2O for PRX and 6.75 to 8.00 ppm for WFN.

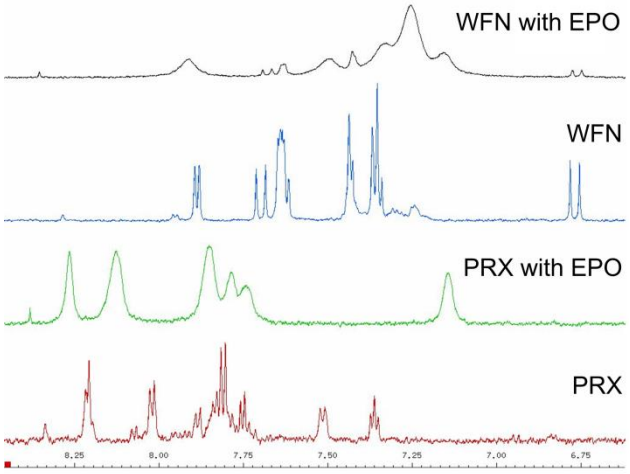

Figure 6.5: Solution-state ^{1}H NMR spectra of WFN and PRX in presence of EPO and in D_2O alone.

The NMR signals of WFN and PRX in D_2O were very sharp (see Figure 6.5), indicating that API-molecules were dispersed in D_2O without substantial aggregation. This was also observed for the other compounds (spectra not shown). All drugs had in common that API-related signals displayed changes in line-width and/or chemical shift in presence of EPO as shown for two examples, WFN and PRX, in Figure 6.5. Peaks derived from compounds could be still clearly observed although the peaks' shapes were comparatively much broader.

1H NMR was further used to measure the diffusion coefficient of the APIs in D2O with and without 0.5% EPO and results are displayed in Table 6.6.

Table 6.6: Diffusion coefficient of APIs in D_2O with and without EPO.

Compound	Diffusion coefficient in $D_2O \times 10^{10}$ [m^2/s]	Diffusion coefficient in EPO 0.5% $\times 10^{10}$ [m^2/s]
BZF	4.65	0.56
FRS	4.73	0.36
IMC	5.25	0.34
MFA	5.50	0.34
PRX	5.43	0.63
TLB	5.40	1.32
WFN	7.00	0.48
EPO	0.38	-

As expected, the much larger polymer EPO showed a lower diffusion coefficient (10 to 15-fold) than the APIs alone and therefore moves slower. The EPO diffusion coefficient was practically unaffected by the different drugs (in the range $5.3 \cdot 10^{-11}$ to $3.7 \cdot 10^{-11}$ m^2/s). By contrast, the diffusion coefficient of the APIs decreased substantially in the presence of EPO down to or even slightly below the diffusion coefficient of EPO.

6.4 Discussion

It is a reasonable assumption that the ionic interaction between the deprotonated drug and protonated amino alkyl group of EPO provides important contribution to the whole interaction. As an example of such a likely molecular association of drug and excipient, the potential EPO-MFA interaction is depicted in Figure 6.6.

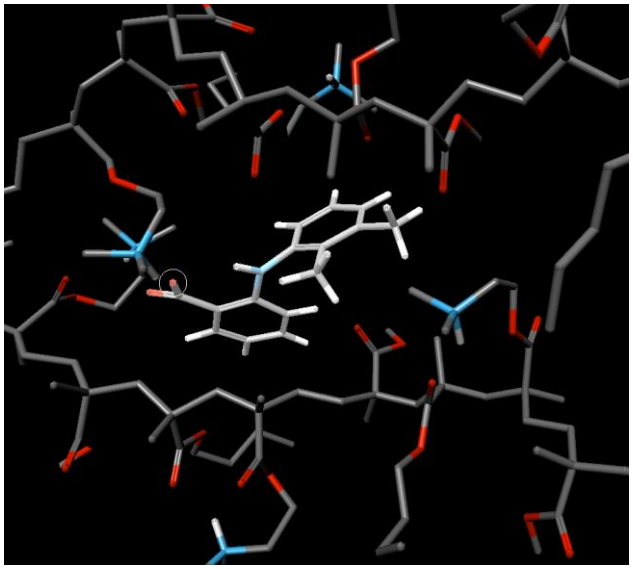

Figure 6.6: Graphical representation of the interaction of ionized molecules and ionized EPO using mefenamic acid as model (light gray).

MFA was selected as an example since its interaction with EPO has been investigated before in studies addressing supersaturation.[171] Figure 6.6 shows that apart from association of the ionic groups, additional interactions e.g. between side chain methyl groups and the aromatic ring, are likely in case of MFA. Especially, the amino group may increase the polarization of the methyl C-H group and thereby favor interaction with an aromatic ring. Similarly, hydrophobic interactions between the dangling EPO side chains and aromatic drug moieties may further strengthen overall association. Higashi et al. studied the interaction mechanism of MFA with EPO by high resolution magic-angle spinning NMR and also divided the molecular interactions into ionic and hydrophobic interactions.[171] They also identified peaks that indicate interactions between the amino alkyl group of EPO and the aromatic systems of MFA.[171] In line with these results, Figure 6.6 shows that interactions with at least three spatial contacts could be viewed as a kind of molecular recognition in the case of MFA and EPO. Thus, EPO might form a kind of a polymeric pocket for MFA and additional interactions are conceivable that further shield MFA from the aqueous environment. Based on the example of MFA, we assume that such specific interaction motifs may also occur with other acidic drugs. In summary, these motifs are the interaction of acidic and positively charged amino alkyl group, the interaction of methyl amino group and aromatic rings, and additional hydrophobic interactions. Even though all

tested compounds can in principle show such interaction motifs, the molecular structures are quite diverse and these structural differences are very likely to influence the specific strength of molecular association between polymer and compound. MFA has a carboxylic acid group whereas other compounds, like PRX, TLB, and WFN, have alternative acidic groups (enolate or sulfonamide). When looking at Table 6.6, it is quite remarkable that the diffusion coefficient of TLB decreases the least in presence of polymer. Comparing all the structures, TLB is the only compound that has only one aromatic ring. All other compounds have at least two aromatic rings. Thus the number of aromatic rings could be important for the polymer-drug interaction, for example in case of MFA, the interaction of the methyl amino group and of the aromatic ring. Such interaction motifs also require that an aromatic ring is spatially arranged close to the amino alkyl side chain of EPO. Therefore molecular flexibility and hence rotatable bonds adjacent to aromatic systems are also very likely associated with a strong polymer-drug interaction and in turn also with a good SE. FRS and WFN showed excellent SE and these drugs are also flexible regarding their spatial arrangement of their aromatic groups.

Theoretically, a certain initial conformation of the polymer might be optimal for drug solubilization. However, at the same time, the presence of API molecules may also influence conformation of the polymer. It is therefore expected that due to these complex molecular interactions, no simple relationship can be established between the polymer concentration and drug solubility. Concentration dependent solubility data were indeed in agreement with this view since there was no general solubilization pattern evidenced for the different compounds (Figures 6.3-6.4). Nonetheless, it is remarkable that most acidic drugs show a solubility maximum at 2% EPO. Drug solubility was measured in a broad concentration range of EPO and solubility could be affected by both the initial conformational structure of the polymer in solution and by the conformation induced by its interaction with the drug.

For most compounds we observed a maximum of SE within the range of polymer concentration investigated. For those which do not show this maximum the curvature of the solubility increase proposed a maximum (or plateau) outside the range of polymer concentration investigated. Eventually, these compounds will show beyond

the tested range also a maximum for SE at a certain polymer concentration. These observed maxima can be explained by steric hindrance of the interactions between EPO and the APIs occurring at high polymer loads. In addition conformational changes of the polymer at high concentration may lead to limited accessibility of the polymeric cavities that enable strong drug association.

The molecular interactions discussed and exemplarily shown in Figure 6.6 were in agreement with our ^{1}H NMR results. Notable was for example that all drugs revealed changes in the aromatic regions, where a change in line-width and/or chemical shift for peaks originated from protons of aromatic rings in presence of EPO. These results are in line with former results, where similar line broadening was observed for MFA due to strong interaction with EPO.[171] Besides spectral information, drug diffusion coefficients of the compounds in presence and absence of EPO were used to monitor the strength of the API polymer interactions in solution.

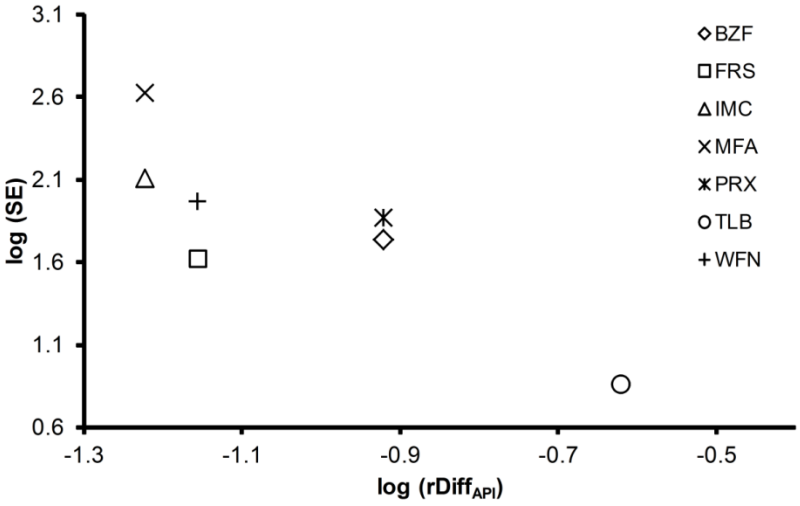

Figure 6.7: SE in presence of polymer (0.5% (w/w)) plotted against the rDiff$_{API}$ defined as the diffusion coefficient of drug with polymer divided by the value of pure drug in D_2O.

A relative diffusion coefficient (rDiff$_{API}$) was considered that holds for the observed value of drug in the presence of polymer normalized by the diffusion coefficient of drug alone (in D_2O). When rDiff$_{API}$ is plotted against the relative SE of the drug (drug solubility in polymer solution normalized by the pure aqueous solubility) there

appears to be a non-linear relationship. A Spearman rank correlation provided a coefficient of $r_{Spearman}$ = -0.83 that supported the view of a significant relationship (p= 0.04). Thus, a decrease of diffusion coefficient ratio correlates well with an observed excipient SE (Figure 6.7). It is expected that APIs diffusion will be increasingly reduced by stronger interaction with EPO and therefore, a relative diffusion coefficient might be used as marker for the strength of drug-excipient interaction in the bulk phase. The approach seems promising because no additional effects of the drug solid state were evidenced in presence of polymer. Based on the identified correlation, it might be in the future possible to formulate an empirical power law that describes SE as a function of $rDiff_{API}$ but this should be based on an even larger dataset than presented in the current study.

The non-linear nature of the relationship is likely due to a complex solid-liquid equilibrium where drug in the bulk phase can be either interacting or non-interacting with polymer. It is possible that presence of drug may induce conformational change of the polymer, thereby influencing its binding. On top of such multiphase consideration, one may also have to account for fractal physics of drug dissolution and diffusion.[118, 177, 178] Such further theoretical research is beyond the scope of the present article. The observed empirical correlation has in any case a great practical relevance because it suggests how the strength of the molecular interaction, expressed by $rDiff_{API}$, may translate into SE. It is here interesting that a moderate change in the strength of molecular interaction can exert a huge effect on solubilization.

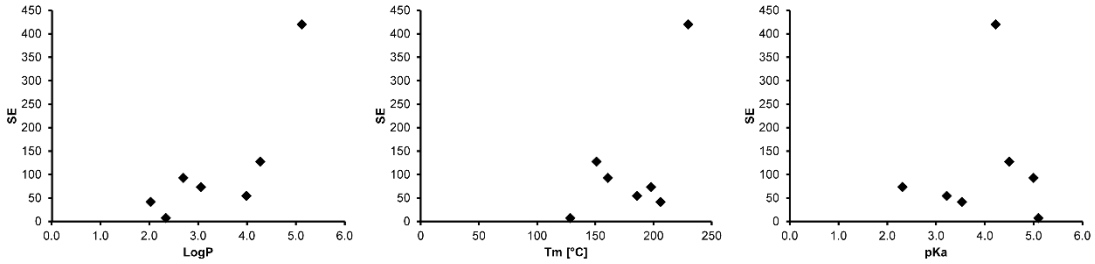

Figure 6.8: Plot of log$P$, melting point (T_m), and pK_a versus solubility enhancement (SE).

Further possible correlations were studied between characteristics of the compounds (used for general solubility prediction)[179] like log*P*, melting point, or pK_a of the APIs and the solubility enhancement by EPO (data shown in Figure 6.8). As a result, the present dataset did not point to a comparatively simple relationship of such a molecular parameter with SE, which was probably due to the complex nature of ionic and relevant hydrophobic interactions of drug and polymer.

6.5 Conclusion

In former studies it was shown that EPO is a very potent polymer for stabilizing amorphous acidic compounds, which can increase oral bioavailability.[170, 171] We studied the influence of EPO in solution on seven crystalline acidic drugs and could show that the observed huge SE was enabled by specific molecular interactions of drug and polymer. Thus, EPO seems to be a very well suitable polymer to formulate anionic drugs in both solid dispersions and in less complex formulations such as solutions or suspensions. The exceptional drug solubilization by EPO may even replace solid dispersions in many cases. This is attractive because simple formulations that are easy to produce and stable upon storage are clearly preferred particularly for early stage development. An important finding was also that a ratio of diffusion coefficients of an API measured by NMR in presence and absence of EPO correlated well with the obtained excipient solubility enhancement. The findings suggested that small changes in the strength of molecular interaction between APIs and EPO may substantially affect drug solubility in the presence of EPO. Based on the comparison of the acidic drugs, a better molecular understanding was achieved for the association of drug and polymer to target maximum solubility. Such findings of molecular pharmaceutics are of practical relevance and it is particularly the early development phase that benefits from such knowledge to formulate poorly soluble drugs, while coping with challenges of limited compound availability and stretched timelines. The results are also interesting for oral solid dosage forms in the later stage of pharmaceutical development where EPO could be used as well for SE.

Chapter 7

Unexpected solubility enhancement of drug bases in presence of a dimethylaminoethyl methacrylate copolymer

Summary

The methacrylate-copolymer Eudragit® EPO (EPO) has previously shown to greatly enhance solubilization of acidic drugs via ionic interactions and by multiple hydrophobic contacts with polymeric side chains. The latter type of interaction could also play a role for solubilization of other compounds than acids. The aim of this study was therefore to investigate the solubility of six poorly soluble bases in presence and absence of EPO by quantitative ultra-pressure liquid chromatography with concomitant X-ray powder diffraction (XRPD) analysis of the solid state. For a better mechanistic understanding, spectra and diffusion data were obtained by ^{1}H nuclear magnetic resonance (NMR) spectroscopy. Unexpected high solubility enhancement (up to 360-fold) was evidenced in presence of EPO despite of the fact that bases and polymer were both carrying positive charges. This exceptional and unexpected solubilization was not due to a change in the crystalline solid state. NMR spectra and measured diffusion coefficients indicated both strong drug-polymer interactions in the bulk solution and diffusion data suggested conformational changes of the polymer in solution. Such conformational changes may have increased the accessibility and extent of hydrophobic contacts thereby leading to increased overall molecular interactions. These initially surprising solubilization results demonstrate

Saal et al. Unexpected solubility enhancement of drug bases in presence of a dimethylaminoethyl methacrylate copolymer, *Molecular Pharmaceutics*, **2018**, 15, 1, 186-192.

that excipient selection should not be based solely on simple considerations of, for example, opposite charges of drug and excipient, but it requires a more refined molecular view. Different solution NMR techniques are here especially promising tools to gain such mechanistic insights.

7.1 Introduction

Poorly water soluble drug candidates are becoming more prevalent in pharmaceutical discovery and development.[1, 180] These candidates can be formulated for oral administration by several strategies including the reduction of the particle size, formulation of the drug in solution, amorphous systems or lipid formulations.[165, 181-183] While such formulation techniques are used in preclinical formulation supply, there are certainly limitations of any sophisticated formulation approaches because of limited compound availability and stretched timelines.[7] Formulation strategies that are widely used in the early phase are solubilization by pH-adjustment, the use of cosolvents, cyclodextrins or surfactants, formulation as suspensions, emulsions, or solid dispersions.[7] Lee et al. reported that in Pfizer 85% out of more than 300 compounds submitted for discovery and pre-clinical injectable formulation development were formulated by pH adjustment, cosolvent addition, or a combination of the two approaches.[184] More complicated and metastable formulations such as solid dispersions are often not the first choice at an early development stage, for example, in preclinical formulation supply. However, much can be learned from the literature on solid dispersions regarding drug-polymer interactions that can be harnessed more broadly in different formulation approaches.[167, 185, 186]

The current work focusses on Eudragit® EPO that was introduced as pharmaceutical polymer for taste masking, moisture protection, enteric film-coating, and sustained release drug delivery[169] but more recently, it was used for solubility enhancement of poorly soluble acidic drugs by stabilizing them in an amorphous state.[170-174] EPO belongs to the family of methacrylic acid copolymers and is composed of

dimethylaminoethyl methacrylate, butyl methacrylate, and methyl methacrylate with a molar ratio of 2:1:1. It is positively charged at pH < 8 in aqueous media and the chemical structure is displayed in Figure 7.1.

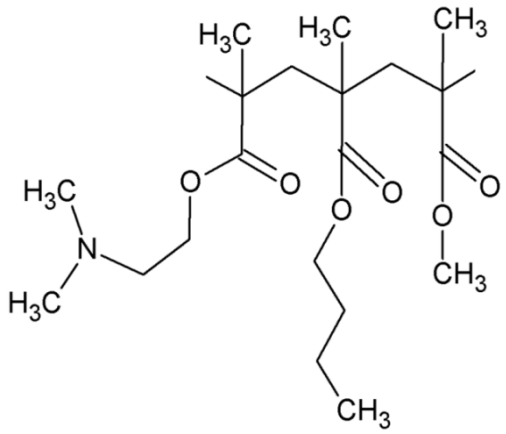

Figure 7.1: Simplified monomer structure of EPO (details are given in the text).

When using EPO as a carrier for amorphous compounds, outstanding results were obtained in terms of solubility and bioavailability enhancement. [170, 172] EPO was not only very potent in stabilizing compounds in an amorphous state but excellent solubilization was recently demonstrated with a range of acidic drugs. [187] Of great importance is here the ionic interaction between the deprotonated acid and protonated amine moieties of the polymer. [171, 187] Moreover, further relevant hydrophobic interactions were evidenced between the polymeric side chains and active pharmaceutical ingredients (APIs). The latter drugs may contain aromatic residues or other lipophilic groups for which such hydrophobic excipient interactions were shown to play a role in solubilization.[187]

Only very few non-acidic compounds have so far been formulated with EPO[188, 189] and to the best of our knowledge, there are no data available using only EPO for solubility enhancement of basic APIs. The latter approach seems at first to be less promising based on the same type of positive charge that is obtained at pH values < 8. However, the gained knowledge of hydrophobic side chain interactions led to the hypothesis that potentially also drug bases may profit from a solubility enhancement

in presence of the copolymer despite of its dimethylaminoethyl groups. We therefore studied the influence of EPO in solution on the solubility and solid state of six poorly water-soluble, basic drugs with chemically diverse characteristics.

7.2 Materials and Methods

7.2.1 Materials

Pimozide (PMZ) and tamoxifen (TMX) were obtained by Sigma Aldrich (Buchs, Switzerland), while carvedilol (CVD) was from AK Scientific, Inc. (Union City, USA). Cinnarizine (CNZ) was purchased from Alfa Aesar (Karlsruhe, Germany), mefloquine (MFQ) was obtained from F. Hoffmann-La Roche Ltd (Basel, Switzerland) and terfenadine (TFD) was from Carbosynth Ltd (Compton, UK). The chemical structures of all model compounds are shown in Figure 7.2 and their physicochemical properties are listed in Table 7.1. Aminoalkyl metacrylate copolymer E, Eudragit EPO, (EPO) was obtained by Evonik (Darmstadt, Germany). Hydrochloric acid (0.1 M) and sodium hydroxide solution (0.1 M) were from Merck KGaA (Darmstadt, Germany).

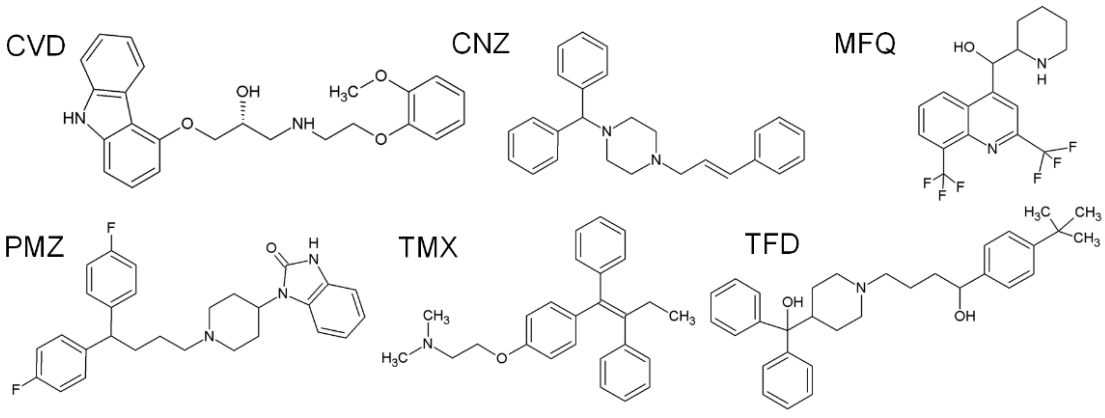

Figure 7.2: Chemical structure of model drug bases and abbreviations used (from left to right in the order of carvedilol, cinnarizine, mefloquine, pimozide, tamoxifen, and terfenadine).

Table 7.1: Molecular weight (Mw), ionization constant (pK_a) and distribution coefficient (log$D$) at pH 6.0 for the different model compounds.

Compound	**Mw [g/mol]**	**pK_a[a]**	**Log$D$[b] (pH 6.0)**
Carvedilol (CVD)	406.5	8.1	0.8
Cinnarizine (CNZ)	368.5	7.8	3.8
Mefloquine (MFQ)	378.1	9.2	1.1
Pimozide (PMZ)	461.2	8.6	3.5
Tamoxifen (TMX)	371.2	9.7	3.7
Terfenadine (TFD)	471.7	9.1	3.6

[a]Measured pK_a-values via photometric titration (Roche internal data).
[b]Values calculated by Marvin Suite (V. 16.5.30, ChemAxon, Douglas Drake, USA).

7.2.2 Sample preparation

Polymer solutions were prepared by dissolving EPO (0.1%, 0.5%, 1%, 2%, 3%, 4%, 5% (w/w)) in deionized water and adjusting all solutions to pH 6.0 by hydrochloric acid and sodium hydroxide at 25°C. Solutions were checked carefully for absence of particles.

7.2.3 Solubility and residual solid analysis

Solubility of compounds in EPO-solutions was determined by using a 96-well assay that was introduced to measure equilibrium solubility in parallel to a solid state analysis of the residual solid (SORESOS)[56] as described before.[90] In brief, APIs were dispensed using the powder-picking-method[103] in a 96-well flat bottom plate (Corning Inc., Durham, USA). After addition of stir bars and polymer solutions (150 µl), mixtures were agitated by head-over-head rotation for 48 h at room temperature. After mixing, the suspensions were carefully transferred into 96-well filter plates and the liquid and solid phase were separated by centrifugation. Filtrates were collected, diluted with N-methyl-2-pyrrolidone and drug content in filtrates was determined using a Waters Acquity Ultra Performance Liquid Chromatographic (UPLC) system equipped with a 2996 Photodiode Array Detector and an Acquity UPLC BEH C18 column (2.1x50 mm, 1.7 µm particle size) from Waters (Milford, USA). An isocratic flow (composition of the mobile phase is listed in Table 7.2) was applied for 0.3 min at a flow rate of 0.75 mL/min. Subsequently, the concentration of solvent B was

linearly increased to 100% within 0.5 min. Solid state analysis of residual solid was performed by X-ray powder diffraction (XRPD) using a STOE Stadi P Combi diffractometer with a primary Ge-monochromator (Cu Kα radiation), imaging plate position sensitive detector (IP-PSD), and a 96-well sample stage as described before.[56] The IP-PSD allowed simultaneous recording of the diffraction pattern on both sides of the primary beam, which were summed up by the software STOE WinXPOW to reduce effects related to poor crystal orientation statistics. Samples were analyzed directly in the 96-well filter plate with an exposure time of 5 min per well.

Table 7.2: UPLC analytic.

	Gradient (A:B)[a] [%]	Detection wavelength [nm]
CVD	80:20	331
CNZ	90:10	230
MFQ	90:10	222
PMZ	90:10	214
TMX	90:10	223
TFD	70:30	260

[a]Mobile phase A: deionized water with 0.1% (v/v) triethylamine adjusted to pH 2.2 with methanesulfonic acid Mobile phase B: acetonitrile

7.2.4 ^{1}H NMR spectroscopy

Solutions for NMR analyses were prepared by suspending APIs for 24 h in a 0.5% (w/w) EPO-solution in deuterium oxide (D_2O) at pH 6.0. Samples were then centrifuged and supernatants (550 µl) were transferred to short disposable 5 mm NMR tubes.

All NMR measurements were performed with a Bruker 600 MHz Avance II spectrometer equipped with a cryogenic QCI probe head at a temperature of 300 K. Spectrometer operation and data processing was done by Topsin 2.1 software (Bruker, Fällanden, Switzerland). For all samples matching/tuning of the probe head and the 90° pulse were determined fully automated. Pseudo 2D ^{1}H diffusion ordered spectroscopy (DOSY) with bipolar gradient pulse pairs and 2 spoil gradients[175] was measured for all samples with presaturation of residual water. Data points (32 k) were

acquired over 18 ppm sweep-width and the interscan delay was set to 1.5 s. SMSQ10.100 shaped bipolar gradient was ramped from 2.65 to 50.35 gauss/cm in 16 equidistant steps. Spectra were processed with a lb = 1 exponential filtering and a diffusion time of 300 ms was used.

Diffusion coefficient *D* was fitted by use of the T_1/T_2 relaxation module implemented within the Topsin 2.1 software (Bruker, Switzerland). For most molecules at least one API and excipient related NMR signal was identified by visual inspection.

7.3 Results

7.3.1 Solubility and residual solid analysis

All excipient solutions were adjusted to pH 6.0 before incubation and following equilibration, the residual solid was analyzed by means of XRPD. Compared to water, all model compounds displayed a good solubility enhancement (SE) in the different EPO-solutions (Fig. 7.3-7.4 and Table 7.5). In addition to the measured aqueous solubilities of the model compounds, adjusted solubility values for pH 6.0 are displayed in Table 7.3. This extrapolation method was based on the Henderson-Hasselbalch equation and it is generally reliable when the experimental solubility value is within one pH unit difference.[190]

Table 7.3: Drug solubility and pH of drug suspensions in water after 24 h incubation time. Aqueous solubilities were adjusted for a pH 6.0.

Compound	Solubility in water (standard deviation, n=3) [mg/ml]	pH in water (standard deviation, n=3)	Adjusted solubility at pH 6.0 [mg/ml]
CVD	0.005 (0.002)	7.2 (0.3)	0.071
CNZ	0.001 (0.001)	6.1 (0.3)	0.001
MFQ	0.063 (0.001)	7.6 (0.1)	2.448
PMZ	0.002 (0.001)	6.8 (0.2)	0.013
TMX	0.008 (0.004)	6.9 (0.0)	0.064
TFD	0.002 (0.001)	6.8 (0.2)	0.013

Table 7.4: pH of drug suspensions in the presence of 0.5%, 2% and 5% EPO after 48 h at room temperature.

Compound	pH in EPO 0.5% after 48 h (standard deviation, n=3)	pH in EPO 2% after 48 h (standard deviation, n=3)	pH in EPO 5% after 48 h (standard deviation, n=3)
CVD	5.9 (0.0)	5.8 (0.1)	6.0 (0.0)
CNZ	5.7 (0.1)	6.0 (0.0)	5.9 (0.0)
MFQ	6.3 (0.1)	6.3 (0.0)	6.4 (0.0)
PMZ	5.8 (0.1)	6.0 (0.0)	6.0 (0.0)
TMX	5.9 (0.1)	5.9 (0.0)	6.0 (0.0)
TFD	5.8 (0.0)	6.1 (0.0)	6.0 (0.0)

pH values were also measured after 48 h for all basic compounds in EPO (0.5%, 2%, and 5%) (Table 7.4). The pH did not change for most compounds, only MFQ caused a pH increase to values of 6.3 and 6.4. Such a pH shift was expected given the dissolution of a basic compound. MFQ reached with 12 mg/ml at an EPO concentration of 5% the highest total solubility, which thereby caused the pH shift.

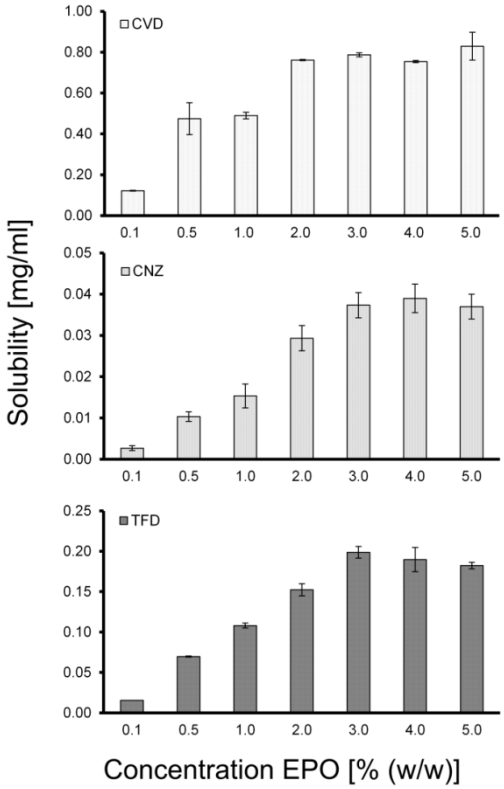

Figure 7.3: Solubility of CVD, CNZ, and TFD in EPO-solutions after 48 h at room temperature.

CVD, CNZ, and TFD (Figure 7.3) solubility reached a plateau at 2% EPO (w/w). In contrast, MFQ, PMZ, and TMX (Figure 7.4) showed an increase of solubility with polymer concentration up to 5% EPO.

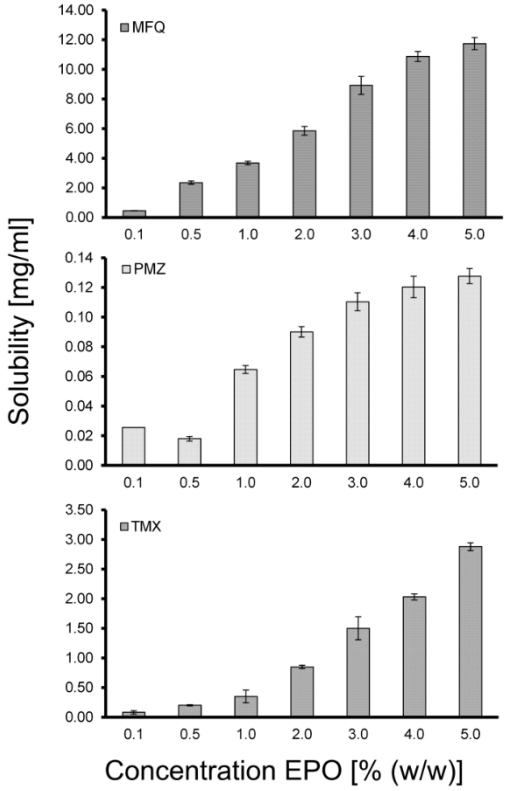

Figure 7.4: Solubility of PMZ, TMX, and MFQ in EPO-solutions after 48 h at room temperature.

Table 7.5: Adjusted solubility enhancement (SE) factors of model compounds in EPO-solutions (0.1-5%) compared to solubility in water (pH 6.0). SE factors were calculated by dividing the solubility of a compound in polymer solutions by the adjusted solubility in water at a pH 6.0. Non-adjusted values are displayed in brackets.

Compound	**SE in EPO**						
	0.1%	0.5%	1.0%	2.0%	3.0%	4.0%	5.0
CVD	1.7	6.7	6.9	10.7	11.1	10.6	11.7
	(24.3)	(94.9)	(97.9)	(152.3)	(157.4)	(150.9)	(165.9)
CNZ	2.7	10.3	15.3	29.3	37.3	39.0	37.0
	(2.7)	(10.3)	(15.3)	(29.3)	(37.3)	(39.0)	(37.0)
MFQ	0.2	1.0	1.5	2.4	3.6	4.4	4.8
	(7.2)	(37.3)	(58.3)	(92.8)	(141.5)	(172.5)	(186.2)
PMZ	2.0	5.4	5.0	6.9	8.5	9.3	9.8
	(12.8)	(35.3)	(32.3)	(45.0)	(55.2)	(60.2)	(63.8)
TMX	1.2	3.1	5.5	13.2	23.4	31.7	45.0
	(10.0)	(25.0)	(43.6)	(105.8)	(187.6)	(253.8)	(359.9)
TFD	2.5	6.6	8.3	11.7	15.3	14.6	14.0
	(16.0)	(43.2)	(54.0)	(76.2)	(99.3)	(94.8)	(91.2)

The true solubility enhancement by the drug-polymer interaction was calculated by comparing the aqueous solubility with the solubility in presence of the excipient at the same pH. Since the dissolution process of acidic or basic compounds influences the pH of unbuffered water, it was not possible to measure both solubilities at the same pH. Therefore, aqueous solubility values were adjusted for constant pH 6.0 according to the Henderson-Hasselbalch equation to calculate true solubility enhancement factors (Table 7.5). Also the non-adjusted values are practically relevant but obtained solubility enhancement is then a confounded effect of molecular excipient interactions as well as pH shift. Another solubility factor could have been a changed solid state during drug dissolution. However, the residual solid analysis confirmed that none of the tested compounds exhibited a solvent-mediated phase transformation. Thus, initial polymorphic forms remained the same during the course of the experiments.

7.3.2 ^{1}H NMR spectroscopy

^{1}H NMR spectra were analyzed to evaluate the interactions between EPO and the different compounds in solution. Peaks originating from protons of aromatic ring systems (present in all API molecules investigated) were observed between 5.50 and 8.50 ppm in D_2O for all APIs.

The NMR signals of all APIs in D_2O were very sharp (see Figure 7.5), indicating that API-molecules were dispersed in D_2O without substantial aggregation. All drugs had in common that API-related signals displayed changes in line-width in presence of EPO as shown for the two examples in Figure 7.5. Peaks derived from compounds could be still clearly observed although the peaks' shapes were comparatively much broader. Such line broadening suggests a form of aggregation and hence restricted molecular tumbling.

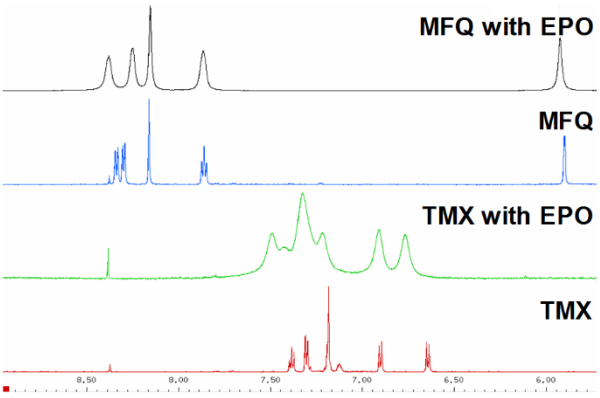

Figure 7.5: Solution-state ^{1}H NMR spectra of MFQ and TMX in the presence of EPO and in D_2O alone.

DOSY ^{1}H NMR was used to determine the diffusion coefficients of the APIs in D_2O with and without 0.5% EPO. Results are displayed in Table 7.6. The diffusion coefficient of EPO in presence of the APIs was also measured.

Table 7.6: Drug diffusion coefficient in D_2O with and without EPO as well as polymer diffusion coefficient in presence of the different APIs.

Compound	**Drug diffusion coefficient in D_2O x 10^{10} [m^2/s]**	**Drug diffusion coefficient in EPO 0.5% x 10^{10} [m^2/s]**	**Diffusion coefficient of EPO with API 0.5% x 10^{10} [m^2/s]**
	$D_{API(D2O)}$	$D_{API(EPO)}$	$D_{EPO(API)}$
CVD	4.60	3.53	0.43
CNZ	4.46	3.04	0.41
MFQ	4.65	2.62	1.03
PMZ	4.02	2.91	0.40
TMX	4.43	0.58	0.44
TFD	3.56	2.28	0.53
EPO*	0.38		

* Reference value of pure EPO in aqueous solution.

As expected, the much larger polymer EPO showed a lower diffusion coefficient in pure D_2O (10 to 15-fold) than the APIs alone. The diffusion coefficient of the APIs decreased in presence of EPO. This reduction was for most drugs rather moderate, whereas a relatively higher reduction in diffusion coefficient was observed with MFQ and most was the change for TMX. Interestingly, the diffusion coefficient of EPO increased in the presence of APIs.

7.4 Discussion

Previous research on the methacrylate-copolymer EPO was primarily motivated by investigating the ionic drug interactions of acids with the protonated amino alkyl group of EPO. [187, 188] Based on NMR data in solution, it was shown that additional hydrophobic molecular interactions with the polymer side chains were providing a notable contribution to overall molecular polymer-API association.[171, 187] These findings led to the present hypothesis that not only acids may benefit form solubilization by EPO. Accordingly, the present work focused on solubilization of basic APIs by EPO even though it may seem at first counterintuitive since both bases and EPO exhibit positive charges at pH values < 8.

Concentration dependent solubility data demonstrated that EPO had a beneficial effect on drug solubility of the basic model drugs. While the present hypothesis was aiming at some solubility enhancement in presence of the polymer, it was rather unexpected and highly remarkable to what extent the bases were showing increased solubilization. No general solubilization pattern was evidenced for the different compounds in the studied concentration range (Figures 7.3 and 7.4), but it is notable that half of the tested basic drugs showed a plateau regarding solubility enhancement starting at 2% EPO. Since for none of the model compounds polymorphic transformation was detected, the observed solubilization was therefore attributed to drug-EPO interactions in the liquid phase and not to a stabilization of a metastable polymorphic drug form. Due to the complexity of the API-polymer-interactions shown already for acidic drugs, [187] the interactions were studied more in detail by means of solution NMR spectroscopy. The NMR spectra of the APIs together with EPO displayed a change in peak width for the aromatic region indicating their interaction with the polymer.

Interesting were also the DOSY NMR findings. The diffusion coefficients of the APIs decreased to some extent in presence of the polymer (Table 7.6) and this change was most pronounced for TMX followed by MFQ. Although TMX, for example, reached high drug solubilization, there was no clear general correlation noted of SE with a change in drug diffusion coefficient. Changes in drug diffusion coefficient can be here primarily attributed to drug binding. Such binding could be readily quantified if the polymer itself keeps its value of the diffusion coefficient in presence of drug. However, this was interestingly not the case and EPO appeared to undergo itself diffusional changes because of the APIs (Table 7.6). Such a clear effect of altered EPO diffusion was not evidenced in a previous study of tested acidic compounds.[187] In the present study, the diffusion coefficient of the macromolecule was evidently diffusing faster in the presence of basic drugs compared to pure water. Faster movement of the polymer must be associated with conformational changes of the swollen macromolecule in solution. The conformation of polyelectrolytes like EPO depends greatly on its concentration in solution. In dilute solutions, the intra-chain interactions usually dominate over the inter-chain ones. [191] Thus, one can effectively consider a single polyelectrolyte chain with counterions surrounding it, whereas in more concentrated solutions, polyelectrolytes chains start to overlap. The

conformation of polyelectrolytes, e.g. EPO in solution is generally highly influenced by the presence and location of counterions.[191, 192] The insertion of additional positively charged drugs in this complex system of EPO chains and counterions is likely to cause structural changes. Since the polyelectrolyte conformation is controlled by the fraction of ionized groups, additional positive charges of the basic APIs that are attached via hydrophobic interactions to the polymer backbone may lead to weakening of electrostatic interactions and can promote conformational change like shrinkage of the polyelectrolyte chains.[191] When the majority of counterions condense to the polymer backbone, polyelectrolyte can even take conformations like spheres that are rather typical for neutral polymers. When the polymer chain shrinks or even forms spherical globules, it would move faster in solution, which is in line with our experimental NMR diffusion results.

The change in the polymeric conformation may help also to explain the observed solubilization pattern. The positively charged APIs are likely associated with the polymer by hydrophobic interactions between the aromatic systems of the compounds and the side chains of the polymer. However, there will be also a non-bound fraction of drugs. This fraction can interact with the free counterions in solution and influences the balance between polymer and counterions. Accordingly, complex drug-excipient interactions as evidenced by the NMR results were obviously forming the basis of the surprisingly high drug solubilization enhancement in EPO solutions.

7.5 Conclusions

EPO was earlier shown to be a potent solubilizer for acidic drugs in different formulation approaches. The present study now provides evidence for six positively charged (basic) compounds whose solubility was enhanced by the polymer EPO. Although some hydrophobic interactions were expected to occur, the high extent of solubility enhancement was surprising given the same positive charge type of aminoalkyl groups that abundantly exist in EPO. Results of ^{1}H-NMR spectroscopy in solution showed that molecular interactions between hydrophobic drug moieties, such as aromatic rings, interact with the polymer. Additionally, conformational changes of

the polymer were suggested by DOSY NMR data and such changes may further point to the hydrophobic interactions with the basic drugs. These findings broaden the application area of EPO, especially for simple formulations like suspensions and solutions that can be used in early phases of the drug development process. Additionally, important insights were gained into the mechanisms of drug-EPO interactions. Our results indicate that beyond obvious charge-driven interactions between APIs and excipients additional (hydrophobic) interactions may play a role and should be considered in excipient selection.

.

Chapter 8

Interactions of dimethylaminoethyl methacrylate copolymer with non-acidic drugs demonstrated high solubilization *in vitro* and pronounced sustained release *in vivo*

Summary

Recent work demonstrated remarkable solubilization effects of methacrylate-copolymer Eudragit EPO (EPO) not only with acidic drugs but interestingly also with poorly soluble basic compounds. The current work studied EPO-mediated solubilization effects first *in vitro* using felodipine (FLP) and tamoxifen (TMX) as model compounds. EPO-containing solutions were subsequently compared in a rat pharmacokinetic study against reference solutions and suspensions. Surprisingly, solution formulations with EPO did not result in an increased relative oral bioavailability. Exposure was reduced for both drugs and plasma-profiles of the EPO solutions showed a delayed and lower maximum plasma concentration compared to the reference formulations. This sustained *in vivo* release was likely due to combined effects of strong drug-polymer interactions and pH-dependent precipitation of the polymer in the rat intestine. Remarkable was that *in vitro* drug-polymer coprecipitates did not reveal crystalline drug by polarized light microscopy. Thus, such a formulation approach provides a rather simple opportunity to modify drug release *in vivo*. However, this may be rather an approach for preclinical formulations, if high peak-to-trough ratios of plasma levels are problematic regarding adverse effects

Saal et al. Interactions of dimethylaminoethyl methacrylate copolymer with non-acidic drugs demonstrated high solubilization *in vitro* and pronounced sustained release *in vivo*, *European Journal of Pharmaceutics and Biopharmaceutics*, **2018**, 125, 68-75.

related to C_{max} or if plasma concentrations drop too fast below required pharmacological concentrations.

8.1 Introduction

Several enabling formulation techniques have been developed for oral delivery of poorly water-soluble drugs. [4, 193] They are either based on methods increasing dissolution rate and/or solubility of drug candidates. Such methods include particle size reduction, crystal modification, self-emulsifying systems, polymeric and lipid nanoparticles, solid dispersions or the use of cosolvents. [6, 7, 9] All of these approaches have specific advantages and limitations. For example, particle size reduction can lead to formulation issues regarding powder flow, electrostatic forces, or wettability; and crystal modifications may not be feasible with all compounds. [64, 161] Formulations based on lipid delivery or on solid dispersion technology are often rather sophisticated and therefore are mainly of interest for later stage pharmaceutical development and for the market, whereas simpler approaches are used for an early formulation phase. [131, 167] The early formulation supply typically comes with additional needs such as simplicity, speed, and possible dosing via gavage. This aim for simplicity is often in contrast to the complex biopharmaceutical task to adequately deliver poorly soluble drugs. In this context, the use of functional copolymers in solutions offers much potential; however it still requires a proper understanding of drug-polymer interactions *in vitro* and *in vivo*.

Eudragit EPO (EPO) was introduced originally as pharmaceutical excipient for taste masking and moisture protection. [169] It belongs to the family of methacrylic acid copolymers and the aminoalkyl chain has a pK_a value of 8. The chemical structure of EPO is displayed in Figure 8.1.

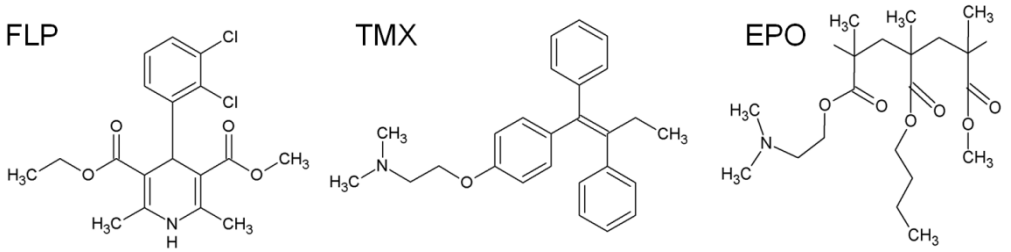

Figure 8.1: Chemical structure of the model drugs felodipine (FLP), tamoxifen (TMX) and Eudragit EPO (EPO).

EPO has further been used for solubility improvement of poorly soluble acidic drugs in solid dispersions and outstanding bioavailability enhancement was evidenced. [170-172] More recently, EPO was applied as a solubilizer to simple solution formulations of acidic drugs. The relevant molecular mechanisms leading to a significant solubility enhancement were analogous to those of solid dispersions. [187] Drug solubilization was promoted by both ionic interactions with deprotonated anionic drugs and hydrophobic interactions between aromatic moieties of pharmaceutical compounds and backbone and alkyl-side chains of the polymer. [171, 187] Since the solubility enhancement is not exclusively caused by ionic interactions, EPO was also shown to be a potent solubilizer also for basic compounds. [187, 194] While the solubility enhancement *in vitro* is rather impressive, it remains to be shown how such polymeric drug solutions would perform *in vivo*.

The present work used felodipine (FLP) and tamoxifen (TMX) formulated as EPO solutions as typical examples of poorly soluble compounds. FLP (pK_a 4.4 (basic), see Table 8.1) is protonated at pH < 4 and can be therefore charged in the stomach, whereas it is mostly unionized in the small intestine. Thus, variations in pH may barely influence its solubility at least in the small intestine. On the other hand, TMX is a more basic compound (pK_a 9.7) and it keeps the protonated form as it passes from the stomach to the intestinal tract. The structures of both compounds are displayed in Figure 1. FLP is a dihydropyridine calcium channel blocker widely used as a potent anti-hypertensive drug [195] whereas TMX is an oral nonsteroidal antiestrogen that has

been considered as a gold standard in the treatment and prevention of all stages of estrogen-receptor-positive breast cancer. [196, 197] However, due to their poor solubility, the oral bioavailability is < 30% and is for TMX additionally reduced by enzymatic degradation.[196]

Table 8.1: Molecular weight (Mw), ionization constant (pK_a), distribution coefficient (log$D$) at pH 6.0 and solubility in fasted state simulated gastric (FaSSGF) and intestinal (FaSSIF) fluid for the different model compounds.

Compound	**Mw [g/mol]**	**pK_a**[a]	**Log$D$**[b] **(pH 6.0)**	**Solubility [mg/ml] at 37°C in**	
				FaSSGF	FaSSIF
Felodipine (FLP)	384.3	4.4 (basic)	3.4	na[c]	0.026 ± 0.001
Tamoxifen (TMX)	371.2	9.7 (basic)	3.7	0.035 ± 0.000	0.230 ± 0.005

[a]Measured pK_a-values via photometric titration (Roche internal data).
[b]Values calculated by Marvin Suite (V. 16.5.30, ChemAxon, Douglas Drake, USA).
[c]na: Value not available, concentration below limit of detection.

Both model compounds were first evaluated for their solubility enhancement in presence of different EPO concentrations *in vitro*. Second, drug-EPO solutions were compared to solutions with cosolvents or pH adjusted solutions, and conventional suspensions in rats to study the influence of EPO on the pharmacokinetics of the drugs *in vivo* at preclinical doses.

8.2 Materials and Methods

8.2.1 Materials

Tamoxifen (TMX) and acetic acid were from Sigma Aldrich (Buchs, Switzerland) and felodipine (FLP) from Melrob-Eurolabs (Congleton, UK). The ionization constant (pK_a) was measured by photometric titration whereas values for the distribution coefficient (log$D$) were calculated by the molecular modeling suite Marvin 16.5.30 (ChemAxon Inc., Douglas Drake, US). Aminoalkyl metacrylate copolymer E, Eudragit EPO, (EPO) was obtained from Evonik (Darmstadt, Germany), methylcellulose (MC) was supplied by Colorcon Inc. (Harleysville, USA) and

polyethylene glycol 400 (PEG 400) was from Clariant SE (Muttenz, Switzerland). Hydrochloric acid (0.1 M) and sodium hydroxide solution (0.1 M) were purchased from Merck KGaA (Darmstadt, Germany). The SIF® powder was purchased from Biorelevant (Croydon, UK) and used to produce original fasted-state simulated intestinal fluid (FaSSIF, pH 6.5) and original fasted-state simulated gastric fluid (FaSSGF, pH 1.6). Although these media were developed to mimic the human situation [101] the classical compositions serve here as an initial experimental model for *in vivo* solubilization in rodents.

8.2.2 Sample preparation

Polymer solutions were prepared by dissolving EPO (3% and 5% (w/w)) or MC (0.5% (w/w)) in deionized water that was acidified and subsequently adjusting to pH 6.0 with hydrochloric acid or sodium hydroxide at 25°C. Solutions were filtered and checked carefully for absence of particles. The dosing solutions employed in the *in vitro* tests and in the *in vivo* study are specified in Table 8.2.

Final formulations were prepared by weighing the required amount of FLP or TMX into a glass bottle, addition of vehicle and stirring for 48 h at room temperature protected from light. TMX dissolved in acetic acid (40 mM) resulted in a final pH of 3.5. The dosing solutions were analyzed by LC-MS/MS using a Waters Acquity UPLC system equipped with an Acquity UPLC BEH phenyl column (2.1x30 mm, 1.7 µm particle size) from Waters (Milford, USA) and a PE Sciex API400 mass spectrometer (AB Sciex Pte. Ltd, Concord, Canada) in a positive ion mode. The analytes were detected by multiple reactions monitoring (MRM). Measured drug concentrations were used for pharmacokinetic calculations. Formulations for groups 1, 2, 4, and 5 were administered as clear solutions, whereas formulations for groups 3 and 6 were fine suspensions.

Table 8.2: Composition and concentrations of dosing solutions.

Compound	Group	Vehicle	Nominal dosing concentration [mg/ml]
Felodipine	1	EPO solution 5% (w/w) pH 6.0	0.4
	2	PEG 400 + water (chaser)	4
	3	MC solution 0.5% (w/w) pH 6.0	0.4
Tamoxifen	4	EPO solution 3% (w/w) pH 6.0	1
	5	Acetic acid (40 mM)	1
	6	MC solution 0.5% (w/w) pH 6.0	1

Final formulations were prepared by weighing the required amount of test article into a glass bottle, adding the vehicle and stirring for 48 h at room temperature protected from light. The dissolution of TMX in acetic acid (40 mM) resulted in a pH of 3.5. The dosing solutions were analyzed by LC-MS/MS using a Waters Acquity UPLC system equipped with an Acquity UPLC BEH phenyl column (2.1x30 mm, 1.7 µm particle size) from Waters (Milford, USA) and a PE Sciex API400 mass spectrometer (AB Sciex Pte. Ltd, Concord, Canada) in a positive ion mode. The analytes were detected by multiple reactions monitoring (MRM). The measured dosing solution concentration was used for pharmacokinetic calculations. Formulations for groups 1, 2, 4, and 5 were administered as clear solutions, whereas formulations for groups 3 and 6 were fine suspensions.

8.2.3 Solubility and residual solid analysis

EPO-solutions for solubility measurements were prepared as described in the section above and adjusted to pH 6.0 with hydrochloric acid or sodium hydroxide at 25°C. Solubility of compounds in EPO-solutions was determined using a slightly modified 96-well SOlubility and REsidual SOlid Screening (SORESOS) assay [56] as described before. [90] In brief, APIs were dispensed using the powder-picking-method [103] in a 96-well flat bottom plate (Corning Inc., Durham, USA). After adding stirring bars and

excipient solutions (150 µl), the plate was sealed with pre-slit silicon caps and the mixtures were agitated by head-over-head rotation for 48 h at room temperature. After mixing, the suspensions were carefully transferred into 96-well filter plates and liquid was separated from residual solid by centrifugation. Filtrates were collected, diluted with N-methyl-2-pyrrolidone and drug content in filtrates was determined using a Waters Acquity Ultra Performance Liquid Chromatographic (UPLC) system equipped with a 2996 Photodiode Array Detector and an Acquity UPLC BEH C18 column (2.1x50 mm, 1.7 µm particle size) from Waters (Milford, USA). The mobile phase consists of a mixture of deionized water with 0.1% (v/v) trimethylamine which was adjusted to pH 2.2 (mobile phase A) and pure acetonitrile (mobile phase B). An isocratic flow with a gradient of 40:60% (A:B) for FLP and a gradient of 90:10% (A:B) for TMX was applied for 0.3 min at a flow rate of 0.75 ml/min. Subsequently, the concentration of solvent B was linearly increased to 100% within 0.5 min. The substances were detected at wavelengths of 238 nm (FLP) and 223 nm (TMX). Solid state analysis of the residual solid was performed by X-ray powder diffraction (XRPD) using a STOE Stadi P Combi diffractometer as described before. [56] Samples were analyzed directly in the 96-well filter plate with an exposure time of 5 min per well.

8.2.4 Precipitation of polymer in presence and absence of APIs

EPO exhibits pH-dependent solubility with highest values at pH< 5.0. Above pH 6.0, the polymer does not dissolve but only swells. The precipitation behavior of polymer solutions (3% and 5%) with and without APIs was studied in pH range 6.0 to 9.0 by adjusting the pH in intervals of 0.5 units. After magnetic stirring for 30 min, solutions and precipitates were visually inspected. The solid state of precipitates was analyzed by XRPD as described above and polarized light images of the precipitates were taken using a Zeiss Axiolab microscope (Carl Zeiss AG, Jena, Germany).

Drug concentration in the supernatant was quantified by UPLC after dilution with N-methyl-2-pyrrolidon as described above. Drug concentration in the precipitated phase

was calculated based on nominal total amounts and measured drug concentrations in the supernatant.

8.2.5 Dynamic image analysis

The particle size and shape of the precipitate of formulations 2 (PEG solution with FLP) and 3 (MC-suspension with FLP) in biorelevant media were assessed by dynamic image analysis with an XPT-C particle analyzer (PS-Prozesstechnik GmbH, Basel, Switzerland) with a peristaltic pump (Ismatec SA, Glattbrugg, Switzerland) that transported the samples through a measuring cell equipped with a Flea 2, 1392 × 1032 pixel CCD camera to analyze the size of precipitated samples (n=1000). Formulations were suspended in biorelevant media in 1:1 (v/v) ratio (FaSSGF) and 1:3.3 (v/v) ratio (FaSSIF). The number of crystals was detected in each sample by analyzing the pictures using the XenParTec software (Version 5.1, TechApp Switzerland). The particle size was expressed as Waddle disk diameter, which is the diameter of a disk with the same area as the detected particle. The particle size and shape of precipitated formulation 2 (PEG solution with FLP) and of formulation 3 (MC-suspension with FLP) in biorelevant media were assessed by dynamic image analysis with an XPT-C particle analyzer (PS-Prozesstechnik GmbH, Basel, Switzerland) with a peristaltic pump (Ismatec SA, Glattbrugg, Switzerland) that transported the samples through a measuring cell equipped with a Flea 2, 1392 × 1032 pixel CCD camera to analyze the size of precipitated samples (n=1000). Formulations were suspended in biorelevant media in 1:1 (v/v) ratio (FaSSGF) and 1:3.3 (v/v) ratio (FaSSIF). The number of crystals was detected in each sample by analyzing the pictures using the XenParTec software (Version 5.1, TechApp Switzerland). The particle size was expressed as Waddle disk diameter, which is the diameter of a disk with the same area as the detected particle.

8.2.6 *In vivo* pharmacokinetics after oral administration

8.2.6.1 Animals and dosing protocol

The non-clinical pharmacokinetic study was conducted at Absorption systems (Exton PA, USA) and the protocol followed established practice and operating procedures. In brief, male Sprague-Dawley rats of 280 g to 310 g were obtained from Hiltop Labs (Scotsdale, USA). The animal experiments were approved by the internal Absorptions Systems IACUC review board and were therefore in accordance with National Institutes of Health guide for the care and use of laboratory animals. [198] Food was withdrawn 12 h prior to the test article administration with water offered *ad libitum.* No food was allowed until four hours post dose. The animals were randomly divided into six groups each with six animals. FLP-formulations were administered at a dose of 4 mg/kg and TMX-formulations at a dose of 10 mg/kg. For group 2, water was immediately administered after administration of the FLP solution in PEG 400 to achieve a 1:10 dilution of the PEG 400 solution *in vivo*. Blood samples (~0.3 ml) were taken from the jugular vein pre-dose and at 15, 30 min and 1, 2, 4, 8 and 24 h following oral administration. Blood samples were collected into heparin. Plasma samples were obtained immediately by centrifuging blood samples at a temperature of 2 to 8°C at 3000 x g for 5 min, after which plasma samples were transferred into polypropylene tubes and stored frozen until further analysis.

8.2.6.2 Determination of felodipine and tamoxifen in plasma

Plasma concentrations of the test articles were determined by LC-MS/MS. Plasma samples of the FLP-group were extracted by liquid-liquid extraction with methyl-t-butyl whereas TMX-samples were extracted by protein precipitation with acetonitrile. Extracted samples were reconstituted in 75:25 acetonitrile: water mixture and chromatographic extraction was performed using a Waters Acquity UPLC system equipped with an Acquity UPLC BEH phenyl column (2.1x30 mm, 1.7 μm particle size) from Waters (Milford, USA).

The column temperature was maintained at 40 °C with water containing 10% ammonium formate buffer (40 mM) (mobile phase A) and acetonitrile containing

10% ammonium formate buffer (40 mM) (mobile phase B) as the mobile phase at a flow rate of 0.8 ml/min. The following gradient program was used for sample separation: 0-0.75 min, 80% A; 0.75-0.80 min, 2% A; 0.8-1.0 min, 80% A. The PE Sciex API400 mass spectrometer (AB Sciex Pte. Ltd, Concord, Canada) was operated in a positive ion mode and the analytes were detected by multiple reactions monitoring (MRM).

8.2.6.3 Pharmacokinetic data analysis

Pharmacokinetic parameters were calculated from the time course of the plasma concentrations and were determined with Phoenix WinNonlin (V. 7.0) software (Certara USA, Inc., Princeton, USA) using a non-compartmental model. The maximum plasma concentration (C_{max}) and the time to reach maximum plasma concentration (t_{max}) after oral dosing were observed from the data. The area under the time-concentration curve (AUC) was calculated using the linear trapezoidal rule with calculation to the last quantifiable data point. Plasma half-life ($t_{1/2}$) was calculated from 0.693/slope of the terminal elimination phase. Mean residence time (MRT) was calculated by dividing the area under the moment curve (AUMC) by the AUC. Any sample below the limit of quantification was treated as zero for pharmacokinetic data analysis.

The software package SigmaPlot V. 11.0 (Scystat Software Inc., San Jose, USA) was used for all statistical calculations. For each compound, an Analysis of the Variance (ANOVA) was comparing the three formulations with respect to the different pharmacokinetic responses. For those analyzes in which $p < 0.05$ was found, the Holm-Sidak-method for pairwise multiple comparison was conducted to study individual differences between groups.

8.3 Results

8.3.1 Solubility and residual solid analysis

A basic physico-chemical characterization of FLP and TMX is shown in Table 8.1. The solubility of FLP and TMX was determined at different polymer concentrations and values were compared to their aqueous solubility. Both compounds exhibited particularly low solubility in pure water; the solubility of FLP and TMX in water was 0.0004 (± 0.0001) mg/ml and 0.008 (± 0.004) mg/ml, respectively. In comparison, presence of EPO increased the aqueous solubility of both compounds substantially. Even at very low polymer concentrations (0.1% (w/w)), the solubility of FLP was 66-fold and of TMX 10-fold enhanced. At the highest tested polymer concentration (5% EPO (w/w)), solubility was 0.5 mg/ml for FLP (1250-fold) and 2.9 mg/ml for TMX (363-fold) (Figure 8.2).

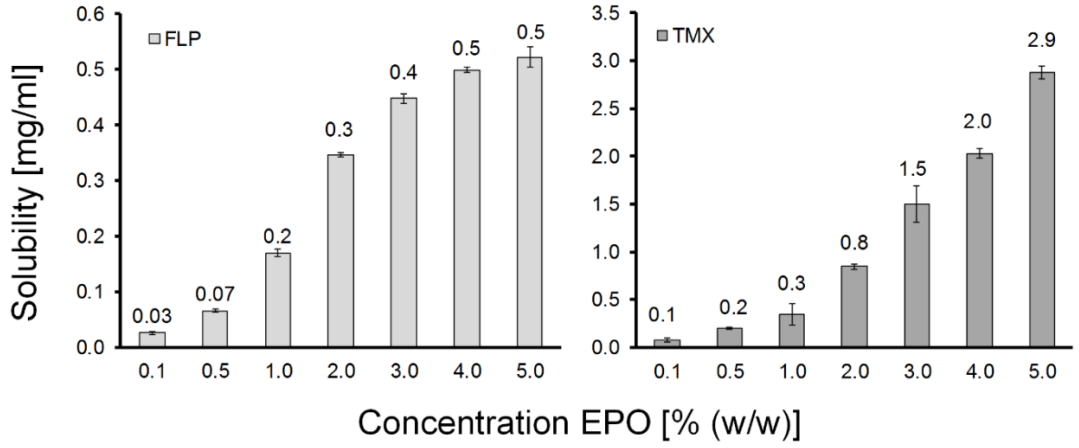

Figure 8.2: Solubility of FLP and TMX in EPO-solutions (pH 6.0) after 48 h equilibration at room temperature.

8.3.2 Precipitation *in vitro* of EPO with and without API

EPO exhibits pH-dependent solubility, dissolves rather fast at pH-values < 5.0 (stomach) and is therefore used for taste masking and moisture protection of

immediate-release solid dosage forms. The precipitation behavior of this polymer from a solution was tested in presence and absence of APIs. EPO precipitated between pH-values of 7.0 and 7.5 (Figure 8.3). Slight differences in precipitation behavior were observed when EPO-solutions with different concentrations were compared. At a higher polymer-concentration (5%) (Figure 8.4) small polymer flakes were visible even at a pH of 7.0. In contrast, at the same pH, the 3%-polymer solution was completely clear.

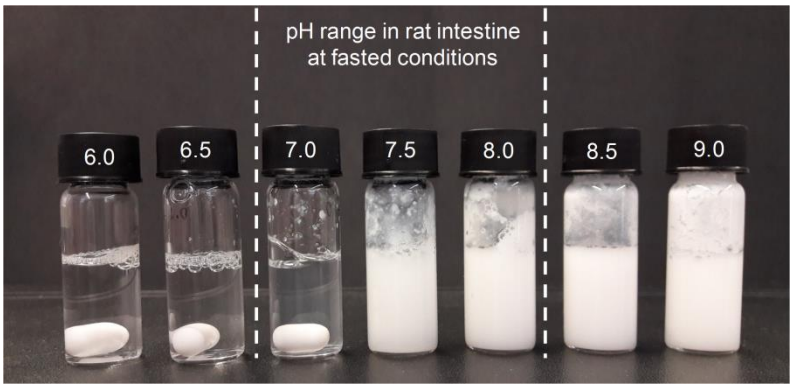

Figure 8.3: Precipitation of EPO (3%-solution) in a pH-range between 6.0 and 9.0. Lines indicate the pH-range of rats' intestine according to Kararli et al.[199]

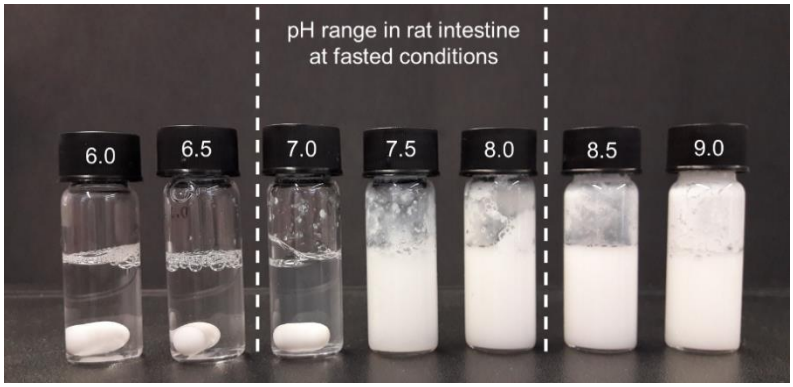

Figure 8.4: Precipitation of EPO (5%-solution) in a pH-range between 6.0 and 9.0. Lines indicate the pH-range of rats' intestine according to Kararli et al.[199]

Concentrations of the APIs in the supernatant were measured and used to calculate drug in the precipitated phase. For both drugs, the amount in the precipitated phase was close to 100% (100% (FLP), 99.6% (TMX)) and almost no drug could be detected in the aqueous phase.

8.3.3 Characterization of the *in vitro* formulations precipitates of FLP

8.3.3.1 Dynamic image analysis

The particle size of the precipitate of formulation 2 (PEG solution with FLP) and of the suspended particles in formulation 3 (MC-suspension with FLP) in biorelevant media was determined by dynamic particle analysis (Table 8.3).

Table 8.3: Measured waddle disk diameter and Heywood circularity factor of FLP-precipitate of PEG 400 solution and MC suspension in biorelevant media (mean values ± SD, n=1000).

Formulation	Medium	Waddle disk diameter [µm]	Heywood circularity factor
PEG 400 solution	FaSSGF	14.80 ± 0.58	0.97 ± 0.01
	FaSSIF	6.61 ± 0.91	0.92 ± 0.04
MC suspension	FaSSGF	5.94 ± 0.26	0.90 ± 0.01
	FaSSIF	6.10 ± 0.22	0.91 ± 0.01

FLP particles of the precipitate from the PEG-solution in FaSSGF were approximately three times larger than those in the MC-suspension. Since FLP is only suspended in the MC-vehicle and not dissolved, it is likely that no precipitation takes place upon dilution in biorelevant media. The shape of the particles did not differ between media and formulations. For all, circularity factors close to one were obtained indicating that the particles' shape in the two-dimensional projection was close to a disk.

8.3.3.2 Solid state analysis of the in vitro *precipitate*

The solid state of the EPO-drug-precipitate at pH 8.0 was analyzed by both XRPD (data not shown) and images obtained by polarized light microscopy (Figure 8.5). The XRPD results showed the absence of birefringent crystalline material in the coprecipitate of polymer and drugs.

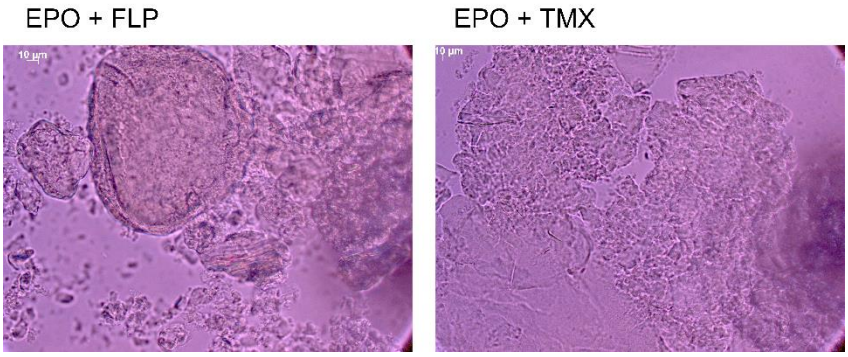

Figure 8.5: Polarized light imaged of coprecipitate (pH 8.0) of EPO with FLP (left) and EPO with TMX (right).

8.3.4 *In vivo* pharmacokinetics after oral administration

8.3.4.1 Felodipine

The plasma concentration-time profiles following a single oral administration of 4 mg/kg FLP in different formulations are presented in Figure 8.6, and the corresponding pharmacokinetic parameters are summarized in Table 8.4.

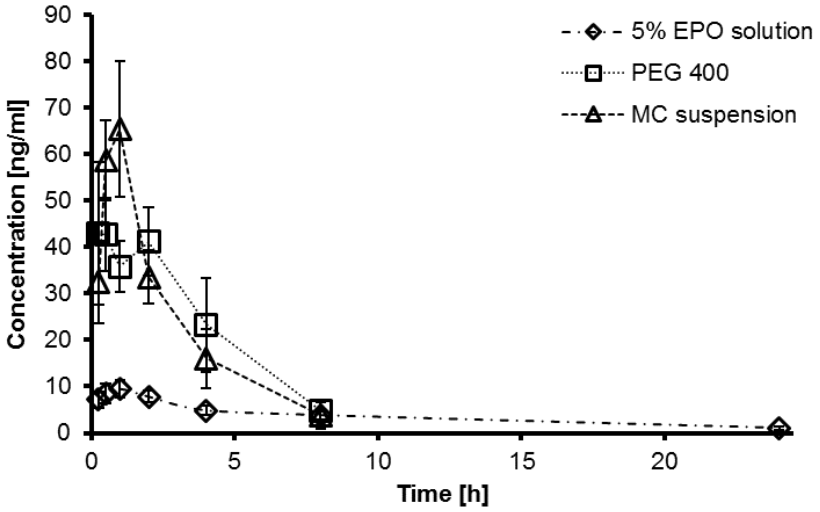

Figure 8.6: Average plasma drug-concentration versus time profiles after oral administration of FLP-formulations in rats. Values are mean ± SD (n=6/group/time point).

Table 8.4: Pharmacokinetic parameters of FLP-formulations after single oral administration of 4 mg/kg body weight to rats. Values are mean ± SD (n=6/group/time point).

Parameters	EPO solution (1)	PEG 400 solution (2)	MC suspension (3)
C_{max} [ng/ml]	10.3 ± 1.4	48.0 ± 11.6	67.4 ± 12.7
t_{max} [h]	2.1 ± 2.9	0.7 ± 0.7	0.8 ± 0.3
AUC_{last} [h ng/ml]	69.0 ± 38.0	195.0 ± 47.8	185.0 ± 31.0
Dose-normalized AUC_{last} [h kg ng/ml/mg]	18.4 ± 10.1	51.5 ± 12.6	39.5 ± 6.6
$t_{1/2}$ [h]	6.4 ± 2.7	2.0 ± 0.4	1.9 ± 0.3

The main pharmacokinetic parameters, C_{max}, $t_{max,}$ and dose-normalized AUC were statistically analyzed regarding differences between the groups. In summary, the post-hoc statistical test revealed differences in C_{max} between formulations 1 and 2 (p< 0.001), 1 and 3 (p< 0.001) as well as 2 and 3 (p= 0.004). There were also significant differences shown in the dose-normalized AUC between formulations 1 and 2 (p< 0.001) as well as 1 and 3 (p= 0.002).

FLP displayed an exposure peak post dosing between 30 minutes and five hours for group 1 (EPO solution), 15 minutes and two hours for group 2 (PEG 400 solution), and 30 minutes and one hour for group 3 (MC-suspension). However, these differences in t_{max} were statistically not significant, which was mainly attributed to high variability displayed by formulation 1. Oral bioavailability (dose-normalized AUC_{last}) was comparable in groups 2 and 3, however bioavailability in group 1 was significantly lower (18.4 vs 51.5 vs 39.5 h·kg ng/ml/mg). C_{max} differed significantly between formulations (10.3 vs 48.0 vs 67.4 ng/ml) and also the half-life was slightly increased in group 1 compared to group 2 and 3 (2.1 vs 0.8 vs 0.7 h).

8.3.4.2 Tamoxifen

The plasma concentration-time profiles of 10 mg/kg TMX following a single oral administration are presented in Figure 8.6. A summary of the average of the pharmacokinetic parameters of all TMX-formulations is shown in Table 8.5. The statistical post-hoc analysis revealed differences between the groups for all

pharmacokinetic parameters. In summary, C_{max} values were different between formulations 4 and 5 ($p< 0.001$) and 4 compared with 6 ($p< 0.001$). Differences in t_{max} were significant between formulations 4 and 5 ($p= 0.005$) as well as 4 and 6 ($p= 0.018$). Finally, the dose-normalized AUC showed differences 4 and 5 ($p= 0.005$) and between 4 and 6 ($p< 0.001$).

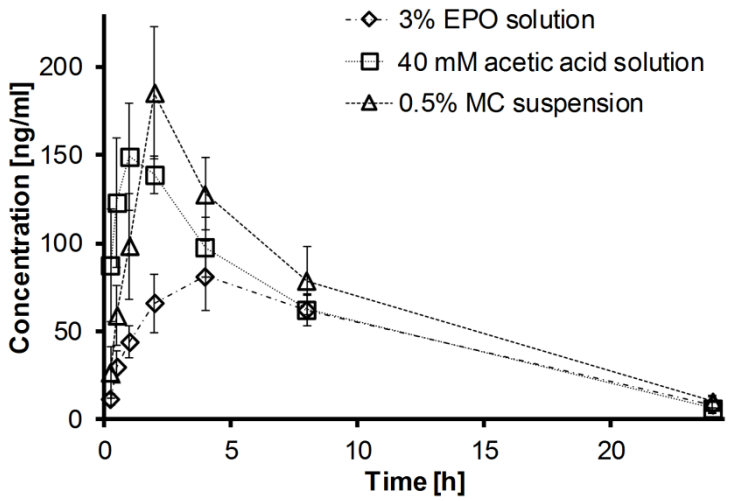

Figure 8.6: Average plasma drug-concentration versus time profiles after oral administration of TMX-formulations in rats. Values are mean ± SD (n=6/group/time point).

Table 8.5: Pharmacokinetic parameters of TMX-formulations after single oral administration of 10 mg/kg body weight to rats. Values are mean ± SD (n=6/group/time point).

Parameters	EPO solution (4)	Acidic solution (5)	MC suspension (6)
C_{max} [ng/ml]	86.2 ± 14.4	157.0 ± 23.4	185.0 ± 37.5
t_{max} [h]	4.0 ± 2.2	1.5 ± 0.5	2.0 ± 0.0
AUC_{last} [h ng/ml]	1077.0 ± 95.8	1358.0 ± 143.0	1633.0 ± 239.0
Dose-normalized AUC_{last} [h kg ng/ml/mg]	133.5 ± 11.9	172.8 ± 18.2	198.4 ± 29.0
$t_{1/2}$ [h]	6.5 ± ND	5.0 ± 0.6	5.5 ± 0.5

ND: not determined

Following oral dosing of 10 mg/kg TMX maximum plasma concentrations post dosing were observed between 2 and 8 hours for group 4 (3% EPO solution), between

1 and 2 hours for group 5 (acetic acid solution) and at 2 hours for group 6 (MC-suspension). Oral bioavailability was significantly higher in groups 5 and 6 compared to group 4. The maximum plasma concentrations (C_{max}) was significantly lower in group 4 compared to groups 5 and 6 (86.2 vs 157.0 vs 185.0 ng/ml).

8.4 Discussion

Pharmaceutical development of poorly soluble drugs needs potent solubilizers to cope with oral delivery challenges. A particularly interesting polymer is EPO and initial work on solubilization was focusing on acidic compounds and on stabilization of the amorphous state. [170, 171] Moreover, it was recently shown that EPO can also greatly enhance solubility of crystalline acids via a mixture of ionic and hydrophobic interactions in the bulk phase. [187] Deprotonated acids would interact to a relevant degree with the dimethylaminoethyl group of the polymer but there were also notable hydrophobic interactions with the polymeric side chains evidenced. NMR data suggested that this contribution was especially important in case of aromatic drugs. [170, 187] Additionally, Kojima et al. evaluated the oral absorption of mefenamic acid from a supersaturated solution obtained by dissolving a cryo-grinded mixture of EPO and mefenamic acid in acetate buffer. [170] This supersaturated solution was compared with a suspension consisting of mefenamic acid in 0.5% carboxymethylcellulose-solution and a dispersion of a physical mixture of EPO and mefenamic acid in acetate buffer. The administration of the supersaturated solution resulted in enhanced oral bioavailability *in vivo*.

For the present study, two compounds were selected that revealed a rather surprising solubility enhancement in combination with EPO. Both are not expected to interact via ionic interactions with the dimethylaminoethyl groups since FLP is apparent neutral and only charged at pH < 4 and TMX is positively charged up to a pH-value of around 9-10. The solubility enhancement is therefore likely caused only by the hydrophobic interactions of the lipophilic and aromatic moieties of the APIs and the side chains of the polymer. A previous study showed pronounced solubility enhancement with the tested bases, which was in line with the current findings of FLP

and TMX together with EPO. [194] Similar to the aforementioned *in vivo* results with mefenamic acid and EPO, the present work addresses the question to which extent the remarkable *in vitro* solubilization by EPO would translate into an enhanced *in vivo* drug exposure for non-acidic model drugs.

In the case of FLP, the oral bioavailability in rats of an EPO-solution was compared with two other liquid formulations with the same dose. Surprisingly, the reference formulations, a cosolvent-solution and a suspension exhibited higher bioavailability than the EPO-solution. Moreover, other pharmacokinetic parameters were affected by the presence of EPO. While the AUC between the suspension and the cosolvent-solution did not differ statistically significant, both C_{max} and bioavailability of the EPO-solution were lower. The time to reach the maximum concentration appeared different, however was not statistically significant. In contrast to the suspension and the cosolvent-solution there was no sharp peak in the first three hours in the EPO-solution group.

In the case of TMX, the reference formulations were a suspension and a pH-adjusted solution. For TMX, the EPO solution also showed the lowest bioavailability. Additionally, the time needed to reach the maximum plasma concentration was significantly delayed in the EPO-solution group (Figure 7).

Oral administration of cosolvents-solutions is followed by a dilution with aqueous media *in vivo* and precipitation is likely to occur during this dilution step. As shown in Table 3, particles originating from precipitation of cosolvent-solution with FLP in biorelevant media had a larger particle size compared to particles in the MC-suspension. Since larger particles have a smaller surface area available for dissolution this may explain the lower C_{max} of the cosolvent-solution compared to the suspension. In contrast, the AUC of both formulations was comparable. Several studies showed that the particle size influences the dissolution rate as well as the oral bioavailability of a compound. [200-202] Since the precipitation takes place as soon as the formulation enters the rats' gastrointestinal tract, it seems that the precipitate can still dissolve and obtain a sufficient bioavailability.

It is likely that the pH-dependent solubility of the polymer is of relevance for the obtained findings. Best solubility is obtained at low pH, which has been utilized, for

example, to enable fast disintegrating tablets. [203, 204] However, EPO was shown to precipitate at elevated pH values. We found that EPO precipitates mainly between pH 7.0 and 7.5 which is in good agreement with literature reports.[205] The pH-range in rats' intestine (at fasted conditions) was reported between 7.1 and 8.0 [199] but it should be added that no final consensus on this exact pH range is given in the literature. [206] For relatively higher pH values, EPO is expected to precipitate in the intestinal passage. A concomitant precipitation of drug and polymer is a likely mechanism that would explain the observed decrease in the maximum plasma concentration as well as the delayed t_{max} for TMX and a decreased AUC for FLP and TMX (Figures 6 and 7). This is also supported by the *in vitro* precipitation results which showed that only a very low amount of API was in the supernatant and that most of the drug co-precipitated with the polymer. Interestingly, previous co-precipitation experiments from EPO-drug solutions e.g. with ondansentron hydrochloride and metoclopramide hydrochloride resulted in drug-polymer-complexes. [203, 204] This complexation of polymer and drugs led to a taste-masked formulation which was releasing the drugs in gastric conditions immediately. Additionally, the authors showed that the drug was still in a crystalline solid state even after complexation with the polymer. Interestingly, our study detected no crystalline drug *in vitro* for FLP and TMX when co-precipitated with the polymer. A polymeric de-swelling and precipitation may have entrapped drug without occurrence of a crystalline drug precipitate. Strong molecular interactions and the drug entrapment in the generated co-precipitate of drug and polymer *in situ* could have caused reduced thermodynamic activity of the active compound thereby leading to a slower release rate.

Even if no or only slight precipitation occurred in a lower pH-range than expected for the rat intestine, [206] strong interactions between the polymer and the drugs might still have affected the kinetics and extent of how the compounds were released and absorbed.

No such pharmacokinetic effects were observed by Kojima et al. compared to the present work. [170] Potential reasons could be (1) the low EPO concentrations in the mefenamic acid study, (2) the high application volume of acetate buffer (for rodent experiments), and (3) that mefenamic acid is charged in the small intestine and will not precipitate. Moreover, the hydrophobic nature of the drug-polymer interactions

makes further a difference to the situation with acids despite of strong interactions of EPO and mefenamic acid.

The finding of changed absorption kinetics is not only academically interesting but may be also technically harnessed. Especially when the exposure is not compromised, such a simple modified release principle could be of great merit in early formulations supply. This early development phase comes with practical limitations of any other sophisticated modified release technology. Furthermore, monolithic modified release systems are rather problematic for rodents. Once checked and validated, an *in situ* generated modified release formulation could provide here an alternative to avoid plasma concentration fluctuations regarding an excessively high C_{max} followed by a possible fast decay to rather low concentration. Such a high peak-to-trough ratio is a typical concern for many drugs especially at the high doses used in preclinical studies. For such drug candidates, ordinary drug solutions with high peak-to-trough ratios may lead to adverse events that are later on the market often encountered by a modified release formulation in the therapeutic dose range. Especially in long term treatment with given adverse effects such as with antipsychotic and antihypertensive drugs or pain medication, there are often modified release formulations employed to avoid large plasma fluctuation. [207] An *in situ* generated modified release formulation based on specific drug-polymer interactions is a very simple approach. A use for market formulations is rather discouraged because more established techniques exist for modified drug release, which, however, require sufficient development time. We see a possible application in preclinical formulations to avoid that drug candidates fail in toxicity studies due to avoidable issues of peak-to-trough toxic kinetics. Furthermore, a modified release technology may provide pharmacokinetic profiles in the preclinical studies similar to those obtained later for the clinical or market formulations.

8.5 Conclusions

The methacrylic copolymer EPO has been shown to effectively solubilize acidic drugs. More recent work demonstrated similar effects also for basic compounds. The present work confirmed these remarkable solubilization effects for FLP and TMX.

This study aimed to show *in vivo* effects of the *in vitro* enhancement of drug solubility. Interestingly, oral exposure was not increased by the presence of the polymer. However, EPO-drug solutions were shown to change pharmacokinetic parameters compared to pH-adjusted solution, cosolvent-solution or simple microsuspension. Delayed and decreased absorption of the drugs were observed and are most likely due to hydrophobic drug polymer interactions and co-precipitation of the compound with polymer in the gastrointestinal tract of the rats. The present results are of interest for several reasons. First, *in vitro* solubilization results due to strong hydrophobic drug-excipient interactions may not translate necessarily into increased *in vivo* absorption, which is of general relevance for *in vitro* characterization. Second, the findings bear a potential technical exploitation of such specific drug-excipient interactions and entrapment by the polymer. The polymeric co-precipitation effect *in vivo* might be used for high-dose animal studies in the early phases of pharmaceutical development like toxicology or pharmacokinetic studies. Thus, high peak-to-trough ratios can be avoided in the preclinical program long before much more resource-intensive modified release formulations can be developed.

Chapter 9

Final remarks and outlook

A successful formulation design is a key process during drug development. However, finding a suitable formulation is challenging, especially during early phases since only a limited amount of compound is available. A more rational excipient selection would help to reduce the number of experiments. Therefore, a better mechanistic understanding of drug-excipient interactions is needed. Even though such molecular interactions have been studied intensively in the pharmaceutical literature, there is a lack of comparatively big datasets about solubility enhancement at a rather low additive concentration. Such rather low excipient concentrations are relevant as model for a diluted oral dosage form and/or have relevance for preclinical formulation vehicles. Moreover, potential solid state changes of the drug have in the past mostly not been considered. The present thesis aimed to improve the mechanistic understanding of such drug-excipient interactions to ultimately provide some guidance in formulation development.

Due to the limited amount of compound that is available in early phases of pharmaceutical development, miniaturized assays are desirable for *in vitro* tests at this stage. We developed a miniaturized X-ray assay for parallel determination of kinetic solubility and solid state transformations. The correction of X-ray pattern with measured background pattern led to detection of much smaller quantities of polymorphic forms in binary mixtures than in previous studies. The parallel study of solvent-mediated phase transformations and drug concentrations provided insights into influences of excipients on the drug in the liquid and the solid phase of the pharmaceutical system. For a more mechanistic study of the solvent-mediated phase changes, dynamic imaging was applied to kinetic measurements. To this end, image analysis was combined with a fractal analysis to gain insights into hydrate crystal growth. Both methods provide time-resolved data on excipient effects on solvent-

mediated phase transformation and drug concentration. An important finding was the differentiation of excipient effects in the solid phase and in the liquid phase of a pharmaceutical system. Knowledge of these kinetic effects can be applied to liquid dosage forms but also to other development of aqueous drug mixtures. Additionally, it is relevant for oral administration of solid dosage forms as they are exposed to aqueous environment after administration and dispersion.

Key excipients for solubilization are surfactants that are commonly used in dosage forms and therefore their influence was studied at low concentrations on solubility and solid state changes of 13 model compounds. The obtained dataset demonstrated high solubilization correlations among pegylated surfactants of similar type but also exceptional solubilization of anionic surfactants. Our results demonstrated further the importance of a solid state characterization of residual drug because surfactants were shown to affect solvent-mediated phase transformation in some cases. Current findings may serve as basis to guide a surfactant screening in preformulation regarding the choice of tested surfactants.

Additionally to surfactants, polymers are widely used in suspensions formulations and are known to influence polymorphic transformations. We showed that EPO is a potent polymer to obtain solubility enhancement of seven crystalline acidic drugs in solution. ^{1}H NMR spectroscopy (including DOSY application) proved to be a suitable tool to study specific molecular interactions of drug and polymer. Additionally to expected ionic interactions, also hydrophobic interactions between the polymer side chains and the aromatic system were identified as crucial. Due to the molecular understanding of drug-polymer interactions, the application of EPO as a solubility enhancer was also tested for six basic compounds that were mostly protonated at physiological pH. Although some hydrophobic interactions were expected to occur, the high extent of solubility enhancement was surprising given the same positive charge type of aminoalkyl groups that abundantly exist in EPO. These findings broaden the application area of EPO, especially for simple formulations like suspensions and solutions that can be used in early phases of the drug development process.

These molecular studies of EPO-drug interactions improved the understanding of *in vitro* results; however, the *in vivo* performance is finally important from a

biopharmaceutical perspective especially, when formulating poorly water-soluble compounds. Therefore, an *in vivo* study in rats with formulations with EPO and a basic (tamoxifen) and a neutral compound (felodipine) was performed. Interestingly, bioavailability could not be improved in presence of the polymer despite of the promising *in vitro* solubilization results. However, kinetic plasma profiles were significantly changed in EPO containing drug solutions and resulted in delayed and decreased absorption of the drugs compared to pH-adjusted solution, cosolvent-solution or simple microsuspension. This result was most likely due to hydrophobic drug polymer interactions and co-precipitation of the compound with polymer in the gastrointestinal tract of the rats and can be used for high-dose *in vivo* studies in the early phases of pharmaceutical development like toxicology or pharmacokinetic studies. Thus, high peak-to-trough ratios can be avoided in the preclinical program long before much more resource-intensive modified release formulations can be developed.

This work provides an improved mechanistic understanding of drug-excipient interactions *in vitro* as well as *in vivo* at low excipient concentrations. However, it was seen that excipient effects especially on the solid state are highly specific between drug and excipient. The findings were still encouraging that with an improved understanding, a more rational excipient selection is possible.

Bibliography

1. Lipinski, C. A.; Lombardo, F.; Dominy, B. W.; Feeney, P. J. Experimental and computational approaches to estimate solubility and permeability in drug discovery and development settings. *Advanced Drug Delivery Reviews* **1997,** *23*, (1-3), 3-25.
2. Amidon, G. L.; Lennernäs, H.; Shah, V. P.; Crison, J. R. A theoretical basis for a biopharmaceutic drug classification: the correlation of in vitro drug product dissolution and in vivo bioavailability. *Pharmaceutical Research* **1995,** *12*, (3), 413-420.
3. Butler, J. M.; Dressman, J. B. The developability classification system: application of biopharmaceutics concepts to formulation development. *Journal of Pharmaceutical Sciences* **2010,** *99*, (12), 4940-4954.
4. Fahr, A.; Liu, X. Drug delivery strategies for poorly water-soluble drugs. *Expert opinion on drug delivery* **2007,** *4*, (4), 403-416.
5. Kawabata, Y.; Wada, K.; Nakatani, M.; Yamada, S.; Onoue, S. Formulation design for poorly water-soluble drugs based on biopharmaceutics classification system: Basic approaches and practical applications. *International Journal of Pharmaceutics.* **2011,** *420*, (1), 1-10.
6. Buckley, S. T.; Frank, K. J.; Fricker, G.; Brandl, M. Biopharmaceutical classification of poorly soluble drugs with respect to "enabling formulations". *European Journal of Pharmaceutical Sciences.* **2013,** *50*, (1), 8-16.
7. Li, P.; Zhao, L. Developing early formulations: Practice and perspective. *International Journal of Pharmaceutics* **2007,** *341*, (1–2), 1-19.
8. Maas, J.; Kamm, W.; Hauck, G. An integrated early formulation strategy – From hit evaluation to preclinical candidate profiling. *European Journal of Pharmaceutics and Biopharmaceutics* **2007,** *66*, (1), 1-10.
9. Strickley, R. G. Solubilizing excipients in oral and injectable formulations. *Pharmaceutical Research* **2004,** *21*, (2), 201-230.
10. Strickley, R. G., Chapter 24 - Formulation in Drug Discovery. In *Annual Reports in Medicinal Chemistry*, John, E. M., Ed. Academic Press: **2008**; Vol. Volume 43, pp 419-451.

11. Dai, W.-G.; Pollock-Dove, C.; Dong, L. C.; Li, S. Advanced screening assays to rapidly identify solubility-enhancing formulations: High-throughput, miniaturization and automation. *Advanced Drug Delivery Reviews* **2008,** *60*, (6), 657-672.
12. Gift, A. D.; Luner, P. E.; Luedeman, L.; Taylor, L. S. Manipulating Hydrate Formation During High Shear Wet Granulation Using Polymeric Excipients. *Journal of Pharmaceutical Sciences* **2009,** *98*, (12), 4670-4683.
13. Jorgensen, A.; Rantanen, J.; Karjalainen, M.; Khriachtchev, L.; Rasanen, E.; Yliruusi, J. Hydrate formation during wet granulation studied by spectroscopic methods and multivariate analysis. *Pharmaceutical Research.* **2002,** *19*, (9), 1285-1291.
14. Wikstroem, H.; Kakidas, C.; Taylor, L. S. Determination of hydrate transition temperature using transformation kinetics obtained by Raman spectroscopy. *Journal of Pharmaceutical and Biomedical Analysis* **2009,** *49*, (2), 247-252.
15. Wikstroem, H.; Rantanen, J.; Gift, A. D.; Taylor, L. S. Toward an understanding of the factors influencing anhydrate-to-hydrate transformation kinetics in aqueous environments. *Crystal Growth and Design* **2008,** *8*, (8), 2684-2693.
16. Gift, A. D.; Luner, P. E.; Luedeman, L.; Taylor, L. S. Influence of Polymeric Excipients on Crystal Hydrate Formation Kinetics in Aqueous Slurries. *Journal of Pharmaceutical Sciences* **2008,** *97*, (12), 5198-5211.
17. Lehto, P.; Aaltonen, J.; Tenho, M.; Rantanen, J.; Hirvonen, J.; Tanninen, V. P.; Peltonen, L. Solvent-Mediated Solid Phase Transformations of Carbamazepine: Effects of Simulated Intestinal Fluid and Fasted State Simulated Intestinal Fluid. *Journal of Pharmaceutical Sciences* **2009,** *98*, (3), 985-996.
18. Lennernäs, H.; Aarons, L.; Augustijns, P.; Beato, S.; Bolger, M.; Box, K.; Brewster, M.; Butler, J.; Dressman, J.; Holm, R.; Julia Frank, K.; Kendall, R.; Langguth, P.; Sydor, J.; Lindahl, A.; McAllister, M.; Muenster, U.; Müllertz, A.; Ojala, K.; Pepin, X.; Reppas, C.; Rostami-Hodjegan, A.; Verwei, M.; Weitschies, W.; Wilson, C.; Karlsson, C.; Abrahamsson, B. Oral biopharmaceutics tools – Time for a new initiative – An introduction to the IMI project OrBiTo. *European Journal of Pharmaceutical Sciences* **2014,** *57*, 292-299.
19. Hilfiker, R.; Berghausen, J.; Blatter, F.; Burkhard, A.; De Paul, S. M.; Freiermuth, B.; Geoffroy, A.; Hofmeier, U.; Marcolli, C.; Siebenhaar, B.; Szelagiewicz, M.; Vit, A.; von Raumer, M. Polymorphism - Integrated approach from high-throughput screening to crystallization optimization. *Journal of Thermal Analysis and Calorimetry* **2003,** *73*, (2), 429-440.
20. Aaltonen, J.; Heinänen, P.; Peltonen, L.; Kortejärvi, H.; Tanninen, V. P.; Christiansen, L.; Hirvonen, J.; Yliruusi, J.; Rantanen, J. In situ measurement of

solvent mediated phase transformations during dissolution testing. *Journal of Pharmaceutical Sciences* **2006,** *95*, (12), 2730-2737.

21. Araya-Sibaja, A. M.; Paulino, A. S.; Rauber, G. S.; Campos, C. E. M.; Cardoso, S. G.; Monti, G. A.; Heredia, V.; Bianco, I.; Beltrano, D.; Cuffini, S. L. Dissolution properties, solid-state transformation and polymorphic crystallization: progesterone case study. *Pharmaceutical Development and Technology* **2014,** *19*, (7), 779-788.
22. Paaver, U.; Lust, A.; Mirza, S.; Rantanen, J.; Veski, P.; Heinamaki, J.; Kogermann, K. Insight into the solubility and dissolution behavior of piroxicam anhydrate and monohydrate forms. *International Journal of Pharmaceutics* **2012,** *431*, (1-2), 111-119.
23. Feenstra, T.; De Bruyn, P. The Ostwald rule of stages in precipitation from highly supersaturated solutions: a model and its application to the formation of the nonstoichiometric amorphous calcium phosphate precursor phase. *Journal of Colloid and Interface Science* **1981,** *84*, (1), 66-72.
24. Brittain, H. G., *Polymorphism in pharmaceutical solids*. CRC Press: **2009**.
25. McCrone, W. Polymorphism. *Physics and chemistry of the organic solid state* **1965,** *2*, 725-767.
26. Hilfiker, R., *Polymorphism: In the Pharmaceutical Industry*. Wiley: Weinheim, **2006**.
27. Vippagunta, S. R.; Brittain, H. G.; Grant, D. J. Crystalline solids. *Advanced Drug Delivery Reviews* **2001,** *48*, (1), 3-26.
28. Hancock, B. C.; Parks, M. What is the true solubility advantage for amorphous pharmaceuticals? *Pharmaceutical Research* **2000,** *17*, (4), 397-404.
29. Yu, L. Amorphous pharmaceutical solids: preparation, characterization and stabilization. *Advanced Drug Delivery Reviews.* **2001,** *48*, (1), 27-42.
30. Chieng, N.; Rades, T.; Aaltonen, J. An overview of recent studies on the analysis of pharmaceutical polymorphs. *Journal of Pharmaceutical and Biomedical Analysis* **2011,** *55*, (4), 618-644.
31. Aaltonen, J.; Alleso, M.; Mirza, S.; Koradia, V.; Gordon, K. C.; Rantanen, J. Solid form screening - A review. *European Journal of Pharmaceutics and Biopharmaceutics* **2009,** *71*, (1), 23-37.
32. Stephenson, G. A.; Forbes, R. A.; Reutzel-Edens, S. M. Characterization of the solid state: quantitative issues. *Advanced Drug Delivery Reviews* **2001,** *48*, (1), 67-90.
33. Campbell Roberts, S. N.; Williams, A. C.; Grimsey, I. M.; Booth, S. W. Quantitative analysis of mannitol polymorphs. X-ray powder diffractometry--exploring preferred orientation effects. *Journal of Pharmaceutical and Biomedical Analysis* **2002,** *28*, (6), 1149-59.

34. Kogermann, K.; Veski, P.; Rantanen, J.; Naelapaa, K. X-ray powder diffractometry in combination with principal component analysis - A tool for monitoring solid state changes. *European Journal of Pharmaceutical Sciences* **2011,** *43*, (4), 278-289.
35. Bugay, D. E. Characterization of the solid-state: spectroscopic techniques. *Advanced Drug Delivery Reviews* **2001,** *48*, (1), 43-65.
36. Heinz, A.; Strachan, C. J.; Gordon, K. C.; Rades, T. Analysis of solid state transformations of pharmaceutical compounds using vibrational spectroscopy. *Journal of Pharmacy and Pharmacoogy.* **2009,** *61*, (8), 971-988.
37. Reich, G. Near-infrared spectroscopy and imaging: Basic principles and pharmaceutical applications. *Advanced Drug Delivery Reviews* **2005,** *57*, (8), 1109-1143.
38. Giron, D. Thermal analysis and calorimetric methods in the characterisation of polymorphs and solvates. *Thermochimica acta* **1995,** *248*, 1-59.
39. Kawakami, K.; Ida, Y. Application of modulated-temperature DSC to the analysis of enantiotropically related polymorphic transitions. *Thermochimica acta* **2005,** *427*, (1), 93-99.
40. Raijada, D.; Bond, A. D.; Larsen, F. H.; Cornett, C.; Qu, H.; Rantanen, J. Exploring the solid-form landscape of pharmaceutical hydrates: Transformation pathways of the sodium naproxen anhydrate-hydrate system. *Pharmaceutical Research* **2013,** *30*, (1), 280-289.
41. Tian, F.; Zeitler, J. A.; Strachan, C. J.; Saville, D. J.; Gordon, K. C.; Rades, T. Characterizing the conversion kinetics of carbamazepine polymorphs to the dihydrate in aqueous suspension using Raman spectroscopy. *Journal of Pharmaceutical and Biomedical Analysis* **2006,** *40*, (2), 271-280.
42. Salameh, A. K.; Taylor, L. S. Physical stability of crystal hydrates and their anhydrates in the presence of excipients. *Journal of Pharmaceutical Sciences* **2006,** *95*, (2), 446-461.
43. Ilevbare, G. A.; Liu, H.; Edgar, K. J.; Taylor, L. S. Effect of binary additive combinations on solution crystal growth of the poorly water-soluble drug, ritonavir. *Crystal Growth and Design* **2012,** *12*, (12), 6050-6060.
44. O'Mahony, M. A.; Seaton, C. C.; Croker, D. M.; Veesler, S.; Rasmuson, A. C.; Hodnett, B. K. Investigation into the mechanism of solution-mediated transformation from FI to FIII Carbamazepine: The role of dissolution and the interaction between polymorph surfaces. *Crystal Growth and Design* **2013,** *13*, (5), 1861-1871.
45. Østergaard, J.; Wu, J. X.; Naelapää, K.; Boetker, J. P.; Jensen, H.; Rantanen, J. Simultaneous UV imaging and Raman spectroscopy for the measurement of solvent-

mediated phase transformations during dissolution testing. *Joutnal of Pharmaceutical Sciences* **2014,** *103*, (4), 1149-1156.

46. Boetker, J. P.; Savolainen, M.; Koradia, V.; Tian, F.; Rades, T.; Müllertz, A.; Cornett, C.; Rantanen, J.; Østergaard, J. Insights into the early dissolution events of amlodipine using UV imaging and Raman spectroscopy. *Molecular Pharmaceutics* **2011,** *8*, (4), 1372-1380.
47. Gendrin, C.; Roggo, Y.; Collet, C. Pharmaceutical applications of vibrational chemical imaging and chemometrics: A review. *Journal of Pharmaceutical and Biomedical Analysis* **2008,** *48*, (3), 533-553.
48. Gordon, K. C.; McGoverin, C. M. Raman mapping of pharmaceuticals. *International Journal of Pharmaceutics* **2011,** *417*, (1–2), 151-162.
49. Wu, J. X.; van den Berg, F.; Rantanen, J.; Rades, T.; Yang, M. Current advances and future trends in characterizing poorly water-soluble drugs using spectroscopic, imaging and data analytical techniques. *Current Pharmaceutical Design* **2014,** *20*, (3), 436-453.
50. Z Zhang, G. G.; Law, D.; Schmitt, E. A.; Qiu, Y. Phase transformation considerations during process development and manufacture of solid oral dosage forms. *Advanced Drug Delivery Reviews* **2004,** *56*, (3), 371-390.
51. Cardew, P. T.; Davey, R. J. The kinetics of solvent-mediated phase transformations. *Proceedings of the Royal Society of London. A. Mathematical and Physical Sciences* **1985,** *398*, (1815), 415-428.
52. Davey, R. J.; Cardew, P. T.; McEwan, D.; Sadler, D. E. Rate controlling processes in solvent-mediated phase transformations. *Journal of Crystal Growth* **1986,** *79*, (1), 648-653.
53. Myerson, A. S., *Molecular modeling applications in crystallization*. Cambridge University Press: New York, **1999**.
54. Murdande, S. B.; Pikal, M. J.; Shanker, R. M.; Bogner, R. H. Aqueous solubility of crystalline and amorphous drugs: Challenges in measurement. *Pharmaceutical Development and Technology* **2011,** *16*, (3), 187-200.
55. Bergström, C. A. S.; Holm, R.; Jørgensen, S. A.; Andersson, S. B. E.; Artursson, P.; Beato, S.; Borde, A.; Box, K.; Brewster, M.; Dressman, J.; Feng, K.-I.; Halbert, G.; Kostewicz, E.; McAllister, M.; Muenster, U.; Thinnes, J.; Taylor, R.; Mullertz, A. Early pharmaceutical profiling to predict oral drug absorption: Current status and unmet needs. *European Journal of Pharmaceutical Sciences* **2014,** *57*, 173-199.

56. Wyttenbach, N.; Alsenz, J.; Grassmann, O. Miniaturized assay for solubility and residual solid screening (SORESOS) in early drug development. *Pharmaceutical Research* **2007,** *24*, (5), 888-898.
57. Alsenz, J.; Kansy, M. High throughput solubility measurement in drug discovery and development. *Advanced Drug Delivery Reviews* **2007,** *59*, (7), 546-567.
58. Dokoumetzidis, A.; Macheras, P. A century of dissolution research: from Noyes and Whitney to the biopharmaceutics classification system. *International Journal of Pharmaceutics* **2006,** *321*, (1), 1-11.
59. Bruner, L.; Tołłoczko, S. Über die Auflösungsgeschwindigkeit fester Körper (III Mitteilung.). *Zeitschrift für Anorganische und Allgemeine Chemie* **1903,** *35*, (1), 23-40.
60. Brunner, E., *Reaktionsgeschwindigkeit in heterogenen Systemen*. Georg-Augusts-Universität, Gottingen.: **1903**.
61. Wang, Y.; Abrahamsson, B.; Lindfors, L.; Brasseur, J. G. Comparison and analysis of theoretical models for diffusion-controlled dissolution. *Molecular Pharmaceutics* **2012,** *9*, (5), 1052-1066.
62. Kuentz, M. Analytical technologies for real-time drug dissolution and precipitation testing on a small scale. *Journal of Pharmacy and Pharmacology* **2015,** *67*, (2), 143-159.
63. Andersson, S. B.; Alvebratt, C.; Bevernage, J.; Bonneau, D.; da Costa Mathews, C.; Dattani, R.; Edueng, K.; He, Y.; Holm, R.; Madsen, C. Interlaboratory validation of small-scale solubility and dissolution measurements of poorly water-soluble drugs. *Journal of Pharmaceutical Sciences* **2016,** *105*, (9), 2864-2872.
64. Morissette, S. L.; Almarsson, O.; Peterson, M. L.; Remenar, J. F.; Read, M. J.; Lemmo, A. V.; Ellis, S.; Cima, M. J.; Gardner, C. R. High-throughput crystallization: polymorphs, salts, co-crystals and solvates of pharmaceutical solids. *Advanced Drug Delivery Reviews.* **2004,** *56*, (3), 275-300.
65. Gardner, C. R.; Almarsson, O.; Chen, H.; Morissette, S.; Peterson, M.; Zhang, Z.; Wang, S.; Lemmo, A.; Gonzalez-Zugasti, J.; Monagle, J.; Marchionna, J.; Ellis, S.; McNulty, C.; Johnson, A.; Levinson, D.; Cima, M. Application of high throughput technologies to drug substance and drug product development. *Computers & Chemical Engineering* **2004,** *28*, (6–7), 943-953.
66. Bharate, S. S.; Vishwakarma, R. A. Thermodynamic equilibrium solubility measurements in simulated fluids by 96-well plate method in early drug discovery. *Bioorganic & Medicinal Chemistry Letters* **2015,** *25*, (7), 1561-1567.

67. Wyttenbach, N.; Janas, C.; Siam, M.; Lauer, M. E.; Jacob, L.; Scheubel, E.; Page, S. Miniaturized screening of polymers for amorphous drug stabilization (SPADS): Rapid assessment of solid dispersion systems. *European Journal of Pharmaceutics and Biopharmaceutics.* **2013,** *84*, (3), 583-598.

68. Alsenz, J.; Meister, E.; Haenel, E. Development of a partially automated solubility screening (PASS) assay for early drug development. *Journal of Pharmaceutical Sciences* **2007,** *96*, (7), 1748-1762.

69. Vandecruys, R.; Peeters, J.; Verreck, G.; Brewster, M. E. Use of a screening method to determine excipients which optimize the extent and stability of supersaturated drug solutions and application of this system to solid formulation design. *International Journal of Pharmaceutics* **2007,** *342*, (1–2), 168-175.

70. Warren, D. B.; Benameur, H.; Porter, C. J. H.; Pouton, C. W. Using polymeric precipitation inhibitors to improve the absorption of poorly water-soluble drugs: A mechanistic basis for utility. *J of Drug Targeting* **2010,** *18*, (10), 704-731.

71. Bevernage, J.; Brouwers, J.; Brewster, M. E.; Augustijns, P. Evaluation of gastrointestinal drug supersaturation and precipitation: Strategies and issues. *International Journal of Pharmaceutics* **2013,** *453*, (1), 25-35.

72. Bevernage, J.; Forier, T.; Brouwers, J.; Tack, J.; Annaert, P.; Augustijns, P. Excipient-mediated supersaturation stabilization in human intestinal fluids. *Molecular Pharmaceutics* **2011,** *8*, (2), 564-570.

73. Elder, D. P.; Kuentz, M.; Holm, R. Pharmaceutical excipients—quality, regulatory and biopharmaceutical considerations. *European Journal of Pharmaceutical Sciences* **2016,** *87*, 88-99.

74. Attwood, D.; Tolley, J. Self association of analgesics in aqueous solution: micellar properties of dextropropoxyphene hydrochloride and methadone hydrochloride. *Journal of Pharmacy and Pharmacology* **1980,** *32*, (1), 533-536.

75. Schreier, S.; Malheiros, S. V.; de Paula, E. Surface active drugs: self-association and interaction with membranes and surfactants. Physicochemical and biological aspects. *Biochimica et Biophysica Acta (BBA)-Biomembranes* **2000,** *1508*, (1), 210-234.

76. Gautschi, N.; Van Hoogevest, P.; Kuentz, M. Molecular insights into the formation of drug-monoacyl phosphatidylcholine solid dispersions for oral delivery. *European Journal of Pharmaceutical Sciences,* **2016**,*in press*

77. Kogermann, K.; Aaltonen, J.; Strachan, C. J.; Pollanen, K.; Heinamaki, J.; Yliruusi, J.; Rantanen, J. Establishing Quantitative In-Line Analysis of Multiple Solid-State Transformations During Dehydration. *Journal of Pharmaceutical Sciences* **2008,** *97*, (11), 4983-4999.

78. Wikstroem, H.; Carroll, W. J.; Taylor, L. S. Manipulating theophylline monohydrate formation during high-shear wet granulation through improved understanding of the role of pharmaceutical excipients. *Pharmaceutical Research* **2008,** *25*, (4), 923-935.
79. Christensen, N. P. A.; Cornett, C.; Rantanen, J. Role of excipients on solid-state properties of piroxicam during processing. *Journal of Pharmaceutical Sciences* **2012,** *101*, (3), 1202-1211.
80. Ilevbare, G. A.; Liu, H.; Edgar, K. J.; Taylor, L. S. Impact of polymers on crystal growth rate of structurally diverse compounds from aqueous solution. *Molecular Pharmaceutics* **2013,** *10*, (6), 2381-2393.
81. Ilevbare, G. A.; Liu, H.; Edgar, K. J.; Taylor, L. S. Inhibition of solution crystal growth of ritonavir by cellulose polymers–factors influencing polymer effectiveness. *CrystEngComm* **2012,** *14*, (20), 6503-6514.
82. Jackson, M. J.; Toth, S. J.; Kestur, U. S.; Huang, J.; Qian, F.; Hussain, M. A.; Simpson, G. J.; Taylor, L. S. Impact of polymers on the precipitation behavior of highly supersaturated aqueous danazol solutions. *Molecular Pharmaceutics* **2014,** *11*, (9), 3027-3038.
83. Ilevbare, G. A.; Taylor, L. S. Liquid–liquid phase separation in highly supersaturated aqueous solutions of poorly water-soluble drugs: implications for solubility enhancing formulations. *Crystal Growth and Design* **2013,** *13*, (4), 1497-1509.
84. Avdeef, A.; Bendels, S.; Tsinman, O.; Tsinman, K.; Kansy, M. Solubility-excipient classification gradient maps. *Pharmaceutical Research* **2007,** *24*, (3), 530-545.
85. Rodriguez-Hornedo, N.; Murphy, D. Surfactant-facilitated crystallization of dihydrate carbamazepine during dissolution of anhydrous polymorph. *Journal of Pharmaceutical Sciences* **2004,** *93*, (2), 449-460.
86. Stahly, G. P. Diversity in single- and multiple-component crystals. The search for and prevalence of polymorphs and cocrystals. *Crystal Growth and Design* **2007,** *7*, (6), 1007-1026.
87. Haleblian, J.; McCrone, W. Pharmaceutical applications of polymorphism. *Journal of Pharmaceutical Sciences* **1969,** *58*, (8), 911-929.
88. Wyttenbach, N.; Birringer, C.; Alsenz, J.; Kuentz, M. Drug-excipient compatibility testing using a high-throughput approach and statistical design. *Pharmaceutical Development and Technology* **2005,** *10*, (4), 499-505.
89. Otsuka, M.; Kinoshita, H. Quantitative determination of hydrate content of theophylline powder by chemometric X-ray powder diffraction analysis. *AAPS PharmSciTech* **2010,** *11*, (1), 204-211.

90. Kirchmeyer, W.; Wyttenbach, N.; Alsenz, J.; Kuentz, M. Influence of excipients on solvent-mediated hydrate formation of piroxicam studied by dynamic imaging and fractal Analysis. *Crystal Growth and Design* **2015,** *15*, (10), 5002-5010.

91. MacFhionnghaile, P.; Hu, Y.; McArdle, P.; Erxleben, A. A comprehensive near infrared spectroscopic study of the limits of quantitative analysis of sulfathiazole polymorphism. *Journal of Near Infrared Spectroscopy* **2013,** *21*, (1), 55-66.

92. Riekes, M. K.; Pereira, R. N.; Rauber, G. S.; Cuffini, S. L.; de Campos, C. E. M.; Silva, M. A. S.; Stulzer, H. K. Polymorphism in nimodipine raw materials: Development and validation of a quantitative method through differential scanning calorimetry. *Journal of Pharmaceutical and Biomedical Analysis* **2012,** *70*, 188-193.

93. Klug, H. P.; Alexander, L. E., *X-ray diffraction procedures*. Chapman & Hall Ltd.: London, **1954**.

94. Tian, F.; Zhang, F.; Sandler, N.; Gordon, K. C.; McGoverin, C. M.; Strachan, C. J.; Saville, D. J.; Rades, T. Influence of sample characteristics on quantification of carbamazepine hydrate formation by X-ray powder diffraction and Raman spectroscopy. *European Journal of Pharmaceutics and Biopharmaceutics.* **2007,** *66*, (3), 466-474.

95. Smith, D. K.; Johnson, G. G.; Wims, A. M. Use of full diffraction spectra, both experimental and calculated, in quantitative powder diffraction analysis. *Australian Journal of Physics* **1988,** *41*, (2), 311-321.

96. European Pharmacopoeia Commission, European Pharmacopoeia. **2013**; monograph 2.9.33, pp 399-345.

97. Edwards, H. G. M.; Lawson, E.; deMatas, M.; Shields, L.; York, P. Metamorphosis of caffeine hydrate and anhydrous caffeine. *Journal of the Chemical Society-Perkin Transactions 2* **1997**, (10), 1985-1990.

98. Sheth, A. R.; Zhou, D. L.; Muller, F. X.; Grant, D. J. W. Dehydration kinetics of piroxicam monohydrate and relationship to lattice energy and structure. *Journal of Pharmaceutical Sciences* **2004,** *93*, (12), 3013-3026.

99. Vrecer, F.; Vrbinc, M.; Meden, A. Characterization of piroxicam crystal modifications. *International Journal of Pharmaceutics.* **2003,** *256*, (1-2), 3-15.

100. Thakkar, A. L.; Jones, N. D.; Rose, H. A.; Tensmeye.Lg; Hall, N. A. Crystallographic data for testosterone hydrate and anhydrate. *Acta Crystallographica Section B-Structural Crystallography and Crystal Chemistry* **1970,** *B 26*, 1184.

101. Galia, E.; Nicolaides, E.; Horter, D.; Lobenberg, R.; Reppas, C.; Dressman, J. B. Evaluation of various dissolution media for predicting in vivo performance of class I and II drugs. *Pharmaceutical Research* **1998,** *15*, (5), 698-705.

102. Biorelevant dissolution media. http://biorelevant.com/ (accessed Feb 18, **2015**).
103. Alsenz, J. Powder Picking: An inexpensive, manual, medium-throughput method for powder dispensing. *Powder Technology* **2011,** *209*, (1-3), 152-157.
104. Macrae, C. F.; Edgington, P. R.; McCabe, P.; Pidcock, E.; Shields, G. P.; Taylor, R.; Towler, M.; van De Streek, J. Mercury: visualization and analysis of crystal structures. *Journal of Applied Crystallography* **2006,** *39*, 453-457.
105. Griesser, U. J.; Burger, A. The effect of water vapor pressure on desolvation kinetics of caffeine 4/5-hydrate. *International Journal of Pharmaceutics* **1995,** *120*, (1), 83-93.
106. Ledwidge, M. T.; Draper, S. M.; Wilcock, D. J.; Corrigan, O. I. Physicochemical characterization of diclofenac N-(2-Hydroxyethyl)pyrrolidine: anhydrate and dihydrate crystalline forms. *Journal of Pharmaceutical Sciences* **1996,** *85*, (1), 16-21.
107. Betigeri, S.; Thakur, A.; Shukla, R.; Raghavan, K. Effect of polymer additives on the transformation of BMS-566394 anhydrate to the dihydrate form. *Pharmaceutical Research* **2008,** *25*, (5), 1043-1051.
108. Gift, A. D.; Southard, L. A.; Riesberg, A. L. Influence of polymeric excipient properties on crystal hydrate formation kinetics of caffeine in aqueous slurries. *Journal of Pharmaceutical Sciences* **2012,** *101*, (5), 1755-1762.
109. Cardew, P. T.; Davey, R. J.; Ruddick, A. J. Kinetics of polymorphic solid-state transformations. *Journal of the Chemical Society Faraday Transactions 2* **1984,** *80*, 659-668.
110. Sheth, A. R.; Bates, S.; Muller, F. X.; Grant, D. J. W. Polymorphism in piroxicam. *Crystal Growth and Design* **2004,** *4*, (6), 1091-1098.
111. Bordner, J.; Richards, J. A.; Weeks, P.; Whipple, E. B. Piroxicam monohydrate: a zwitterionic form, C15H13N3O4S. H2O. *Acta Crystallographica Section C: Crystal Structure Communications* **1984,** *40*, (6), 989-990.
112. Kojić-Prodić, B.; Ružić-Toroš, Ž. Structure of the anti-inflammatory drug 4-hydroxy-2-methyl-N-2-pyridyl-2H-1λ6, 2-benzothiazine-3-carboxamide 1, 1-dioxide (piroxicam). *Acta Crystallographica Section B: Structural Crystallography and Crystal Chemistry* **1982,** *38*, (11), 2948-2951.
113. Thompson, R.; Dixon, A. In *Population-balance models for solution-facilitated phase transformations*, Proceedings of the Royal Society of London A: Mathematical, Physical and Engineering Sciences, **1987**; The Royal Society: pp 369-381.
114. Laaksonen, T.; Aaltonen, J. Modeling solid-state transformations occurring in dissolution testing. *International Journal of Pharmaceutics* **2013,** *447*, (1), 218-223.
115. Kopelman, R. Fractal reaction kinetics. *Science* **1988,** *241*, (4873), 1620-1626.

116. Macheras, P.; Dokoumetzidis, A. On the Heterogeneity of Drug Dissolution and Release. *Pharmaceutical Research* **2000,** *17*, (2), 108-112.
117. Pippa, N.; Dokoumetzidis, A.; Demetzos, C.; Macheras, P. On the ubiquitous presence of fractals and fractal concepts in pharmaceutical sciences: a review. *International Journal of Pharmaceutics* **2013,** *456*, (2), 340-352.
118. Niederquell, A.; Kuentz, M. Biorelevant dissolution of poorly soluble weak acids studied by UV imaging reveals ranges of fractal-like kinetics. *International Journal of Pharmaceutics* **2014,** *463*, (1), 38-49.
119. Kogermann, K.; Aaltonen, J.; Strachan, C. J.; Pollanen, K.; Veski, P.; Heinamaki, J.; Yliruusi, J.; Rantanen, J. Qualitative in situ analysis of multiple solid-state forms using spectroscopy and partial least squares discriminant modeling. *Journal of Pharmaceutical Sciences* **2007,** *96*, (7), 1802-1820.
120. The GNU image manipulation program.http://gimp.org/ (accessed Feb 09, **2015**).
121. Karperien, A. FracLac for ImageJ. http//rsb.info.nih.gov/ij/plugins/fraclac/FLHelp/Introduction.htm. **1999-2013.**
122. Rasband, W. S. ImageJ, U.S. National Institutes of Health, Bethesda, Maryland, USA, http://imagej.nih.gov/ij/. **1997-2014**.
123. Dathe, A.; Eins, S.; Niemeyer, J.; Gerold, G. The surface fractal dimension of the soil–pore interface as measured by image analysis. *Geoderma* **2001,** *103*, (1), 203-229.
124. Kashchiev, D.; Van Rosmalen, G. Review: nucleation in solutions revisited. *Crystal Research and Technology* **2003,** *38*, (7-8), 555-574.
125. Fini, A.; Fazio, G.; Rabasco, A. M.; Fernández-Hervás, M. J.; Holgado, M. A. Effect of the temperature on a hydrate diclofenac salt. *International Journal of Pharmaceutics* **1999,** *181*, (1), 95-106.
126. Fini, A.; Garuti, M.; Fazio, G.; Alvarez-Fuentes, J.; Holgado, M. A. Diclofenac salts. I. fractal and thermal analysis of sodium and potassium diclofenac salts. *Journal of Pharmaceutical Sciences* **2001,** *90*, (12), 2049-2057.
127. Havlin, S.; Ben-Avraham, D. Diffusion in disordered media. *Advances in Physics* **1987,** *36*, (6), 695-798.
128. Pellett, M.; Castellano, S.; Hadgraft, J.; Davis, A. The penetration of supersaturated solutions of piroxicam across silicone membranes and human skin in vitro. *Journal of Controlled Release* **1997,** *46*, (3), 205-214.
129. Chen, L. R.; Wesley, J. A.; Bhattachar, S.; Ruiz, B.; Bahash, K.; Babu, S. R. Dissolution behavior of a poorly water soluble compound in the presence of Tween 80. *Pharmaceutical Research* **2003,** *20*, (5), 797-801.

130. Marvin Suite 2014, ChemAxon. http://www.chemaxon.com. (accessed on Dec 19, **2014**).

131. Kuentz, M.; Holm, R.; Elder, D. P. Methodology of oral formulation selection in the pharmaceutical industry. *European Journal of Pharmaceutical Sciences* **2016,** *87*, 136-163.

132. Wilson, C. G.; Halbert, G. W.; Mains, J. The gut in the beaker: Missing the surfactants? *International Journal of Pharmaceutics.* **2016,** *514*, (1), 73-80.

133. Attwood, D., Florence,A. T., *Surfactant systems: their chemistry, pharmacy and biology*. Chapman & Hall: London, **1983**.

134. Christian, S. D.; Scamehorn, J. F., *Solubilization in surfactant aggregates*. CRC Press: **1995**.

135. Ismail, A.; Gouda, M. W.; Motawi, M. Micellar solubilization of barbiturates I: Solubilities of certain barbiturates in polysorbates of varying hydrophobic chain length. *Journal of Pharmaceutical Sciences* **1970,** *59*, (2), 220-224.

136. Gouda, M. W.; Ismail, A.; Motawi, M. Micellar solubilization of barbiturates II: Solubilities of certain barbiturates in polyoxyethylene stearates of varying hydrophilic chain length. *Journal of Pharmaceutical Sciences* **1970,** *59*, (10), 1402-1405.

137. Tomida, H.; Yotsuyanagi, T.; Ikeda, K. E. N. Solubilization of steroid hormones by polyoxyethylene lauryl ether. *Chemical & Pharmaceutical Bulletin* **1978,** *26*, (9), 2832-2837.

138. Liu, G. G.; Roy, D.; Rosen, M. J. A simple method to estimate the surfactant micelle− water distribution coefficients of aromatic hydrocarbons. *Langmuir* **2000,** *16*, (8), 3595-3605.

139. Sprunger, L.; Acree, W. E.; Abraham, M. H. Linear free energy relationship correlation of the distribution of solutes between water and sodium dodecyl sulfate (SDS) micelles and between gas and SDS micelles. *Journal of Chemical Information and Modeling* **2007,** *47*, (5), 1808-1817.

140. Storm, S.; Jakobtorweihen, S.; Smirnova, I.; Panagiotopoulos, A. Z. Molecular dynamics simulation of sds and ctab micellization and prediction of partition equilibria with cosmomic. *Langmuir* **2013,** *29*, (37), 11582-11592.

141. Kirchmeyer, W.; Grassmann, O.; Wyttenbach, N.; Alsenz, J.; Kuentz, M. Miniaturized X-ray powder diffraction assay (MixRay) for quantitative kinetic analysis of solvent-mediated phase transformations in pharmaceutics. *Journal of Pharmaceutical and Biomedical Analysis* **2016,** *131*, 195-201.

142. BASF SE, Technical Information Kolliphor HS 15. https://industries.basf.com/en/documentDownload.8805243791829.Kolliphor%C2%AE%20HS%2015%20-%20Technical%20Information.pdf (accessed Mar 29, **2017**).

143. BASF SE, Technical information Kolliphor EL. https://industries.basf.com/en/documentDownload.8805244447189.Kolliphor%C2%AE%20EL%20-%20Technical%20Information.pdf (accessed Mar 29, **2017**).

144. Ong, J. T. H.; Manoukian, E. Micellar solubilization of timobesone acetate in aqueous and aqueous propylene glycol solutions of nonionic surfactants. *Pharmaceutical Research* **1988,** *5*, (11), 704-708.

145. Dawson, R., Elliott, DC, Elliott, WH, Jones, KM, *Data for Biochemical Research*. Oxford Science Publications: Oxford, **1986**.

146. Khan, A. M.; Shah, S. S. Determination of critical micelle concentration (CMC) of sodium dodecyl sulfate (SDS) and the effect of low concentration of pyrene on its CMC using ORIGIN software. *Journal of the Chemical Society of Pakistan* **2008,** *30*, (2), 186.

147. Steffy, D.; Nichols, A.; Kiplagat, G. In *Effectiveness of the Surfactant Dioctyl Sodium Sulfosuccinate (DOSS) to Disperse Oil in a Changing Marine Environment*, AGU Fall Meeting Abstracts, **2011**; p 1621.

148. Constantinides, P. P.; Scalart, J.-P. Formulation and physical characterization of water-in-oil microemulsions containing long- versus medium-chain glycerides. *International Journal of Pharmaceutics* **1997,** *158*, (1), 57-68.

149. Housaindokht, M. R.; Nakhaei Pour, A. Study the effect of HLB of surfactant on particle size distribution of hematite nanoparticles prepared via the reverse microemulsion. *Solid State Sciences* **2012,** *14*, (5), 622-625.

150. Koos, E.; Johannsmeier, J.; Schwebler, L.; Willenbacher, N. Tuning suspension rheology using capillary forces. *Soft Matter* **2012,** *8*, (24), 6620-6628.

151. Reis, S.; Moutinho, C. G.; Pereira, E.; de Castro, B.; Gameiro, P.; Lima, J. L. β-Blockers and benzodiazepines location in SDS and bile salt micellar systems: an ESR study. *Journal of Pharmaceutical and Biomedical analysis* **2007,** *45*, (1), 62-69.

152. Rub, M. A.; Khan, F.; Azum, N.; Asiri, A. M.; Marwani, H. M. Micellization phenomena of amphiphilic drug and TX-100 mixtures: fluorescence, UV-visible and 1 H NMR study. *Journal of the Taiwan Institute of Chemical Engineers* **2016,** *60*, 32-43.

153. Shareef, A.; Angove, M. J.; Wells, J. D.; Johnson, B. B. Aqueous solubilities of estrone, 17β-estradiol, 17α-ethynylestradiol, and bisphenol A. *Journal of Chemical & Engineering Data* **2006,** *51*, (3), 879-881.

154. Bhat, P. A.; Rather, G. M.; Dar, A. A. Effect of surfactant mixing on partitioning of model hydrophobic drug, naproxen, between aqueous and micellar phases. *The Journal of Physical Chemistry B* **2009,** *113*, (4), 997-1006.

155. Grzesiak, A. L.; Matzger, A. J. New form discovery for the analgesics flurbiprofen and sulindac facilitated by polymer-induced heteronucleation. *Journal of Pharmaceutical Sciences* **2007,** *96*, (11), 2978-2986.

156. Hansen, L. K.; Perlovich, G. L.; Bauer-Brandl, A. The 1:1 hydrate of diflunisal. *Acta Crystallographica Section E* **2001,** *57*, (5), o477-o479.

157. Poole, C. F.; Atapattu, S. N.; Poole, S. K.; Bell, A. K. Determination of solute descriptors by chromatographic methods. *Analytica chimica acta* **2009,** *652*, (1), 32-53.

158. Yang, S.; Bumgarner, J. G.; Kruk, L. F.; Khaledi, M. G. Quantitative structure-activity relationships studies with micellar electrokinetic chromatography influence of surfactant type and mixed micelles on estimation of hydrophobicity and bioavailability. *Journal of Chromatography A* **1996,** *721*, (2), 323-335.

159. Feeney, O. M.; Crum, M. F.; McEvoy, C. L.; Trevaskis, N. L.; Williams, H. D.; Pouton, C. W.; Charman, W. N.; Bergström, C. A.; Porter, C. J. 50 years of oral lipid-based formulations: Provenance, progress and future perspectives. *Advanced Drug Delivery Reviews* **2016,** *101*, 167-194.

160. Arnold, Y. E.; Imanidis, G.; Kuentz, M. In vitro digestion kinetics of excipients for lipid-based drug delivery and introduction of a relative lipolysis half life. *Drug development and Industrial Pharmacy* **2012,** *38*, (10), 1262-1269.

161. Müller, R. H.; Jacobs, C.; Kayser, O. Nanosuspensions as particulate drug formulations in therapy: Rationale for development and what we can expect for the future. *Advanced Drug Deliery Reviews* **2001,** *47*, (1), 3-19.

162. Tommasini, S.; Raneri, D.; Ficarra, R.; Calabro, M. L.; Stancanelli, R.; Ficarra, P. Improvement in solubility and dissolution rate of flavonoids by complexation with beta-cyclodextrin. *Journal of Pharmaceutical and Biomedical Analysis* **2004,** *35*, (2), 379-387.

163. Davis, M. E.; Brewster, M. E. Cyclodextrin-based pharmaceutics: Past, present and future. *Nature Reviews Drug Discovery* **2004,** *3*, (12), 1023-1035.

164. Loftsson, T.; Brewster, M.; Másson, M. Role of cyclodextrins in improving oral drug delivery. *American Journal of Drug Delivery* **2004,** *2*, (4), 261-275.

165. Humberstone, A. J.; Charman, W. N. Lipid-based vehicles for the oral delivery of poorly water soluble drugs. *Advanced Drug Deliery Reviews* **1997,** *25*, (1), 103-128.

166. Constantinides, P. Lipid Microemulsions for Improving Drug Dissolution and Oral Absorption: Physical and Biopharmaceutical Aspects. *Pharmaceutical Research* **1995,** *12*, (11), 1561-1572.

167. Serajuddin, A. T. M. Solid dispersion of poorly water-soluble drugs: Early promises, subsequent problems, and recent breakthroughs. *Journal of Pharmaceutical Sciences* **1999,** *88*, (10), 1058-1066.

168. Vasconcelos, T.; Sarmento, B.; Costa, P. Solid dispersions as strategy to improve oral bioavailability of poor water soluble drugs. *Drug Discovery Today* **2007,** *12*, (23–24), 1068-1075.

169. Gallardo, D.; Skalsky, B.; Kleinebudde, P. Controlled release solid dosage forms using combinations of (meth)acrylate copolymers. *Pharmceutical Development and Technology* **2008,** *13*, (5), 413-423.

170. Kojima, T.; Higashi, K.; Suzuki, T.; Tomono, K.; Moribe, K.; Yamamoto, K. Stabilization of a supersaturated solution of mefenamic acid from a solid dispersion with Eudragit® EPO. *Pharmaceutical Research* **2012,** *29*, (10), 2777-2791.

171. Higashi, K.; Yamamoto, K.; Pandey, M. K.; Mroue, K. H.; Moribe, K.; Yamamoto, K.; Ramamoorthy, A. Insights into atomic-level interaction between mefenamic acid and Eudragit EPO in a supersaturated solution by high-resolution magic-angle spinning NMR spectroscopy. *Molecular Pharmaceutics* **2014,** *11*, (1), 351-357.

172. Li, J. L.; Lee, I. W.; Shin, G. H.; Chen, X. G.; Park, H. J. Curcumin-Eudragit® E PO solid dispersion: A simple and potent method to solve the problems of curcumin. *European Journal of Pharmaceutics and Biopharmaceutics* **2015,** *94*, 322-332.

173. Priemel, P. A.; Laitinen, R.; Grohganz, H.; Rades, T.; Strachan, C. J. In situ amorphisation of indomethacin with Eudragit® E during dissolution. *European Journal of Pharmaceutics and Biopharmaceutics* **2013,** *85*, (3, Part B), 1259-1265.

174. Doreth, M.; Löbmann, K.; Grohganz, H.; Holm, R.; Lopez de Diego, H.; Rades, T.; Priemel, P. A. Glass solution formation in water - In situ amorphization of naproxen and ibuprofen with Eudragit® E PO. *Journal of Drug Delivery Science and Technology* **2016,** *34*, 32-40.

175. Wu, D. H.; Chen, A. D.; Johnson, C. S. An improved diffusion-ordered spectroscopy experiment incorporating bipolar-gradient pulses. *Journal of Magnetic Resonance, Series A* **1995,** *115*, (2), 260-264.

176. Marvin Suite 2015, ChemAxon http://www.chemicalize.org/ (accessed on Nov 19, **2015**).

177. Farin, D.; Avnir, D. Use of fractal geometry to determine effects of surface morphology on drug dissolution. *Journal of Pharmaceutical Sciences* **1992,** *81*, (1), 54-57.

178. Pippa, N.; Merkouraki, M.; Pispas, S.; Demetzos, C. DPPC:MPOx chimeric advanced Drug Delivery nano Systems (chi-aDDnSs): Physicochemical and structural

characterization, stability and drug release studies. *International Journal of Pharmaceutics* **2013,** *450*, (1–2), 1-10.

179. Ran, Y.; Yalkowsky, S. H. Prediction of drug solubility by the general solubility equation (GSE). *Journal of Chemical Information and Computer Sciences* **2001,** *41*, (2), 354-357.
180. Bergström, C. A.; Norinder, U.; Luthman, K.; Artursson, P. Experimental and computational screening models for prediction of aqueous drug solubility. *Pharmaceutical Research* **2002,** *19*, (2), 182-188.
181. Van den Mooter, G. The use of amorphous solid dispersions: A formulation strategy to overcome poor solubility and dissolution rate. *Drug Discovery Today: Technologies* **2012,** *9*, (2), e79-e85.
182. Kuentz, M. Lipid-based formulations for oral delivery of lipophilic drugs. *Drug Discovery Today: Technologies* **2012,** *9*, (2), e97-e104.
183. Desai, P. P.; Date, A. A.; Patravale, V. B. Overcoming poor oral bioavailability using nanoparticle formulations – opportunities and limitations. *Drug Discovery Today: Technologies* **2012,** *9*, (2), e87-e95.
184. Lee, Y.-C.; Zocharski, P. D.; Samas, B. An intravenous formulation decision tree for discovery compound formulation development. *International Journal of Pharmaceutics* **2003,** *253*, (1–2), 111-119.
185. Song, Y.; Yang, X.; Chen, X.; Nie, H.; Byrn, S.; Lubach, J. W. Investigation of drug–excipient interactions in lapatinib amorphous solid dispersions using solid-state NMR spectroscopy. *Molecular Pharmaceutics* **2015,** *12*, (3), 857-866.
186. Taylor, L. S.; Zografi, G. Spectroscopic characterization of interactions between PVP and indomethacin in amorphous molecular dispersions. *Pharmaceutical Research* **1997,** *14*, (12), 1691-1698.
187. Saal, W.; Ross, A.; Wyttenbach, N.; Alsenz, J.; Kuentz, M. A systematic study of molecular interactions of anionic drugs with a dimethylaminoethyl methacrylate copolymer regarding solubility enhancement. *Molecular Pharmaceutics* **2017,** *14*, (4), 1243-1250.
188. Higashi, K.; Seo, A.; Egami, K.; Otsuka, N.; Limwikrant, W.; Yamamoto, K.; Moribe, K. Mechanistic insight into the dramatic improvement of probucol dissolution in neutral solutions by solid dispersion in Eudragit E PO with saccharin. *Journal of Pharmacy and Pharmacology* **2015**.
189. Kanaya, H.; Ueda, K.; Higashi, K.; Yamamoto, K.; Moribe, K. Stabilization mechanism of nitrazepam supersaturated state in nitrazepam/Eudragit®

EPO/saccharin solution revealed by NMR measurements. *Asian Journal of Pharmaceutical Sciences* **2016,** *11*, (1), 58-59.

190. Völgyi, G.; Baka, E.; Box, K. J.; Comer, J. E. A.; Takács-Novák, K. Study of pH-dependent solubility of organic bases. Revisit of Henderson-Hasselbalch relationship. *Analytica Chimica Acta* **2010,** *673*, (1), 40-46.
191. Dobrynin, A. V.; Rubinstein, M. Theory of polyelectrolytes in solutions and at surfaces. *Progress in Polymer Science* **2005,** *30*, (11), 1049-1118.
192. Solis, F. J.; de la Cruz, M. O. Collapse of flexible polyelectrolytes in multivalent salt solutions. *The Journal of Chemical Physics* **2000,** *112*, (4), 2030-2035.
193. Pouton, C. W. Formulation of poorly water-soluble drugs for oral administration: physicochemical and physiological issues and the lipid formulation classification system. *European Journal of Pharmaceutical Sciences* **2006,** *29*, (3), 278-287.
194. Saal, W.; Ross, A.; Wyttenbach, N.; Alsenz, J.; Kuentz, M. Unexpected solubility enhancement of drug bases in prsenece of a dimethylamoniethyl methacrylate copolymer **2017,** *15*, (1), 186-192.
195. Lundahl, J.; Regårdh, C.; Edgar, B.; Johnsson, G. Relationship between time of intake of grapefruit juice and its effect on pharmacokinetics and pharmacodynamics of felodipine in healthy subjects. *European Journal of Clinical Pharmacology* **1995,** *49*, (1-2), 61-67.
196. Jaiyesimi, I. A.; Buzdar, A. U.; Decker, D. A.; Hortobagyi, G. N. Use of tamoxifen for breast cancer: twenty-eight years later. *Journal of Clinical Oncology* **1995,** *13*, (2), 513-529.
197. Jordan, V. C. Tamoxifen: a most unlikely pioneering medicine. *Nature Reviews Drug Discovery* **2003,** *2*, (3), 205-213.
198. National Research Council, *Guide for the care and use of laboratory animals*. National Academies Press: **2010**.
199. Kararli, T. T. Comparison of the gastrointestinal anatomy, physiology, and biochemistry of humans and commonly used laboratory animals. *Biopharmaceutics & Drug Disposition* **1995,** *16*, (5), 351-380.
200. Mosharraf, M.; Nyström, C. The effect of particle size and shape on the surface specific dissolution rate of microsized practically insoluble drugs. *International Journal of Pharmaceutics* **1995,** *122*, (1), 35-47.
201. Jinno, J.-i.; Kamada, N.; Miyake, M.; Yamada, K.; Mukai, T.; Odomi, M.; Toguchi, H.; Liversidge, G. G.; Higaki, K.; Kimura, T. Effect of particle size reduction on dissolution and oral absorption of a poorly water-soluble drug, cilostazol, in beagle dogs. *Journal of Controlled Release* **2006,** *111*, (1–2), 56-64.

202. Noyes, A. A.; Whitney, W. R. The rate of solution of solid substances in their own solutions. *Journal of the American Chemical Society* **1897,** *19*, (12), 930-934.

203. Khan, S.; Kataria, P.; Nakhat, P.; Yeole, P. Taste masking of ondansetron hydrochloride by polymer carrier system and formulation of rapid-disintegrating tablets. *AAPS PharmSciTech* **2007,** *8*, (2), E127-E133.

204. Randale, S. A.; Dabhi, C. S.; Tekade, A. R.; Belgamwar, V. S.; Gattani, S. G.; Surana, S. J. Rapidly disintegrating tablets containing taste masked metoclopramide hydrochloride prepared by extrusion–precipitation method. *Chemical and Pharmaceutical Bulletin* **2010,** *58*, (4), 443-448.

205. Lizio, R.; Damm, M.; Petereit, H.-U. Evonik Röhm GmbH, A*queous carbonated medium containing an amino (meth) acrylate polymer or copolymer*. US 8,951,558 B2, **2015**.

206. McConnell, E. L.; Basit, A. W.; Murdan, S. Measurements of rat and mouse gastrointestinal pH, fluid and lymphoid tissue, and implications for in-vivo experiments. *Journal of Pharmaceutics and Pharmacology* **2008,** *60*, (1), 63-70.

207. Sheehan, J. J.; Reilly, K. R.; Fu, D.-J.; Alphs, L. Comparison of the peak-to-trough fluctuation in plasma concentration of long-acting injectable antipsychotics and their oral equivalents. *Innovations in Clinical Neuroscience* **2012,** *9*, (7-8), 17-23.

List of Abberivations

AH	anhydrate
ANOVA	analysis of variance
API	active pharmaceutical ingredient
ASP	acetylsalicylic acid
AUC	area under the curve
AUMC	area under the moment curve
BCS	biopharmaceutical classification system
BZF	bezafibrate
CAF	caffeine
CAFAH	caffeine anhydrate
CAFH	caffeine hydrate
CBZ	carbamazepine
CCD	charged-coupled device
CEL	cremophor EL, synonymous name is Kolliphor EL
C_{max}	maximum plasma concentration
CMC	critical micelle concentration
CNZ	cinnarizine
CSD	Cambridge structural database
CVD	carvedilol
DCS	developability classification system
DFL	diflunisal
DOSS	dioctyl sodium sulfosuccinate
DOSY	diffusion ordered spectroscopy
DPL	dipyridamole
DSC	differential scanning calorimetry
DVS	dynamic vapor sorption
EPO	Eudragit EPO
ESL	estradiol
FaSSIF	fasted state simulated intestinal fluid
FaSSGF	fasted state simulated gastric fluid

FLP	felodipine
FLU	flurbiprofen
FRS	furosemide
GI	gastrointestinal
H	hydrate
HLB	hydrophilic lipophilic balance
HPL	haloperidol
HPLC	high performance liquid chromatography
HPMC	hydroxypropylmethylcellulose
HT	high throughput
IBU	ibuprofen
IMC	isothermal microcalorimentry (Chapter 2)
IMC	indomethacine (Chapter 6)
IP-PSD	imagine plate position sensitive detector
IR	infrared
MFA	mefenamic acid
MFQ	mefloquine
MRT	mean residence time
NaCMC	sodium caboxymethyl cellulose
NIR	near infrared
NMR	nuclear magnetic resonance
NPX	naproxen
P80	polysorbate 80
PDL	pindolol
PGN	progesterone
PMZ	pimozide
PLM	polarized light microscopy
PLS	partial least square analysis
PRX	piroxicam
PRXAH	piroxicam anhydrate
PRXMH	piroxicam monohydrate
OrBiTo	oral biopharmaceutical tools
RT	room temperature
$rDiff_{API}$	relative diffusion coefficient
SDS	sodium dodecyl sulfate
SE	solubility enhancement

SEM	scanning electron microscopy
SLE	solid-liquid phase equilibrium
SOLU	Solutol, synonymous name is Kolliphor HS 15
SORESOS	solubility and residual solid screening
ss-NMR	solid state nuclear magnetic resonance
SUCM	sucrose monolaurate
$t_{1/2}$	plasma half-life
TES	testosterone
TESAH	testosterone anhydrate
TESMH	testosterone monohydrate
TFD	terfenadine
TGA	thermogravimetric analysis
TLB	tolbutamide
t_{max}	time to reach maximum plasma concentration
TMX	tamoxifen
UPLC	ultra performance liquid chromatography
UV	ultra violet
WFN	warfarin
XRPD	X-ray powder diffraction

List of Symbols

h	thickness of the diffusion layer
i	empirically determined exponent
j	empirically determined exponent
k	Boltzmann constant (Chapter 2.1.2 and 4)
k	Noyes-Whitney constant (Chapter 2.2)
k_1	Bruner-Tolloczko constant
k_N	secondary nucleation rate constant
l	empirically determined exponent
log$D$	distribution coefficient
log$P$	partitioning coefficient
pK_a	acid dissociation constant
t	time
x_i	mass fraction of standard i

A'	kinetic factor proportional to the number of nucleation-active centers
B'	shape and homogeneity factor
C	concentration
C_S	saturation solubility
D	diffusion coefficient
D	fractal dimension (Chapter 4)
D_2O	deuterium oxide
I	intensity
J_1	primary nucleation rate
J_2	secondary nucleation rate
N	number of boxes
S	drug supersaturation
S	thermodynamic solubility
S_0	intrinsic solubility
S_{app}	apparent solubility
S_i	observed intensity

T	temperature
T_m	melting temperature
V	volume
γ	interfacial energy
ε	box size
v_0	molecular volume of crystalline phase
ρ_S	suspension density
σ	supersaturation
ω	agitation rate

List of Figures

List of Tables